

2008

Structure of the Southern Skagit Gneiss Complex, North Cascades, Washington

Erin Kathleen McLaren Shea
San Jose State University

Follow this and additional works at: https://scholarworks.sjsu.edu/etd_theses

Recommended Citation

Shea, Erin Kathleen McLaren, "Structure of the Southern Skagit Gneiss Complex, North Cascades, Washington" (2008). *Master's Theses*. 3625.

DOI: <https://doi.org/10.31979/etd.hjb2-kupm>

https://scholarworks.sjsu.edu/etd_theses/3625

This Thesis is brought to you for free and open access by the Master's Theses and Graduate Research at SJSU ScholarWorks. It has been accepted for inclusion in Master's Theses by an authorized administrator of SJSU ScholarWorks. For more information, please contact scholarworks@sjsu.edu.

INFORMATION TO USERS

This manuscript has been reproduced from the microfilm master. UMI films the text directly from the original or copy submitted. Thus, some thesis and dissertation copies are in typewriter face, while others may be from any type of computer printer.

The quality of this reproduction is dependent upon the quality of the copy submitted. Broken or indistinct print, colored or poor quality illustrations and photographs, print bleedthrough, substandard margins, and improper alignment can adversely affect reproduction.

In the unlikely event that the author did not send UMI a complete manuscript and there are missing pages, these will be noted. Also, if unauthorized copyright material had to be removed, a note will indicate the deletion.

Oversize materials (e.g., maps, drawings, charts) are reproduced by sectioning the original, beginning at the upper left-hand corner and continuing from left to right in equal sections with small overlaps.

ProQuest Information and Learning
300 North Zeeb Road, Ann Arbor, MI 48106-1346 USA
800-521-0600

UMI[®]

STRUCTURE OF THE
SOUTHERN SKAGIT GNEISS COMPLEX,
NORTH CASCADES, WASHINGTON

A Thesis

Presented to

The Faculty of the Department of Geology

San José State University

In Partial Fulfillment

of the Requirements for the Degree

Master of Science

by

Erin Kathleen McLaren Shea

December 2008

INFORMATION TO USERS

The quality of this reproduction is dependent upon the quality of the copy submitted. Broken or indistinct print, colored or poor quality illustrations and photographs, print bleed-through, substandard margins, and improper alignment can adversely affect reproduction.

In the unlikely event that the author did not send a complete manuscript and there are missing pages, these will be noted. Also, if unauthorized copyright material had to be removed, a note will indicate the deletion.



UMI Microform 1463410

Copyright 2009 by ProQuest CSA

All rights reserved. This microform edition is protected against unauthorized copying under Title 17, United States Code.

ProQuest CSA
789 E. Eisenhower Pkwy
P.O. Box 1346
Ann Arbor, MI 48108-3218

©2008

Erin Kathleen McLaren Shea

ALL RIGHTS RESERVED

SAN JOSÉ STATE UNIVERSITY

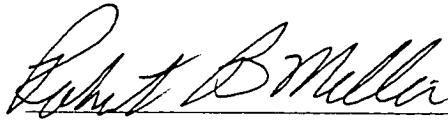
The Undersigned Thesis Committee Approves the Thesis Titled

STRUCTURE OF THE
SOUTHERN SKAGIT GNEISS COMPLEX,
NORTH CASCADES, WASHINGTON

by

Erin Kathleen McLaren Shea

APPROVED FOR THE DEPARTMENT OF GEOLOGY

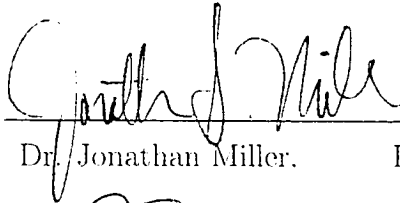


13 November 2008

Dr. Robert Miller,

Department of Geology

Date



11/13/08

Dr. Jonathan Miller,

Department of Geology

Date



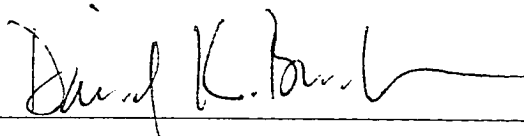
11/13/08

Dr. Richard Sedlock,

Department of Geology

Date

APPROVED FOR THE UNIVERSITY



12/1/08

Associate Dean

Office of Graduate Studies and Research

Date

ABSTRACT
STRUCTURE OF THE SOUTHERN SKAGIT GNEISS COMPLEX,
NORTH CASCADES, WASHINGTON

Erin Shea

The crystalline core of the North Cascades is part of a thick Cretaceous-Eocene continental magmatic arc. The Skagit Gneiss Complex (SGC), composed of NW-striking, partially migmatitic ortho- and paragneisses, comprises the highest grade rocks of the arc. Geological mapping and U-Pb zircon geochronology from this study indicate that the southern SGC can be subdivided into five sub-units ranging in age from at least 76 Ma to 60 Ma. Foliation in the southern SGC is NW-striking and dips moderately to steeply NE or SW. Lineation is SE-trending and has gentle to moderate plunge. Two periods of non-coaxial deformation are recorded in the study area: a period of high-temperature shear (≥ 450 °C) and a later period of low-temperature shear (≤ 450 °C). At least four phases of folds are evident in the study area and range in age from mid-Cretaceous or older to ~ 49 Ma. The first two phases are relatively small (centimeter- to meter-wavelength) and constrained to specific rock units. The final two phases are relatively large (kilometer-wavelength) and affect most rocks older than 49 Ma.

ACKNOWLEDGEMENTS

I would like to express my deepest gratitude to my advisor, Robert Miller, for his guidance in researching and writing this thesis. My thesis committee, Professors Jonathan Miller, Richard Sedlock, and Ellen Metzger provided welcome insight and assistance. Thank you to Ian and Tyler Philips, Morgan Mendoza, Brad Bruerer, Aaron Rutledge, and Shannon Leslie, my field assistants, who suffered greatly in extreme temperatures and working conditions in the pursuit of data. Noah McLean was a geochronology guru, and along with Zach Michels and Brigid Doran, was always willing to talk about the North Cascades with me. Kyle Gilpin provided endless patience, editing, and support (and field assistance). Finally, I would like to thank Sam Bowring for allowing me to use his fantastic geochronology lab and without whom this thesis never would have been written.

Financial support was provided by the U.S. Geological Survey EDMAP Program, Geological Society of America Graduate Research Grant, and National Science Foundation Grant EAR-0511062.

DEDICATION

For Michael Burton

The scientist only imposes two things, namely truth and sincerity, imposes them upon himself and upon other scientists.

-Schrödinger

Table of Contents

	Page
INTRODUCTION	1
Regional Geology	1
Skagit Gneiss Complex	5
ROCK UNITS	7
Cascade River-Holden Assemblage	7
Bearcat Ridge Orthogneiss	11
Skagit Gneiss Complex	12
Migmatite	13
Heterogeneous Gneisses	16
Ferry Peak Orthogneiss	18
Old Maid Orthogneiss	21
Cub Lake Orthogneiss	23
Gray Gneiss	24
Sunrise Lake Pluton	26
Cooper Mountain Batholith	28
Railroad Creek Pluton	30
Dikes of Intermediate Composition	30
GEOCHRONOLOGY	33
Ferry Peak Orthogneiss (ES-32)	36
Bearcat Ridge Orthogneiss (ES-19)	36
Gray Gneiss (ES-02)	39
Cooper Mountain Batholith (BNC-326-1)	39

METAMORPHISM	46
STRUCTURE	47
Foliation	47
Lineation	50
Non-Coaxial Shear	54
High-Temperature Non-Coaxial Shear	54
Low-Temperature Non-Coaxial Shear	57
Folds	60
F2 Folds	60
F3 Folds	61
F4 Folds	61
F5 Folds	65
Dikes of Intermediate Composition	65
DISCUSSION	69
Intrusive History	69
Deformation History	76
CONCLUSIONS	83
REFERENCES CITED	85

List of Illustrations

Figure	Page
1. Fault-bounded Domains of the North Cascades	3
2. Geologic Map of the Crystalline Core of the North Cascades	4
3. Simplified Map of the Study Area	8
4. Contact Between the Bearcat Ridge Orthogneiss and Cascade River-Holden Assemblage	9
5. Migmatite Xenolith	14
6. Heterogeneous Gneiss and Migmatite	15
7. Xenolith of the Cascade River-Holden Assemblage	17
8. Garnets in the Ferry Peak Orthogneiss	20
9. Mingling of the Old Maid Orthogneiss and Gray Gneiss	22
10. Xenoliths of the Ferry Peak Orthogneiss in the Gray Gneiss	25
11. Mingling of Quartz Diorite and Leuco-tonalite in the Sunrise Lake Pluton	27
12. Xenoliths of Ferry Peak Orthogneiss in the Cooper Mountain Batholith	29
13. Xenolith of Heterogeneous Gneiss in Mafic Dike	32
14. Concordia Plot for the Ferry Peak Orthogneiss	37
15. Magnified Concordia Plot for the Ferry Peak Orthogneiss	38
16. Concordia Plot for the Bearcat Ridge Orthogneiss	40
17. Concordia Plot for the Gray Gneiss	41
18. Magnified Concordia Plot for the Gray Gneiss	42
19. Concordia Plot for the Cooper Mountain batholith	44
20. Magnified Concordia Plot for the Cooper Mountain Batholith	45
21. Simplified Map of Foliations in the Study Area	48

22.	Lower Hemisphere Stereographic Projection of Poles to Solid-state Foliations in the Study Area	49
23.	Stereographic Projection of Poles to Magmatic Foliations in the Study Area	51
24.	Simplified map of Lineations in the Study Area	52
25.	Stereographic Projection of Lineations in the Cascade River-Holden Assemblage, SGC, and Bearcat Ridge Orthogneiss	53
26.	Melt-filled Ductile Shear Zones in the Ferry Peak Orthogneiss	56
27.	Micro-faulted Plagioclase in a Thin Section of the Gray Gneiss	58
28.	Ductile Shear Zones in a Medium-Grained Biotite-Tonalite	59
29.	F2 Folds in a Xenolith of the Cascade River-Holden Assemblage	62
30.	Openly Folded Xenolith of the Cascade River-Holden Assemblage Contained in the Ferry Peak Orthogneiss	63
31.	Crenulated Foliation in the Ferry Peak Orthogneiss	64
32.	Simplified Map of Foliation in the Study Area Combined with Data from Miller (1987) and Unpublished Data (R.B. Miller).	66
33.	Simplified Map of Lineations in the Study Area Combined with Data from Miller (1987) and Unpublished Data (R.B. Miller)	67
34.	Lower Hemisphere Stereographic Projection of Poles to Dikes in the Study Area	68
35.	Schematic Sketch of the Southern SGC	74
36.	Simplified Map of Non-Coaxial Deformation in the Study Area	79

Plate

1.	Bedrock Geologic Map of the Study Area	In Pocket
2.	Cross Section A-A'	In Pocket

3.	Cross Section B-B'	In Pocket
4.	Cross Section C-C'	In Pocket

Table

1.	Zircon U-Pb Isotopic Data	35
----	-------------------------------------	----

INTRODUCTION

The study of exhumed crust in magmatic arcs is often overlooked in comparison to collisional orogens such as the Himalayas; in particular, models of lateral and vertical crustal flow have been developed almost exclusively for collisional orogens. The behavior of the lower crust in contractional magmatic arcs is significantly less well-understood. The exhumed crust from ancient magmatic arcs provides an opportunity to examine this region of the crust. This study investigated how models of crustal flow apply to the exhumed remnants of a very thick (≥ 55 km) Cretaceous- to-Eocene contractional magmatic arc in the North Cascades of Washington (Miller and Paterson, 2001).

In particular, this study focused on the southern part of the Skagit Gneiss Complex (SGC), which is composed of the highest grade, and possibly the most deeply exhumed, metamorphic rocks within the Cascades arc (Whitney, 1992a). The ultimate goal of research in the SGC is to understand the dynamics of mid-to-deep crustal flow in continental arcs during orogenesis. The structures, contacts, and ages of the southern SGC are of particular interest due to the juxtaposition of the complex with older orthogneisses and metasedimentary rocks. Additionally, the SGC is composed of ortho- and paragneiss bodies of varying ages that aid in the determination of the timing of specific deformational stages.

Regional Geology

The North Cascades were divided by Misch (1966, 1968) into three fault-bounded belts: a western belt of Paleozoic and Mesozoic oceanic and arc-derived accreted rocks (Western domain), an eastern belt composed of unmetamorphosed Jurassic and Cretaceous strata (Methow basin), and a central

belt of extensively intruded, highly metamorphosed schist and gneiss (Cascades crystalline core domain) (Fig. 1). This study concentrated on the crystalline core of the North Cascades (Cascades core).

The Cascades core is the southernmost extension of the ~1500-km-long Coast Plutonic Complex that stretches from southeast Alaska to northern Washington (e.g., Rubin et al., 1990). The crystalline core is bounded by two faults, the Straight Creek fault to the west and the Ross Lake fault zone to the east (Figs. 1 and 2) (Misch, 1966; Miller, 1994). The North Cascades region records a history of pre-Late Cretaceous accretion, mid-Cretaceous deformation, metamorphism, and plutonism, and Eocene transtension and plutonism (e.g., Tabor et al., 1989). The early (96-85 Ma) history of the Cascades core was marked by intrusion, amphibolite-facies metamorphism, regional shortening, and crustal thickening to ≥ 55 km (Miller and Paterson, 2001). This mid-Cretaceous shortening and crustal thickening resulted from the final suturing of the Wrangellia terrane to the North American continent (Monger et al., 1982; McGroder, 1991). Shortening was expressed at shallow levels (< 10 km) as southwest-directed thrusting (Brandon et al., 1988) and at deeper levels (10-40 km) as folds, associated axial-planar foliation and southwest-vergent reverse shear zones (Miller et al., 2006).

Later magmatism, metamorphism, and deformation were concentrated in the northeastern part of the Cascades core. The post-metamorphic, high-angle Entiat fault divides the Cascades core into two regions: the Wentachee block to the southwest and the Chelan block to the northeast (Fig. 1) (Tabor et al., 1989). Radiometric cooling ages in the Wenatchee block are largely Late Cretaceous, whereas cooling ages in the Chelan block are early Tertiary (e.g., Haugerud et al., 1991). Eocene transtension produced dextral strike-slip faulting along the continental margin, non-marine sedimentary basin development, and magmatism

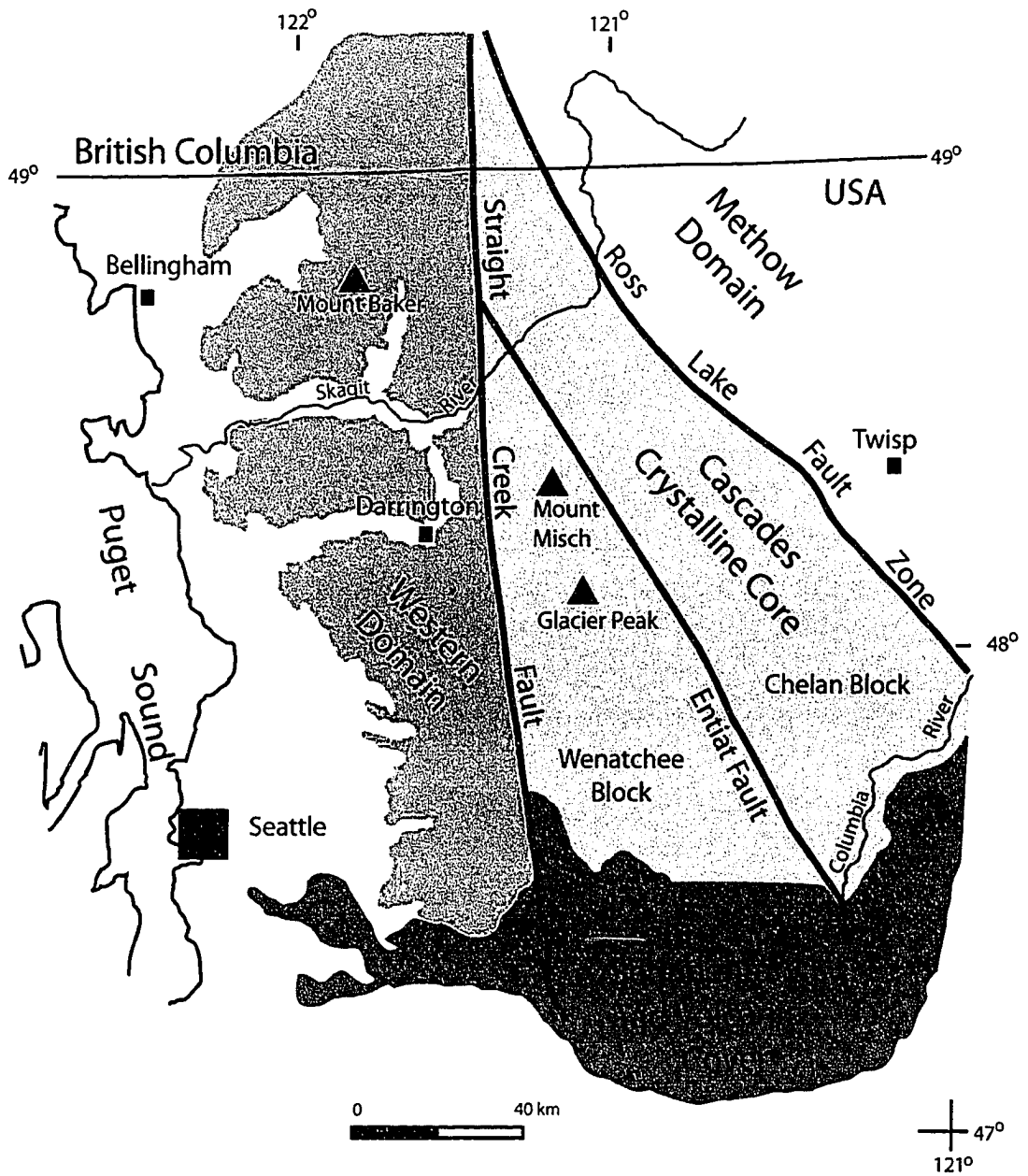


Fig. 1. Northwestern part of Washington State, showing fault-bounded domains of the North Cascades. Modified from Tabor et al. (1989).

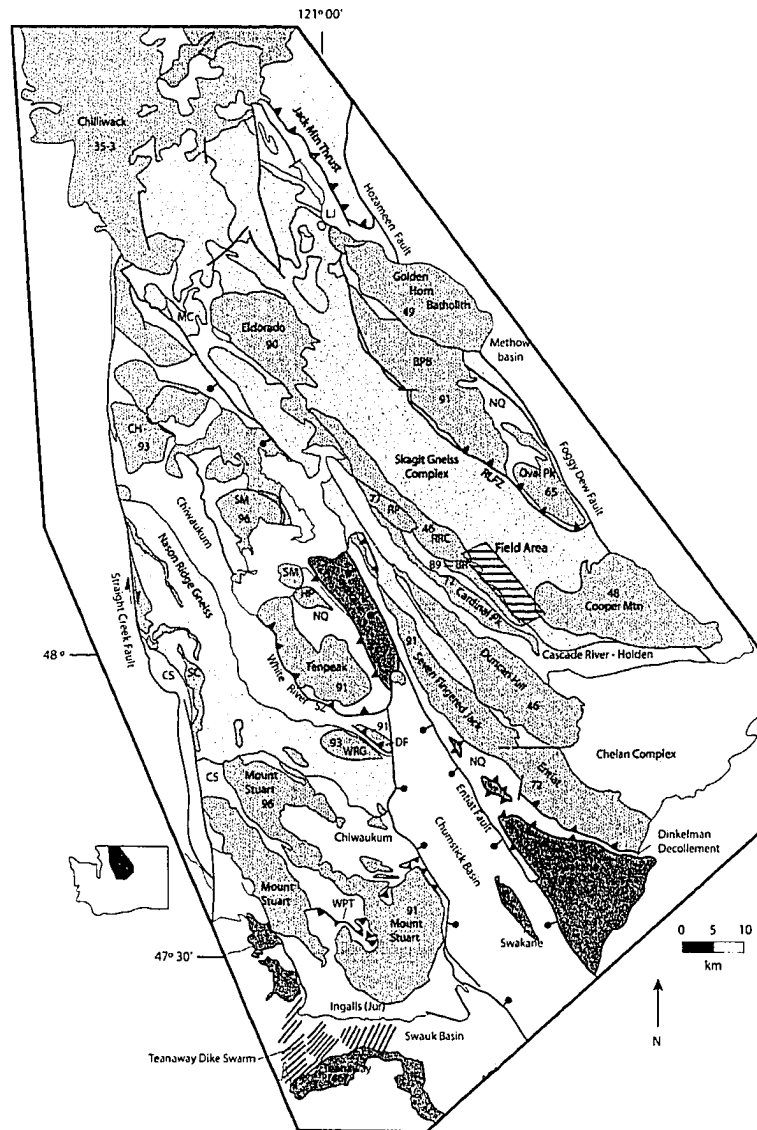


Fig. 2. Northwestern part of the crystalline core of the North Cascades. Patterned rocks are plutons and crystallization ages are numbers within each unit. BPB- Black Peak batholith, BR- Bearcat Ridge Orthoneiss, CH- Chaval pluton, CS- Chiwaukum Schist, DF- Dirtyface pluton, HP- High Pass pluton, LJ- Little Jack unit, MC- Marble Creek pluton, NQ- Napeequa unit, RLFZ- Ross Lake fault zone, RP- Riddle Peaks pluton, RRC- Railroad Creek pluton, RM- Ruby Mountain, SC- Sloan Creek plutons, SM- Sulphur Mountain pluton, WPT- Windy Pass thrust, WRG- Wenatchee Ridge Gneiss. Study area outlined with a striped pattern. Modified from Miller et al. (2006) and Tabor et al. (2003).

(Johnson, 1985). Eocene transtensional basins contain thick sections of non-marine strata of the Swauk, Chuckanut, and Chumstick formations (Johnson, 1985). These units are deformed by N-to-NW trending folds that have wavelengths of a kilometer or more (Tabor et al., 1984). Intermediate to mafic Eocene dike swarms generally record arc-parallel extension (Haugerud et al., 1991; Doran et al., 2007). This extension direction is variable, possibly due to complex spatial and/or temporal variations in the strain field (Doran et al., 2007). Ductile deformation in the Eocene is recorded by a NW-trending stretching lineation in the SGC, movement along the Dinkelman decollement (Fig. 2), and distributed shear in the Swakane Gneiss (Haugerud et al., 1991; Paterson et al., 2004; Miller et al., 2007). Long wavelength folds as young as 49 Ma in the SGC and surrounding units suggest that transpression was also important during the Eocene (Shea et al., 2007).

Skagit Gneiss Complex

The SGC is an ~150-km-long and ~20-30-km-wide, northwest-striking unit in the Cascades core with a broadly antiformal structure (Fig. 2). Units adjacent to the SGC include non-migmatitic meta-supracrustal rocks, discrete plutons, and orthogneisses generally not associated with the SGC. The SGC is composed of both ortho- and paragneisses that are in places migmatitic (Misch, 1968). Paragneiss is an important constituent in the northern half of the complex, and orthogneiss makes up most of the southern half (Haugerud et al., 1991; Miller et al., 1994). These orthogneisses vary in composition from leucogranodiorite to diorite (Misch, 1966) and overall are more felsic than the tonalitic orthogneisses found elsewhere in the Cascades core (Miller et al., 1994). Foliation in the gneiss complex generally strikes NW. Dip direction is NE or SW and ranges from gentle to steep (Haugerud et al., 1991). Foliation describes a large antiform that is present along the length of

the complex (Misch, 1966; Tabor et al., 1989). Lineations are NW- or SE- to NNE- or SSW-trending with subhorizontal to moderate plunges. Work by Whitney (1992a, b) and Gordon et al. (2008) have determined that migmatitic rocks of the SGC reached pressures of at least 8 kbar at peak temperatures between 650 and 800°C. These pressures suggest that protoliths of the SGC were buried to a depth of at least 25 km, with the highest recorded pressures towards the center of the antiform (Whitney, 1992a).

ROCK UNITS

The southern SGC is bounded in the study area by the Bearcat Ridge Orthogneiss (89-69 Ma) on the southwest and the Cooper Mountain batholith (48 Ma) on the southeast (Fig. 3; Plate 1). To the east, the complex is intruded by the Sunrise Lake pluton (49 Ma) (McLean et al., 2006) and in the northwestern corner of the study area, the Railroad Creek pluton intrudes both the Bearcat Ridge Orthogneiss and the SGC (Fig. 3; Plate 1). Additionally, xenoliths and bodies of the Cascade River-Holden assemblage are present in all plutons and orthogneiss bodies in the study area. Late dikes of mainly intermediate composition are observed throughout the area and cross-cut all units but the Sunrise Lake pluton, Cooper Mountain batholith, and Railroad Creek pluton.

Cascade River-Holden Assemblage

The Triassic Cascade River-Holden assemblage is defined by Cater and Wright (1967) as consisting mainly of hornblende schist and gneiss with significant amounts of calc-silicate rock and biotite schist. Based on mineral modes, the protoliths of this unit are interpreted as mafic volcanic rocks, calc-silicates, and greywackes (Cater and Wright, 1967; Miller et al., 1994). In the eastern part of the field area (east of Lake Chelan), the Cascade River-Holden assemblage crops out as isolated rafts and xenoliths (1-10 m long) in the SGC, Sunrise Lake pluton, and Cooper Mountain batholith. To the west, the unit forms map-scale bodies and one- to three-meter-thick layers bodies concordantly intruded by the Bearcat Ridge Orthogneiss (Fig. 4). An elongate septum of the assemblage is present on the eastern margin of the migmatite unit of the SGC (discussed below). Many outcrops of the assemblage along the shore of Lake Chelan are partially migmatitic and

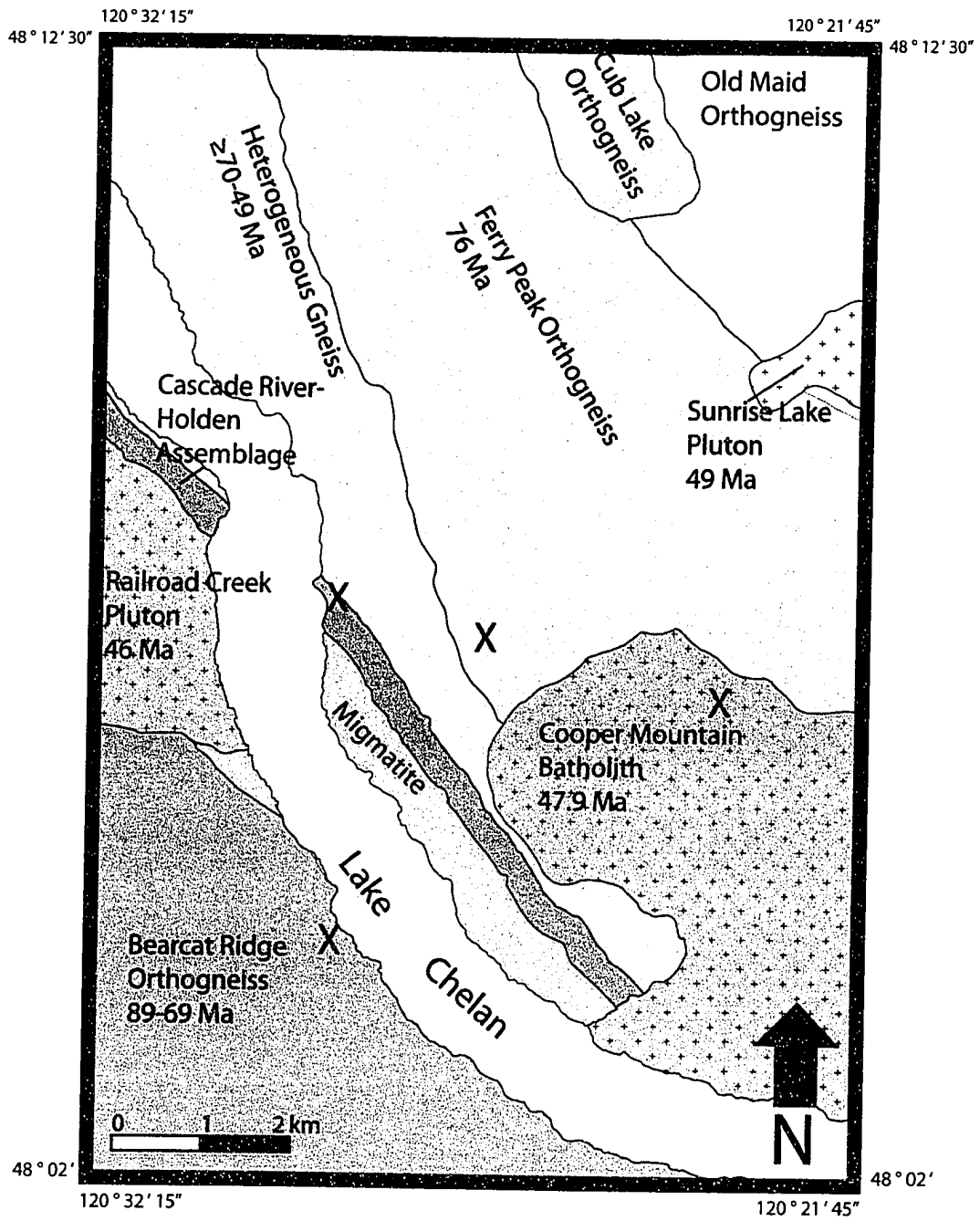


Fig. 3. Simplified map of the study area. Plus pattern signifies units with a magmatic foliation. "X"s indicate geochronology sample sites.



Fig. 4. Contact between the Bearcat Ridge Orthogneiss (lower) and amphibolite of the Cascade River-Holden assemblage (upper). Note the isoclinal folds in the upper right of the photo (outlined by black dashes). Pencil for scale

contain concordant veinlets of leucocratic intrusive rocks.

Contacts of the Cascade River-Holden assemblage with adjacent units are sharp. In the western part of the study area (west of Lake Chelan), contacts are concordant to foliation and have a northwest strike and moderate southwest dip. In the eastern part of the study area, xenolith foliations are broadly parallel to foliation in the host rocks of the SGC. Foliation in the assemblage is defined by aligned biotite, elongate quartz, and compositional layering. Lineation is distinguished by aligned biotite and hornblende, and by elongate quartz aggregates.

In the study area, the Cascade River-Holden assemblage mainly consists of biotite and hornblende schists. Many outcrops display less-abundant interlayered calc-silicate rocks. Biotite schist of the Cascade River-Holden assemblage is fine- to medium-grained and compositionally layered at a sub-centimeter scale. Compositional layering is also evident at a centimeter-scale as biotite- and hornblende-rich layers alternating with more leucocratic bands. Typical assemblages consist of biotite, quartz, hornblende, plagioclase, \pm garnet. Biotite is deformed into mica fish and commonly forms tails on more resistant plagioclase and garnet porphyroblasts. Quartz is present as elongate ribbons that contain blocky subgrains and recrystallized grains. Hornblende is anhedral and fractured. Plagioclase is anhedral to subhedral and typically contains bent deformation twins. Large plagioclase porphyroclasts are commonly fractured. Mosaics of recrystallized plagioclase are evident in many samples. Garnet ranges in diameter from 120 μm to 500 μm and is generally anhedral with inclusions of biotite and quartz.

Amphibolite of the Cascade River-Holden assemblage is fine-grained, equigranular, and marked by millimeter-scale layering of plagioclase- and hornblende-rich material. Typical assemblages consist of hornblende, plagioclase, biotite, sphene, quartz, \pm clinopyroxene. Calc-silicate minerals occur in specific

layers within the amphibolite. Recrystallization is common in plagioclase, hornblende, quartz, and clinopyroxene, forming a mosaic texture. Hornblende is subhedral and is present as recrystallized mosaics and elongate grains. Plagioclase is subhedral and contains lamellar twins, deformation twins, and normal zoning. Bent grains of plagioclase are common. Biotite is deformed into fish and commonly wraps around more resistant grains. Quartz forms both recrystallized and elongate grains. Non-recrystallized grains contain bulging grain boundaries and subgrains. Sphene grains range from anhedral to euhedral and are $\leq 300 \mu\text{m}$ in length. Clinopyroxene crystals are small ($\leq 300 \mu\text{m}$) and subhedral.

Calc-silicate rocks were observed in two outcrops in the study area. These rocks have recrystallized mosaics of plagioclase, diopside, and minor quartz, biotite, hornblende, and sphene. Several distinct zones in the rocks are defined by variations in grain sizes, which range from fine- to coarse-grained. Minor compositional layering of felsic and mafic minerals is highly localized. Plagioclase is characterized by lamellar twins, minor bent grains, and microfractures. Diopside is weakly elongate and microfractured. Quartz is largely present as late veins composed of elongate grains. Biotite is almost entirely altered to chlorite. Rare hornblende is small and anhedral. Sphene is subhedral and occurs in concentrated layers.

Bearcat Ridge Orthogneiss

The Late Cretaceous (89-69 Ma) Bearcat Ridge Orthogneiss was described by Cater (1982) as a series of roughly concordant, northwest-striking deformed plutons that extended from Bearcat Ridge, 10 km NW of the study area, to the shore of Lake Chelan. The unit is present in the western-most part of the study area as a series of elongate bodies that range in thickness from 1 to 100 m. These bodies vary in composition from granodioritic gneiss to muscovite-bearing tonalitic leucogneiss.

More mafic hornblende-bearing gneisses described by Cater (1982) are not present. Rare sheets containing large (up to 1.5×0.5 cm) euhedral muscovite crystals are found in the unit. These sheets are at least 5 m wide, and possibly much wider, as it was not possible to determine an upper limit due to cover. As described above, the unit concordantly intrudes the Cascade River-Holden assemblage with sharp contacts (Fig. 4). The eastern contact of the Bearcat Ridge Orthogneiss with migmatite of the SGC is obscured by Lake Chelan. To the north, the unit is intruded by the Railroad Creek pluton. Foliation strength varies from well-foliated to mylonitic; S=L and $S \geq L$ fabrics are most common. Any magmatic fabric present in the initial intrusions has been overprinted by later solid-state fabrics.

The most common mode of the Bearcat Ridge Orthogneiss is plagioclase (40%), quartz (30%), biotite (15%), potassium feldspar (15%), \pm garnet, \pm muscovite, \pm sphene. Thin section analysis shows an assemblage of recrystallized biotite, quartz, potassium feldspar, and plagioclase. Foliation within the gneiss is distinguished by aligned plagioclase, biotite, and quartz. Lineation is defined by elongate quartz and biotite. Some plagioclase forms sigma and delta porphyroclasts that are ~ 1 cm long. These grains vary between anhedral and subhedral. Myrmekite is common. Plagioclase contains deformation twins and subgrains, indicating deformation at temperatures of ≥ 600 °C (Passchier and Trouw, 2005). Quartz is present as both recrystallized and deformed grains that contain bulging grain boundaries and subgrains. Biotite forms elongate stringers and small “fish”. Alteration of biotite to chlorite is common. Garnet in the Bearcat Ridge Orthogneiss is small (≤ 1 mm) and sub-idiomorphic to xenomorphic, and has biotite and muscovite tails. Muscovite is highly elongate and, in places, boudinaged. Aligned muscovite is included in plagioclase and potassium feldspar. Accessory sphene is typically small and xenomorphic.

Skagit Gneiss Complex

A major aspect of this study was the subdivision of the southern SGC into individual paragneiss and orthogneiss units. From oldest to youngest, these units are: migmatite, Ferry Peak Orthogneiss, Old Maid Orthogneiss, Cub Lake Orthogneiss, and Gray Gneiss. Additionally, the western part of the SGC in the study area is composed of many gneisses that are difficult to assign to a specific sub-unit. These rocks are grouped into a unit referred to as the heterogeneous gneisses. One of the units described above, the Ferry Peak Orthogneiss, was previously defined by R.B. Miller (pers. comm.).

Migmatite

Several types of migmatite are present in the southern SGC, but stromatic (layered), ophalmitic (augen), and schollen (raft) migmatites are the most common. Schlieren migmatite is also present in isolated outcrops. The migmatite outcrops are grouped into a northwest-striking, ~3-km-wide unit that is bounded by a septa of Cascade River-Holden assemblage to the northeast and Bearcat Ridge Orthogneiss to the southwest (Fig. 3; Plate 1). The contact between the migmatite and Cascade River-Holden assemblage is sharp. Heterogeneous gneisses intrude some migmatite outcrops that contain both sharp and gradational contacts (Figs. 5 and 6). The contact of the migmatite with the Bearcat Ridge Orthogneiss is covered, but occurs over ≤ 100 m across strike.

Migmatites of the southern SGC are commonly cut by concordant to discordant plagioclase- and quartz-dominated pegmatite intrusions (Fig. 6). These intrusions have contacts that vary from sharp to gradational. Layers in the stromatic migmatite range between 0.5 m and 1.0 m in thickness and are generally concordant



Fig. 5. Migmatite xenolith intruded by intermediate rocks of the heterogeneous gneiss along the shore of Lake Chelan. Pencil for scale.

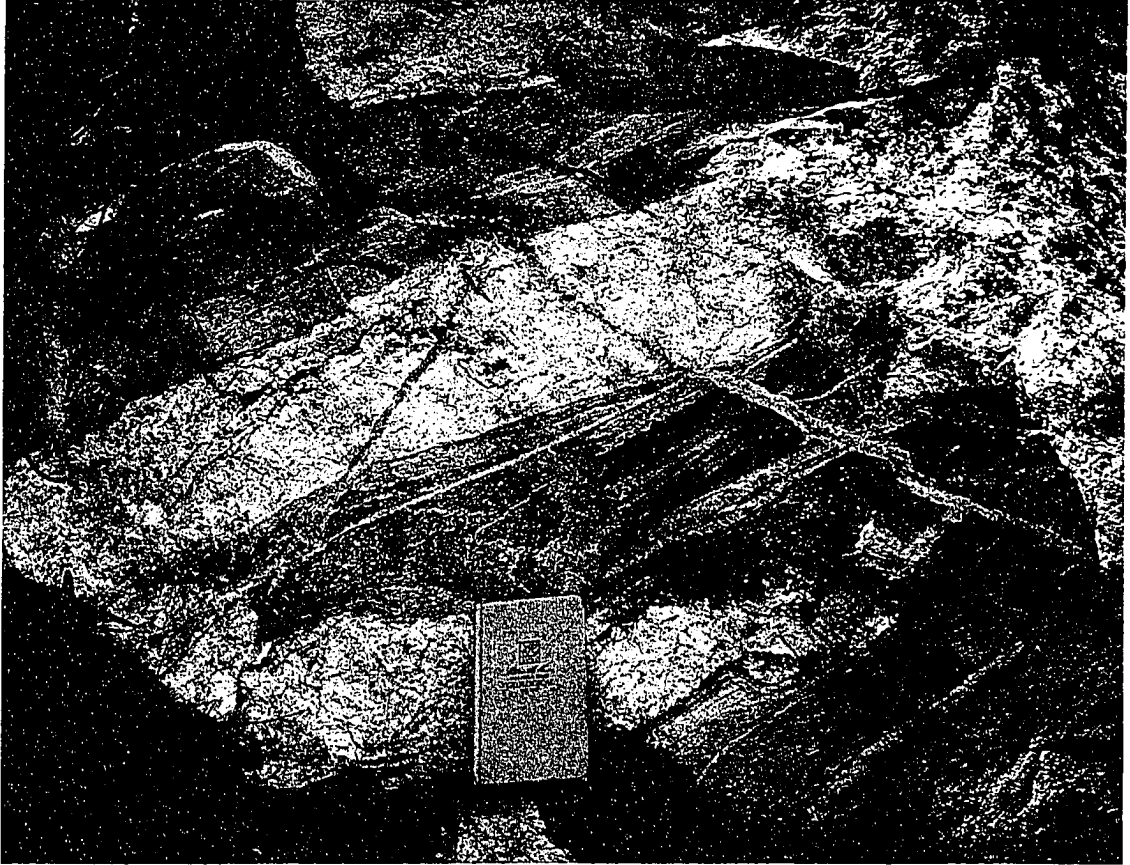


Fig. 6. Quartz diorite member of the heterogeneous gneiss unit and migmatite. Note the interdigitations of fine-grained gneiss into the heterogeneous gneiss. Also, note gradation of diorite to migmatite in lower right corner.

to foliation. The melanosome is composed of medium-grained biotite, hornblende, quartz, and plagioclase. The leucosome is composed of plagioclase, quartz, and minor biotite. Both the leucosome and melanosome display elongate quartz parallel to layering and foliation. Rare outcrops contain garnets that vary from millimeter to centimeter scale. Solid-state deformation is evident throughout the SGC migmatite.

Heterogeneous Gneisses

The heterogeneous gneisses are a northwest-striking assemblage of tonalitic to quartz dioritic gneisses found along and above the eastern shore of Lake Chelan (Fig. 3; Plate 1). Rocks of the heterogeneous gneiss are in both sharp (Fig. 5) and gradational (Fig. 6) contact with the migmatite unit and Ferry Peak Orthogneiss. The main body of heterogeneous gneiss is separated from the migmatite by a thin septa of Cascade River-Holden assemblage. This septa is heavily intruded by the heterogeneous gneisses. Xenoliths of the Cascade River-Holden assemblage are common throughout the heterogeneous gneisses (Fig. 7).

The heterogeneous gneisses can be divided into two main sub-groups; felsic gneisses and intermediate-composition gneisses. Both sub-groups occur in sheets that range from meters to tens of meters in thickness. Felsic gneisses are generally fine- to medium-grained and have a tonalitic protolith. Of the samples studied, the mode was generally plagioclase (50%), biotite (10%), and quartz (40%), \pm potassium feldspar, \pm garnet. Intermediate-composition gneisses are medium- to coarse-grained and have a quartz diorite protolith. Of the samples studied, the mode was generally plagioclase (50%), quartz (20%), and biotite/hornblende (30%). Both felsic and mafic gneisses range from equigranular to porphyritic and contain subhedral to anhedral grains. Plagioclase displays lamellar twins, deformation twins, and bent grains. Recrystallization of plagioclase into mosaics is common. Biotite grains are



Fig. 7. Cascade River-Holden assemblage xenolith in tonalitic member of the heterogeneous gneisses along the eastern shore of Lake Chelan. Field notebook for scale.

typically elongate and show evidence for recrystallization. Quartz grains are elongate, contain blocky subgrains, and are recrystallized into mosaics. Rare potassium feldspar is typically perthitic and microfractured. Myrmekite is also common. Garnet is subhedral and several millimeters in diameter.

Ferry Peak Orthogneiss

The Ferry Peak Orthogneiss (~76 Ma) is a northwest-striking body of tonalitic orthogneiss centrally located in the study area (Fig. 3; Plate 1). The unit is several kilometers wide and at least 6 km long. Xenoliths of Cascade River-Holden assemblage aligned parallel to foliation in the gneiss are common. The Ferry Peak Orthogneiss is intimately intruded in many outcrops by leucocratic pegmatite that ranges in thickness from 10 cm to 50 cm and has a foliation concordant to that of the main gneiss. Contacts between the pegmatite and the main orthogneiss are commonly gradational and difficult to distinguish. The pegmatite is considered part of the Ferry Peak Orthogneiss because of its abundance within the orthogneiss and because its fabric and deformation so strongly resemble that of the orthogneiss. In the southern part of the orthogneiss, meter-thick dikes of granodiorite similar to the Cooper Mountain batholith intrude the orthogneiss with sharp contacts. These dikes become progressively more common and increase in thickness with proximity to the batholith. The Ferry Peak Orthogneiss is well-lineated and foliated in the solid-state throughout the field area; $L \geq S$ or $L=S$ fabrics are most common.

The Ferry Peak Orthogneiss varies from medium- to coarse-grained and is composed of plagioclase (40%), quartz (30%), biotite (20%), potassium feldspar (10%) and extremely rare hornblende, garnet, and sillimanite. Accessory minerals are sphene, zircon, and Fe-Ti oxides. In hand sample, foliation and lineation are apparent in long biotite stringers that typify the unit. In thin section, plagioclase is

typified by quartz intergrowths, deformation twins, bent grains, and local recrystallization. Quartz grains are large, have subgrains and bulging grain boundaries, and are recrystallized through subgrain rotation. Biotite is elongate and is commonly altered to chlorite. Potassium feldspar grains are relatively large (~ 0.5 cm), display undulose extinction, and are microfractured. Hornblende and garnet occur in rare, isolated outcrops. Garnet is 3-4 cm in diameter and idioblastic. Foliation wraps around the crystals, implying pre- or syn-tectonic formation (Fig. 8). Hornblende, found in garnet-bearing outcrops, is anhedral to subhedral; grains measure up to 1.5 mm across. Similarly, sillimanite, present as fibrolite, forms deformed mats in outcrops that also contain garnet and hornblende. There is no evidence that this fibrolite is the result of muscovite breakdown. The source (metamorphic or igneous) of the garnet and sillimanite is uncertain.

The pegmatite of the Ferry Peak Orthogneiss is trondhjemitic to tonalitic and is composed of quartz, plagioclase, potassium feldspar, and biotite. The pegmatite is well-foliated and -lineated. In thin section, pegmatite shows recrystallized biotite, quartz, and plagioclase. Quartz and plagioclase both form recrystallized mosaics. Plagioclase displays bent grains, deformation twins, relict oscillatory zoning, and core and mantle structure. Quartz intergrowths in plagioclase are common but have no specific orientation. Quartz has blocky subgrains, grain boundary bulging, and evidence for subgrain rotation. Potassium feldspar is microfractured and poikilitic, containing biotite and quartz inclusions.

The relationship of the Ferry Peak Orthogneiss to most of the surrounding rock units, excepting the Cooper Mountain batholith, is difficult to determine due to a lack of exposed contacts. However, a transect along Prince Creek provides insight into the relationship between the orthogneiss and the heterogeneous gneiss and migmatite units (Plate 2). The contact between the heterogeneous gneisses and



Fig. 8. Ferry Peak Orthogneiss with large, sub-idioblastic garnet. Note the strong foliation defined by elongate biotite and plagioclase.

Ferry Peak Orthogneiss appears gradational; nearer the orthogneiss, outcrops of heterogeneous gneisses more strongly resemble the Ferry Peak rocks. In particular, the heterogeneous gneisses increase in grain size and feldspars take on an augen-like appearance. The heterogeneous gneisses also are less mafic closer to the Ferry Peak Orthogneiss.

A particularly interesting outcrop between the two gneisses consists of hornblende-garnet tonalite. Garnets in this tonalite are large (~2 cm) and are mantled by hornblende, intergrown biotite and plagioclase, and intergrown hornblende and garnet. A complete study of samples from this outcrop is beyond the scope of this paper, and is left as an enticement to future workers.

Old Maid Orthogneiss

The Old Maid Orthogneiss is exposed in the far eastern part of the field area (Fig. 3; Plate 1), and is a fine- to medium-grained granodioritic leucogneiss intruded by many 4- to 5-cm-thick pegmatitic dikelets that cross-cut the foliation (Fig. 9). The unit is homogeneous and is distinguishable from the adjacent Cub Lake Orthogneiss to the northwest based on modal mineralogy: the Cub Lake Orthogneiss has a higher fraction of potassium feldspar. The contact between these units is obscured by soil, but is no more than 30 m wide. To the east, the contact is similarly obscured where the unit is adjacent to garnet-bearing biotite paragneiss. To the west, the orthogneiss intrudes the Ferry Peak Orthogneiss, as evidenced by Ferry Peak xenoliths in the Old Maid Orthogneiss. The Old Maid Orthogneiss is cut by the Gray Gneiss, but in places the two are mingled (Fig. 9). The Old Maid Orthogneiss is truncated on the south by the Sunrise Lake pluton. Foliation and lineation in the Old Maid Orthogneiss are moderately developed and defined by aligned biotite, elongate quartz, and deformed plagioclase grains. Overall, L=S and

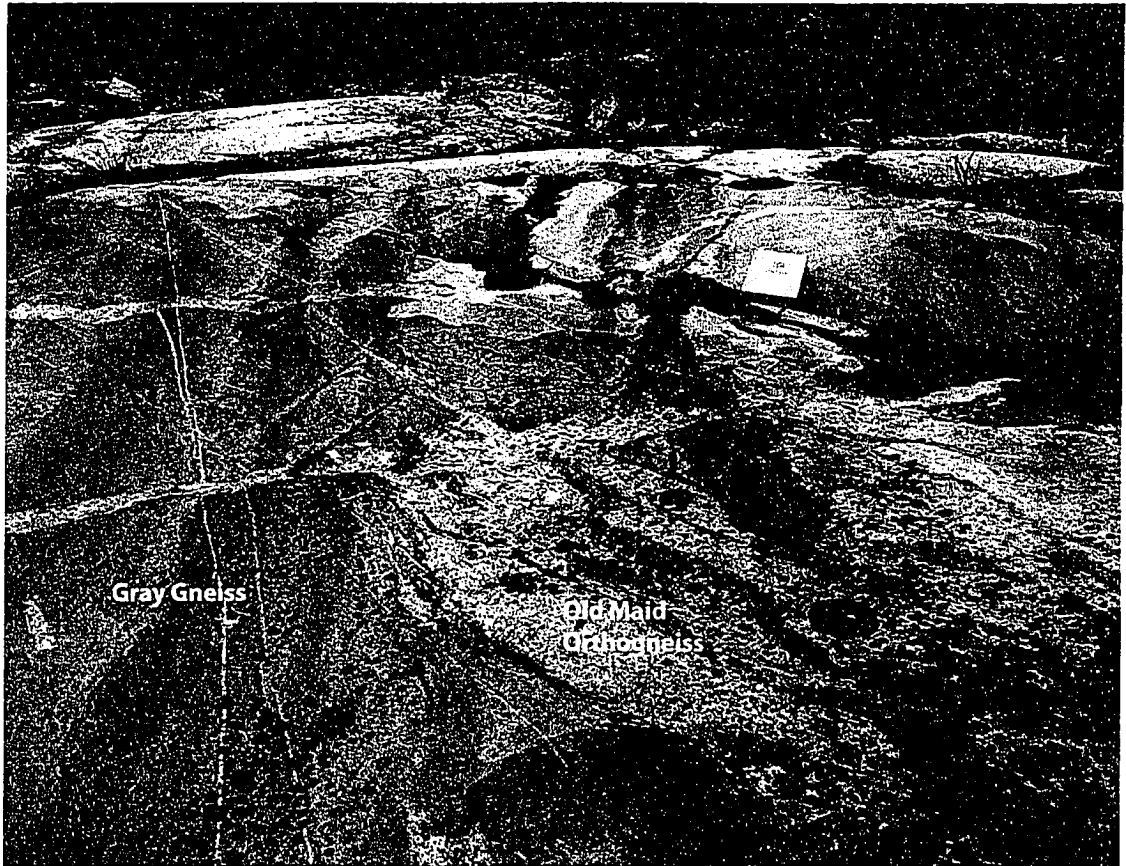


Fig. 9. Outcrop of Old Maid Orthogneiss and Gray Gneiss in which the two are mingled. Note the thin, leucocratic dikes, that cross-cut the Old Maid Orthogneiss. Notebook (18 cm long) for scale.

fabrics are dominantly solid-state.

The approximate modal mineralogy of the Old Maid Orthogneiss is biotite (10%), quartz (30%), plagioclase (40%), and potassium feldspar (20%). The rock is roughly equigranular and has subhedral to anhedral grains. In thin section, elongate biotite wraps around plagioclase. Quartz forms long blocky grains containing subgrains and having aspect ratios of $\sim 3:1$. Plagioclase is bent, has deformation twins, and commonly includes biotite. Potassium feldspar is large, blocky, and microfractured. These grains have plagioclase and biotite inclusions and are altered to sericite. Myrmekite is common. Recrystallized minerals in the Old Maid Orthogneiss are quartz, biotite, plagioclase, and potassium feldspar, indicating temperatures of ≥ 450 °C (Passchier and Trouw, 2005).

Cub Lake Orthogneiss

The Cub Lake Orthogneiss is a deformed, pink-colored granodioritic leucogneiss exposed in the northern part of the study area between the Ferry Peak Orthogneiss and Old Maid Orthogneiss (Fig. 3; Plate 1). Similar to most bodies in the SGC, the Cub Lake Orthogneiss strikes northwest. Xenoliths of plagioclase-quartz pegmatite, interpreted as part of the Old Maid Orthogneiss based on composition, are scattered throughout the Cub Lake Orthogneiss and range in size from centimeter to meter scale. The contact of the Cub Lake Orthogneiss with the Old Maid Orthogneiss to the east is covered, but is less than 30 m thick. Composite fabric in the Cub Lake Orthogneiss consists of a magmatic fabric overprinted by a moderate to weak solid-state fabric that is discernable in thin section. Foliation and lineation in the Cub Lake Orthogneiss are moderately developed and foliation is stronger than lineation ($S \geq L$) throughout.

The Cub Lake Orthogneiss is medium-grained and has a color index varying

between 15 and 20. The gneiss is composed of plagioclase (35%), quartz (30%), potassium feldspar (20%), and biotite (15%), \pm sillimanite. In thin section, plagioclase is weakly deformed and has bent grains, deformation twins, and lamellar twins. Relict oscillatory zoning indicates an igneous protolith. Small biotite inclusions are common. Elongate quartz grains have blocky subgrains and bulging grain boundaries, and show evidence for grain boundary migration recrystallization (serrated grain boundaries). Potassium feldspar is large and subhedral, and contains biotite and quartz inclusions. Microfractures and alteration to sericite are common. Biotite is tabular and weakly deformed. Sillimanite is present as deformed fibrolite mats and rare acicular grains, but the origin (igneous or metamorphic) of this mineral is not clear. However, there is no evidence that this fibrolite is the result of muscovite breakdown.

Gray Gneiss

The Gray Gneiss consists of a series of fine-grained, well-foliated and -lineated tonalitic sills and dikes of dark gray gneiss that are present throughout the SGC, but does not comprise a mappable unit. The Gray Gneiss intrudes the Ferry Peak Orthogneiss, Cub Lake Orthogneiss, Old Maid Orthogneiss, and Sunrise Lake pluton. Intrusions of the Gray Gneiss vary in thickness from 0.5 to 10.0 m and have sharp contacts with the host rock. These contacts are concordant to the northwest-striking foliation within the Gray Gneiss and are subparallel to the host-rock foliation. Small (≤ 40 cm long) xenoliths of host rocks are common near the sill margins (Fig. 10). Fabrics in the Gray Gneiss are dominantly solid-state and range from $S \geq L$ to $S \leq L$.

The Gray Gneiss is composed of plagioclase (50%), quartz (30%), and biotite (20%). Accessory minerals include allanite, sphene, zircon, and apatite. In thin



Fig. 10. Xenoliths of a Ferry Peak Orthogneiss in a dike of Gray Gneiss. Note the sharp, straight boundaries of xenoliths

section, the gneiss is distinguished by zoned plagioclase surrounded by highly deformed quartz. Quartz occurs as discrete lenses and displays core and mantle structure, subgrains, and sutured grain boundaries. Large plagioclase grains are subhedral and characterized by relict zoning, deformation twins, and lamellar twins. Most large plagioclases are microfractured, whereas small grains are euhedral and not fractured. Bent and elongate biotite wraps around more resistant plagioclase, and large biotite grains are commonly kinked.

Sunrise Lake Pluton

First described by McLean et al. (2006), the Sunrise Lake pluton is a young (49 Ma) tonalitic to dioritic body that crops out as an approximately 2-km-wide finger at the eastern edge of the study area (Fig. 3; Plate 1). Where studied for this project, the Sunrise Lake pluton is dominantly quartz diorite, but also contains tonalite. Mingling of Sunrise Lake pluton quartz diorite and tonalite is seen in some outcrops; enclaves of tonalite mix down to the grain scale with the more mafic Sunrise Lake rocks, producing several different rock types depending on the degree of mingling (Fig. 11). Xenoliths (10 cm-10 m) of Cascade River-Holden amphibolite are intruded by millimeter- to centimeter-thick sills similar in composition to the surrounding pluton. Foliation is dominantly magmatic within the pluton and has a weak solid-state overprint. Foliation and lineation are defined by aligned plagioclase, hornblende, and biotite.

In the study area, the Sunrise Lake pluton has a color index of ~45. Mafic minerals are dominantly hornblende and biotite. Felsic minerals include plagioclase (40%) and quartz (10%). Accessory phases are zircon and iron-titanium oxides. Plagioclase is generally subhedral and contains simple twins. Oscillatory zoning is apparent in most plagioclase grains. Aspect ratios of plagioclase are approximately

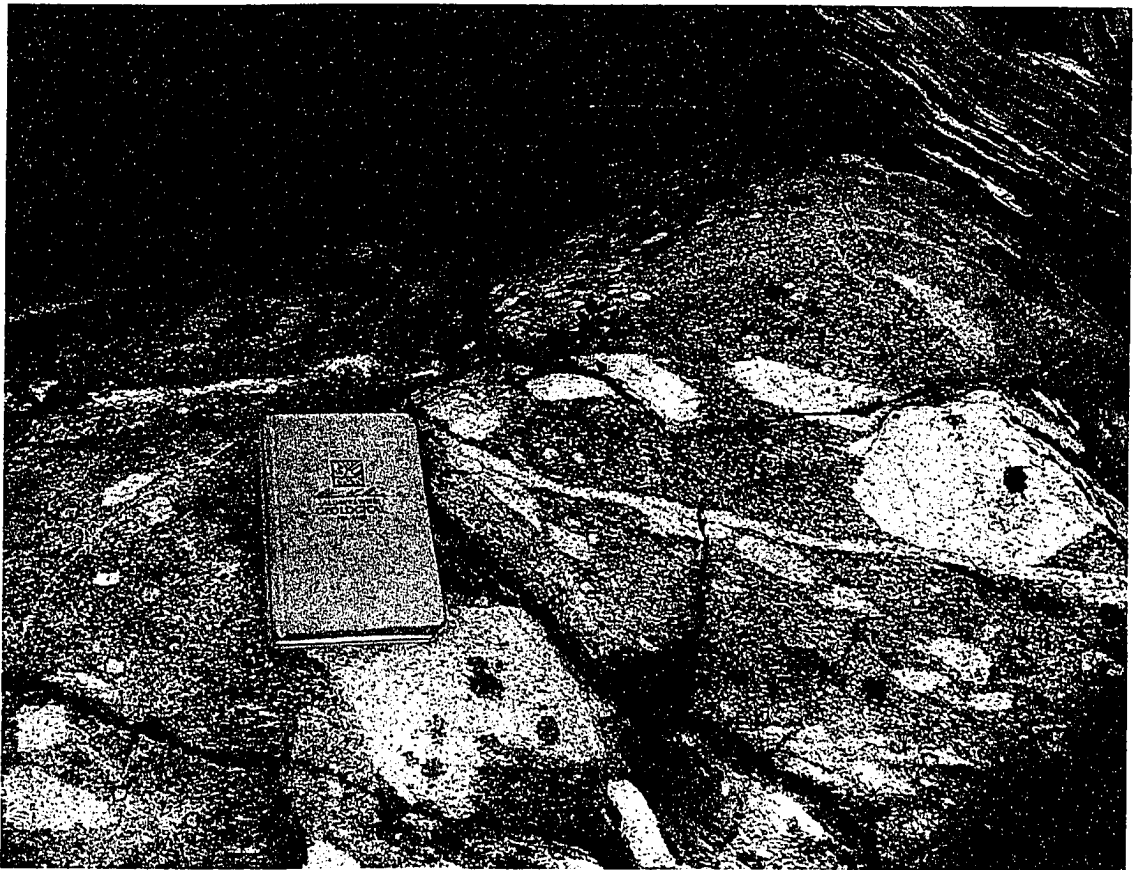


Fig. 11. Mingling of quartz diorite and leuco-tonalite in the Sunrise Lake pluton.

2:1. Quartz is anhedral, has rare subgrains, and occurs as disconnected lenses or pods. Biotite is tabular and subhedral, and is commonly intergrown with hornblende. Biotite also replaces hornblende along cleavage planes. Hornblende is recrystallized into mosaics. Many hornblende grains are cored by small augite grains.

Cooper Mountain Batholith

The Cooper Mountain batholith intrudes the southernmost part of the SGC in the study area. Unlike units in the SGC, the Cooper Mountain batholith does not strike northwest. The northwestern part of the batholith forms a pronounced protrusion in map view (Fig. 3; Plate 1). Contacts of the Cooper Mountain batholith with the Ferry Peak Orthogneiss are irregularly shaped, and many xenoliths of the gneiss occur in the margin of the batholith (Fig. 12). Xenoliths range in scale from 10 to 50 cm. The best exposure of the contact of the Cooper Mountain batholith is along the eastern shoreline of Lake Chelan, where the batholith intrudes heterogeneous gneisses and SGC migmatite and encloses abundant, 5- to 10-m-long xenoliths of the Cascade River-Holden assemblage. The contact between the batholith and heterogeneous gneisses/migmatite is sharp and marked by chilled margins in the batholith ranging up to several centimeters thick. Working towards the contact from the north, the heterogeneous gneisses/migmatite are increasingly intruded by “fingers” of granodiorite that eventually merge into the larger plutonic body. These fingers occur as meter-thick dikes ~3 km from the pluton and become progressively thicker with proximity to the batholith.

The Cooper Mountain batholith in the study area ranges from fine- to medium-grained and equigranular to porphyritic granodiorite. Modal mineralogy is plagioclase (30%), biotite (20%), potassium feldspar (30%), and quartz (20%). Plagioclase and potassium feldspar range from subhedral to euhedral. Plagioclase

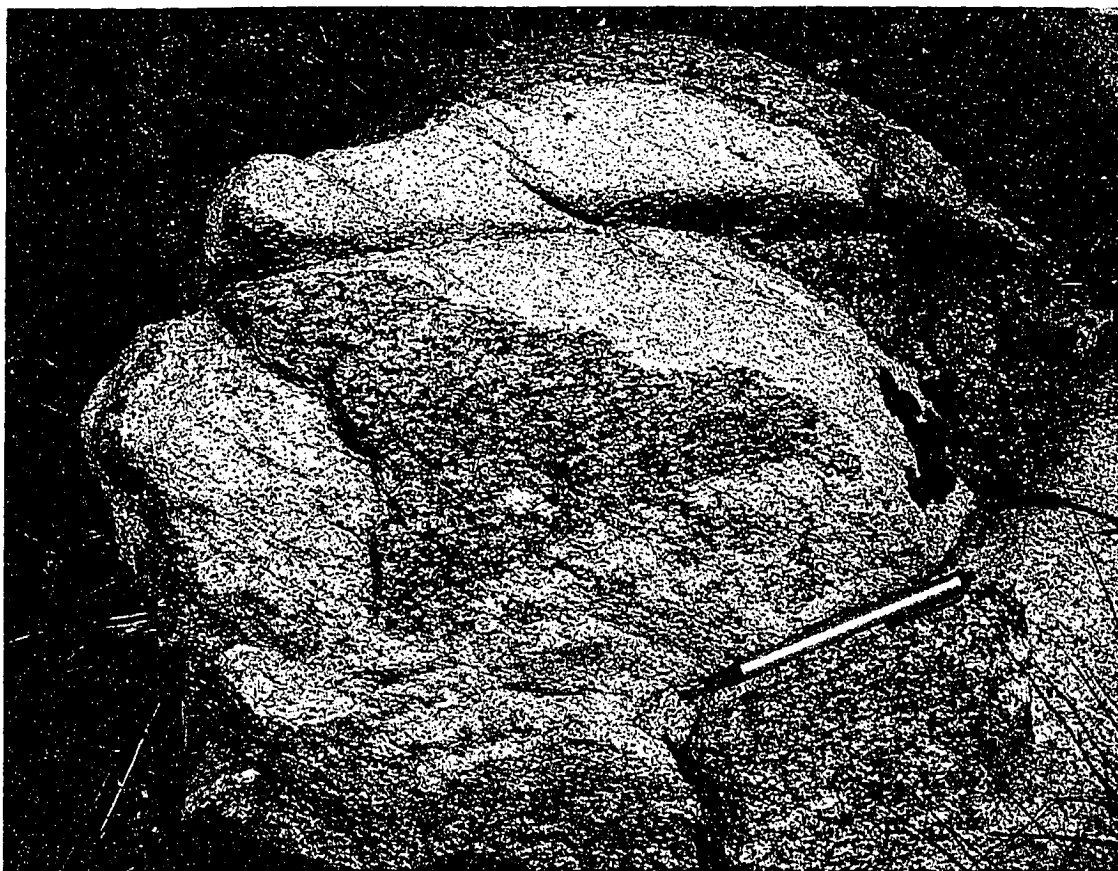


Fig. 12. Xenoliths of the Ferry Peak Orthogneiss in fine-grained equigranular Cooper Mountain batholith.

contains oscillatory zoning, and some grains are cored by aligned inclusions of biotite. Potassium feldspar is poikilitic and has inclusions of biotite, plagioclase, and quartz that are aligned parallel to zone boundaries. Minor perthite and myrmekite are also present. Quartz is anhedral and has rare subgrains, but no recrystallization. Magmatic foliation in the Cooper Mountain batholith is moderately to weakly developed and is defined by aligned biotite and plagioclase. Lineation is weak to absent. Quartz shows a very weak solid-state fabric.

Railroad Creek Pluton

The Railroad Creek pluton is a medium- to fine-grained, hypidiomorphic granodiorite-tonalite with a color index of 10-15. Within the field area, the pluton intrudes the Bearcat Ridge Orthogneiss and SGC migmatite to the south and Cascade River-Holden assemblage to the north. Both contacts are obscured by soil, but are interpreted as sharp due to an abrupt change in rock type over a distance of 50 m for the southern contact and 5 m for the northern one. A few xenoliths of Cascade River-Holden assemblage lie in the pluton close to the contact with the assemblage. In the study area, the pluton is tonalitic. Composition is plagioclase, quartz, biotite, and rare hornblende. The lack of potassium feldspar differentiates these outcrops from those described by Cater (1982), who studied a much larger part of the pluton. Subhedral plagioclase phenocrysts occur in some outcrops. Foliation and lineation are weak to absent except near pluton margins. Where present, fabrics are defined by aligned biotite, plagioclase, and hornblende.

Dikes Of Intermediate Composition

Throughout the map area, rock units are cut by late, one- to two-meter thick andesitic-basaltic dikes. These dikes generally have a fine-grained, equigranular

texture, but plagioclase-phyric dikes are also present. Plagioclase phenocrysts range from 0.5 to 2.0 cm in length. Dikes generally consist of pyroxene, plagioclase, and iron-titanium oxides. Host rock xenoliths, ranging in length from 1 to 30 cm, are common near dike margins (Fig. 13). Similar dikes can be found throughout the SGC and may be related to the Eocene dike swarms found to the south [e.g., Teanaway Dike swarm (Doran and Miller, 2006; Doran et al., 2007)]. These dikes cut the Bearcat Ride Orthogneiss and sub-units of the SGC, but were not observed in the Sunrise Lake pluton, Cooper Mountain batholith, or Railroad Creek pluton.



Fig. 13. Xenolith of leucocratic heterogeneous gneiss in mafic dike.

GEOCHRONOLOGY

No high-precision radiometric ages were available for rocks in the study area. To remedy this problem, zircons of varying sizes and shapes were obtained from four of the rock units described above: the Ferry Peak Orthogneiss (ES-32), Bearcat Ridge Orthogneiss (ES-19), Cooper Mountain batholith (BNC-326-1), and Gray Gneiss (ES-02) (Fig. 3). Isotopic dates were determined by single- and partial-grain zircon U-Pb isotope dilution thermal ionization mass spectrometry (ID-TIMS) at the MIT Geochronology Laboratory. Data are summarized in Table 1.

Grains chosen for analysis were extracted using standard crushing, Wilfley table, heavy liquid, and magnetic separation. Following extraction, a representative array of zircons was selected from each sample and processed according to the chemical abrasion techniques described in Mattinson (2005). Selected grains were annealed by heating for 60 hours at 900 °C. CL images of grains were taken using a JEOL JXA-733 electron microprobe. Grains for analysis were selected using these images; primary importance was placed on finding grains with oscillatory zoning, lack of an inherited core, and little or no metamorphic rim. Large grains were broken into smaller pieces.

Selected grains were then transferred to Teflon microcapsules, placed in a Parr vessel and leached in HF for 14 hours at 180 °C to remove radiation-damaged areas. The acid solution was removed, and fractions were rinsed in ultrapure H₂O and fluxed on a hotplate at ~80 °C for an hour each in concentrated HNO₃ and in 6 M HCl. The fractions were then ultrasonically cleaned for 5 minutes, then placed back on the hotplate for an additional 30 min. The HCl solution was removed and the zircon fractions were rinsed three times in ultrapure H₂O and placed in cleaned Teflon microcapsules. Fractions were spiked with a ²³³U-²³⁵U-²⁰⁵Pb tracer (ET535)

with 29 M HF and 30% HNO₃. These capsules were placed in Parr vessels at ~210 °C for 48 hours. After this 48 hour period, samples were dried to fluorides. Samples were then re-dissolved in 6 M HCl for 12 h at 180 °C. U and Pb were isolated using HCl-based, single-column, anion exchange chemistry (Krogh, 1973) and loaded together in a silica gel-H₃PO₄ emitter solution onto Re filaments.

U and Pb isotopic measurements were performed on the MIT VG Sector-54 multicollector thermal-ionization mass spectrometer. Pb was measured by peak-hopping on the Daly detector. U was measured using static Faraday detectors.

Table 1. U-Pb isotopic data from zircon in the southern Skagit Gneiss Complex

Fractions	Date (Ma)				Composition				Isotopic Ratios				corr. coeff.				
	$^{206}\text{Pb}/^{238}\text{U}^a$	$\pm 2\sigma$ abs.	$^{207}\text{Pb}/^{235}\text{U}^a$	$\pm 2\sigma$ abs.	$^{207}\text{Pb}/^{206}\text{Pb}^a$	$\pm 2\sigma$ abs.	Pb _c (pg) ^b	Dis. % ^c	Th/U	Pb ^d / _c	$^{206}\text{Pb}/^{238}\text{U}^c$	%error $\pm 2\sigma$ ^f		$^{207}\text{Pb}/^{235}\text{U}^c$	%error $\pm 2\sigma$ ^f	$^{207}\text{Pb}/^{206}\text{Pb}^c$	%error $\pm 2\sigma$ ^f
BNCS26-1																	
zM11	47.878	0.036	48.010	0.242	54.607	13.852	0.27	12	0.135	15.2	0.00745	0.07629	0.04842	0.51522	0.04711	0.49479	0.33649
zM4	63.178	0.035	64.501	0.137	113.899	31.438	0.34	45	0.134	31.1	0.00985	0.05520	0.06558	0.21907	0.04830	0.20925	0.30925
zL3a	62.139	0.064	62.305	0.571	68.732	31.471	0.28	10	0.079	7.5	0.00969	0.10419	0.06328	0.94544	0.04739	0.80667	0.48710
zL3b	60.317	0.094	60.268	1.110	58.308	53.505	0.29	-3	0.084	7.0	0.00940	0.15665	0.06115	1.89783	0.04718	1.79310	0.69135
zM13	47.947	0.028	48.139	0.143	57.704	8.533	0.30	17	0.216	24.6	0.00747	0.05883	0.04855	0.30472	0.04717	0.28886	0.35905
zL2b	47.972	0.033	47.927	0.261	45.685	12.433	0.44	-5	0.068	13.9	0.00747	0.06910	0.04833	0.55816	0.04693	0.52851	0.47949
zM6	53.186	0.036	53.456	0.119	64.653	6.968	0.55	18	0.177	34.6	0.00828	0.06722	0.05404	0.22803	0.04730	0.21125	0.38786
ES-19																	
zL1b	73.415	0.038	73.493	0.063	76.091	2.746	0.33	4	0.041	210.4	0.01141	0.05141	0.07505	0.08826	0.04753	0.07114	0.59195
zM16	77.701	0.053	77.817	0.300	81.421	15.808	0.40	5	0.183	24.7	0.01213	0.06874	0.07965	0.40088	0.04764	0.38368	0.33047
zM18	88.078	0.058	88.267	0.271	93.355	14.249	0.29	6	0.244	20.9	0.01376	0.06656	0.09082	0.32022	0.04788	0.30339	0.35014
zM19	68.531	0.033	68.732	0.093	75.717	4.977	0.33	10	0.103	79.3	0.01069	0.04840	0.07003	0.13955	0.04753	0.12954	0.37281
zM5	68.606	0.073	68.871	0.516	78.124	29.277	0.39	12	0.163	10.9	0.01070	0.10630	0.07018	0.77470	0.04757	0.73939	0.39313
zL1a	74.476	0.036	74.591	0.067	78.285	3.120	0.30	5	0.033	178.6	0.01162	0.04906	0.07623	0.09320	0.04758	0.07863	0.53700
zL1c	74.390	0.039	74.478	0.155	77.297	8.063	0.49	4	0.036	64.9	0.01161	0.05299	0.07611	0.21572	0.04756	0.20572	0.30728
ES-32																	
zM8	75.288	0.039	75.408	0.119	79.230	6.061	0.35	5	0.178	61.9	0.01175	0.05253	0.07709	0.16361	0.04760	0.15102	0.39091
zM2	84.713	0.068	85.019	0.413	93.657	22.883	0.24	10	0.363	14.7	0.01323	0.08024	0.08734	0.50693	0.04789	0.48574	0.33769
zM9	77.538	0.045	77.641	0.185	80.833	9.519	0.53	4	0.246	23.8	0.01210	0.05868	0.07946	0.24799	0.04763	0.23266	0.37147
zS13a	76.869	0.066	76.712	0.581	71.805	27.216	0.55	-7	0.213	7.7	0.01200	0.08653	0.07848	0.78658	0.04745	0.74553	0.51698
zM4	76.501	0.039	76.439	0.132	74.514	6.334	0.35	-3	0.215	82.5	0.01194	0.05095	0.07819	0.17894	0.04750	0.16742	0.36123
zM6	76.032	0.039	76.138	0.136	79.478	7.082	0.22	4	0.230	66.2	0.01186	0.05099	0.07787	0.18520	0.04760	0.17594	0.31480
zM7	77.016	0.040	76.904	0.142	73.460	6.768	0.40	-5	0.217	60.1	0.01202	0.05284	0.07868	0.19186	0.04748	0.18137	0.33086
ES-02																	
zM1	60.241	0.051	60.544	0.312	72.508	18.590	0.30	17	0.371	13.7	0.00939	0.08406	0.06144	0.53160	0.04746	0.50447	0.39113
zS15	77.051	0.065	77.277	0.522	83.970	28.319	0.93	8	0.184	7.5	0.01203	0.08488	0.07908	0.70174	0.04769	0.66732	0.45609
zM7	83.480	0.056	83.311	0.199	78.242	9.285	0.32	-7	0.370	33.8	0.01304	0.06711	0.08551	0.24864	0.04758	0.23415	0.34451
zS10	47.935	0.075	48.123	0.587	57.529	35.287	0.43	17	0.372	3.4	0.00746	0.15747	0.04853	1.24799	0.04716	1.19813	0.37343
zS7	47.764	0.064	47.750	0.791	47.072	39.128	0.50	-1	0.415	3.1	0.00744	0.13396	0.04815	1.69595	0.04696	1.61542	0.62637

^aCalculations are based on the decay constants of Jaffey et al. (1971).

^bTotal weight of common Pb (including ^{208}Pb).

^c% discordance = $100 \times (^{206}\text{Pb}/^{238}\text{U} \text{ date} - ^{207}\text{Pb}/^{206}\text{Pb} \text{ date})$.

^dRatio of radiogenic Pb (including ^{208}Pb) to common Pb. All common Pb is assumed to be laboratory blank.

^eCorrected for fractionation, spike, and laboratory blank.

^fErrors propagated using the algorithms of Schmitz and Schoene (2007).

Ferry Peak Orthogneiss (ES-32)

Sample ES-32 was collected from an area of deformed Ferry Peak Orthogneiss on a ridge west of Ferry Peak (Fig. 3). Field relationships indicate that the gneiss is one of the oldest rocks in the study area (described above). The sample is a medium- to coarse-grained tonalite leucogneiss and has elongate biotite stringers typical of the orthogneiss. Thin section analysis found zircons in biotite, plagioclase, and less commonly quartz.

Zircons from the Ferry Peak Orthogneiss are euhedral, colorless, clear, and have aspect ratios of 5:2. Zircons commonly contained oscillatory zoning, and many contained inherited cores with significant overgrowths. Seven zircon fractions gave ages that range from 84 Ma to 75 Ma. The youngest date (75.2 Ma) is likely the crystallization age of the orthogneiss. However, the crystallization age of the orthogneiss is taken as ~ 76 Ma due to the broad spread of dates centered around 76 Ma (Figs. 14 and 15). The span of dates suggest inheritance of older zircons, since chemical abrasion likely removed the parts of zircon that experienced Pb-loss.

Bearcat Ridge Orthogneiss (ES-19)

Sample ES-19 was collected approximately 1000 m above the western shore of Lake Chelan (Fig. 3). The sample was collected from a ≥ 2 m thick sheet of fine-grained biotite-tonalite leucogneiss that intruded rocks of the Cascade River-Holden assemblage. Zircons are chiefly found in plagioclase, but also in biotite and quartz.

Zircons in the Bearcat Ridge Orthogneiss are euhedral, colorless, clear, and have aspect ratios of 5:2. Obvious cores with oscillatory-zoned overgrowths are common. Seven grains from the Bearcat Ridge Orthogneiss were analyzed. These

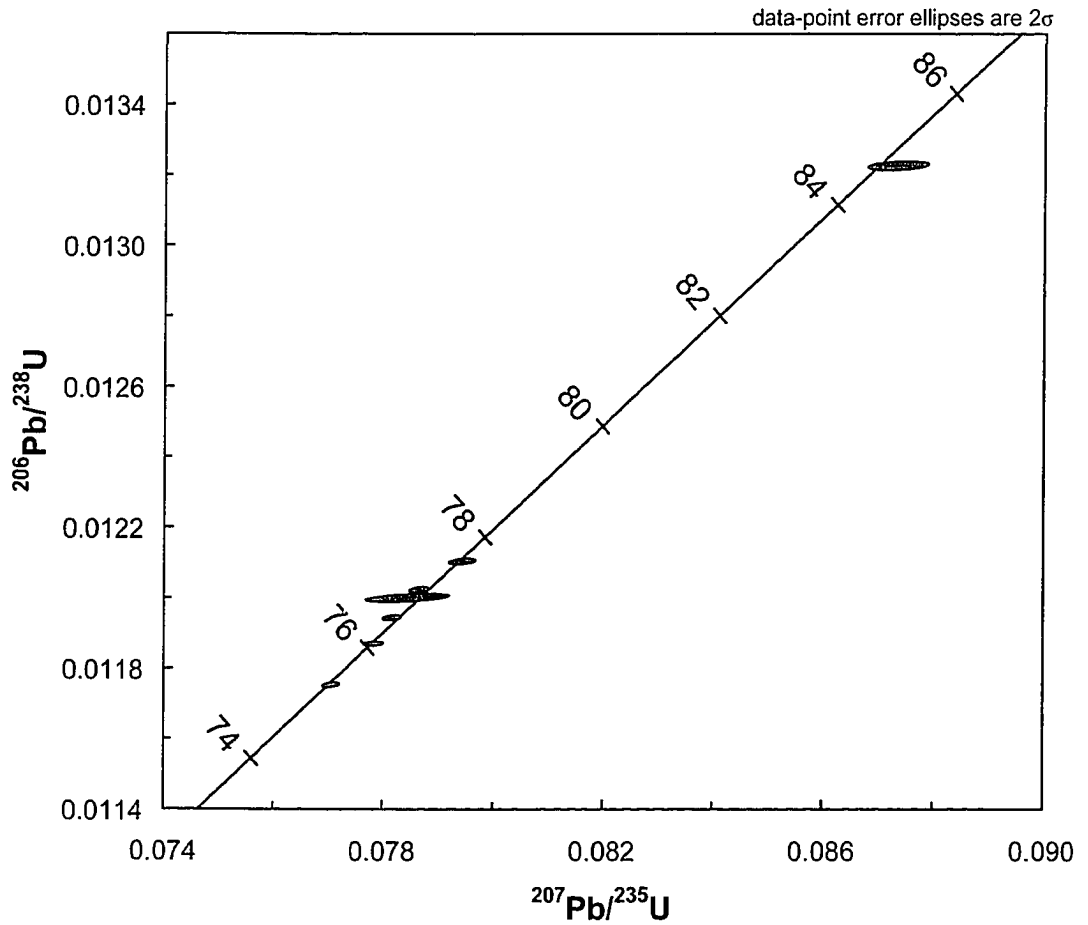


Fig. 14. Concordia plot of all analyzed zircons from the Ferry Peak Orthogneiss (ES-32).

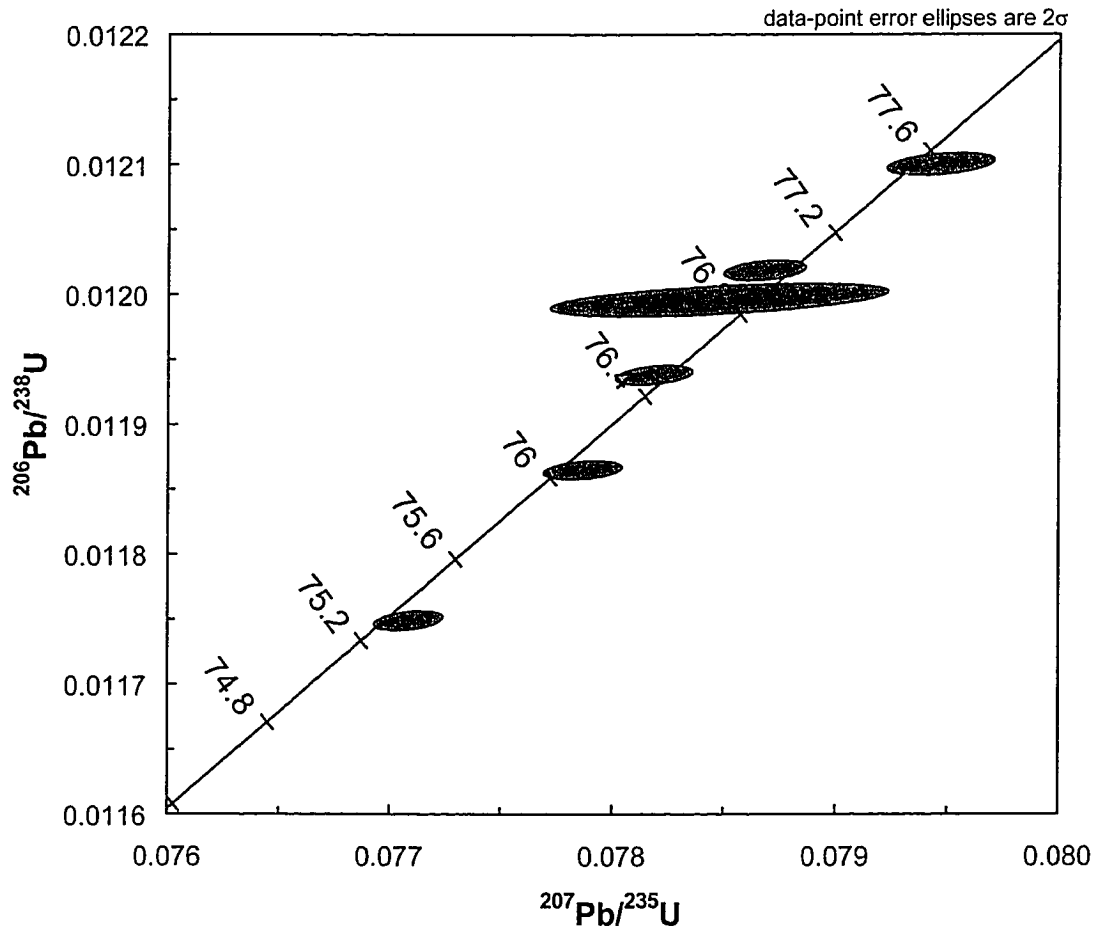


Fig. 15. Magnified concordia plot of analyzed zircons from the Ferry Peak Orthogneiss (ES-32). Plot is focused on zircons near the inferred crystallization age.

zircons gave ages that ranged from 88 Ma to 68 Ma (Fig. 16). All of the fractions were concordant to slightly discordant within 2σ uncertainty. Two fractions gave ages of approximately 68 Ma, which is interpreted as the crystallization age of the tonalite protolith. Given the textural observations noted above, the older fractions are likely to contain inherited zircon.

Gray Gneiss (ES-02)

Sample ES-02 was collected ~50 m from the Prince Creek Campground along the eastern shore of Lake Chelan (Fig. 3). The outcrop contained several xenoliths of banded gneiss that are associated with the heterogeneous gneiss found along Lake Chelan. The sample included part of a late-forming leucocratic veinlet that was cut off using a rock saw prior to crushing. The sample is a fine-grained, biotite-tonalite with minor granophyric texture. Zircons in thin section are distributed in biotite, plagioclase, and less commonly quartz.

Zircons from the Gray Gneiss are subhedral to euhedral, colorless, and clear. Many grains contained obvious cores with oscillatory-zoned overgrowths. Average zircon aspect ratio was 5:2, but wider, more rounded grains were also present (aspect ratio 3:2). Six fractions were analyzed and ages ranged from 83 Ma to 47 Ma (Fig. 17). All of the fractions gave ages that were concordant or slightly discordant. Two distinct populations can be distinguished; one at ~62-60 Ma and another at ~47 Ma (Fig. 18). It is possible that some of the leucocratic veinlet was analyzed along with the gray gneiss, giving the two age populations. Further zircon analysis of the veinlet is pending.

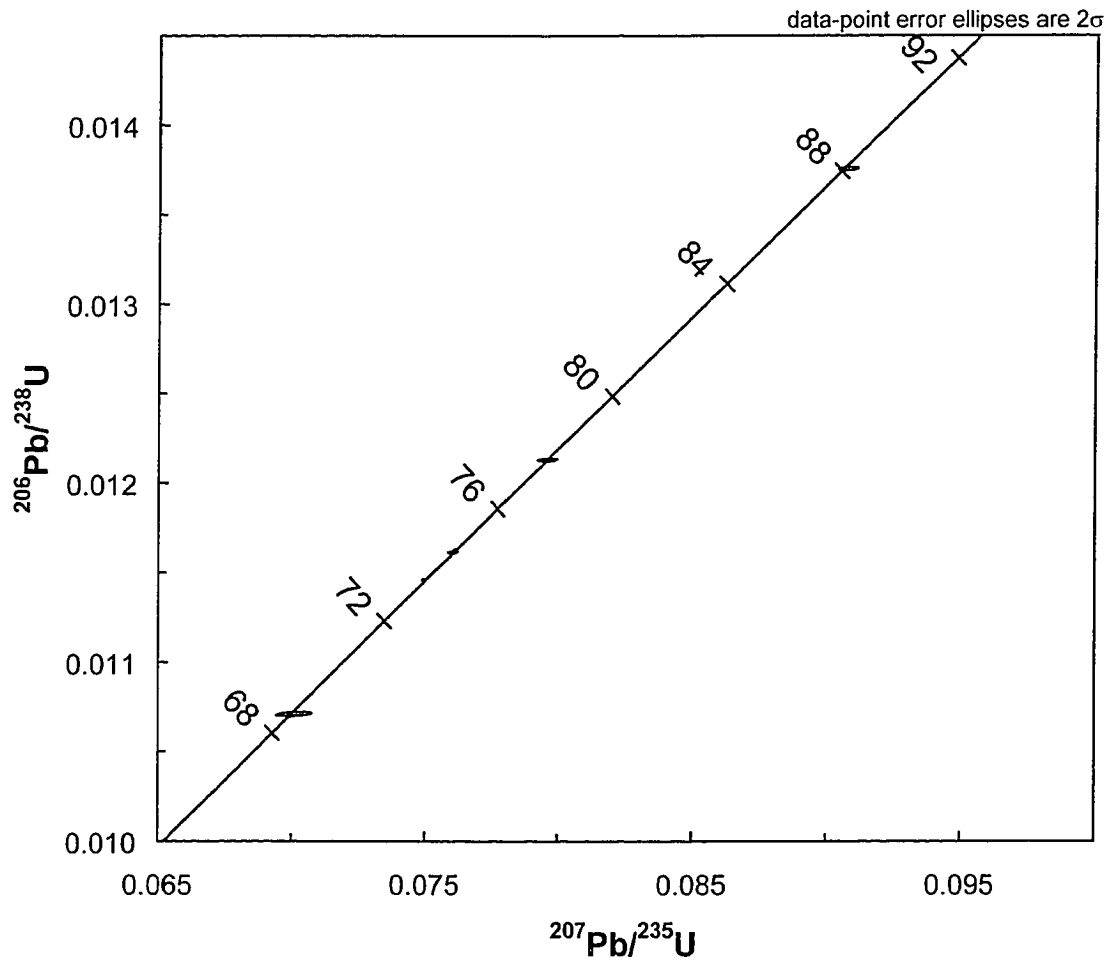


Fig. 16. Concordia plot for zircons from the Bearcat Ridge Orthogneiss (ES-19).

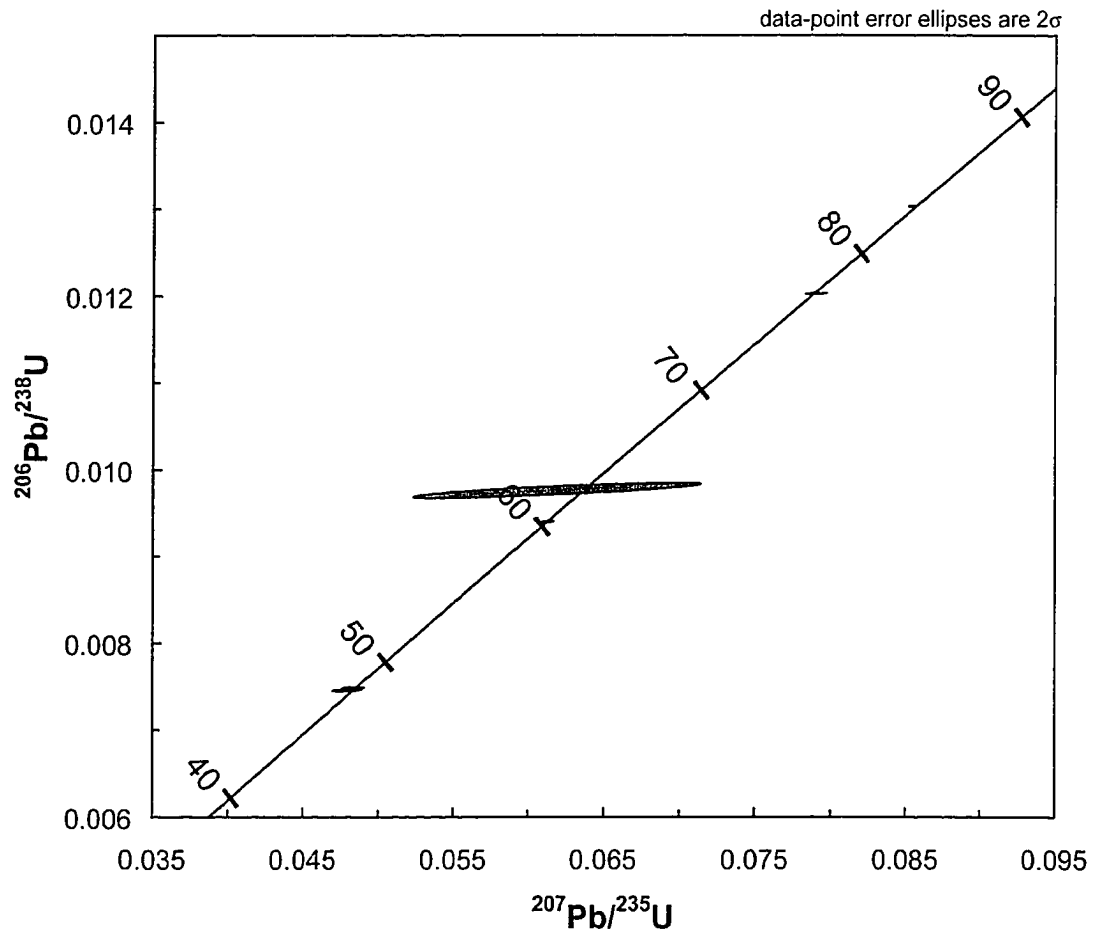


Fig. 17. Concordia plot of all analyzed zircons from the Gray Gneiss (ES-02).

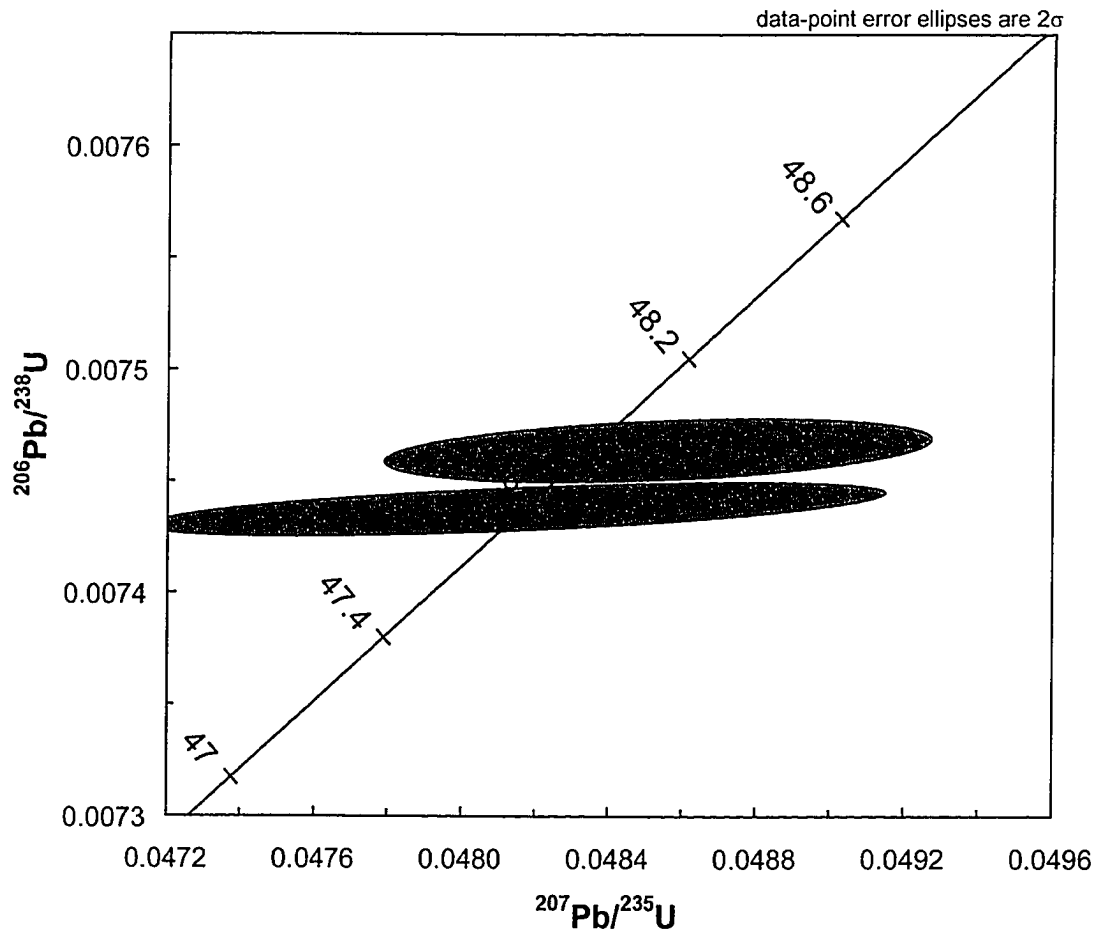


Fig. 18. Magnified concordia plot of the Gray Gneiss (ES-02). Plot is focused on the youngest zircon ages.

Cooper Mountain Batholith (BNC-326-1)

Sample NC-326-1 was collected by R.B. Miller and E. Shea along a ridge of Uno Peak ~800 m from the contact with the Ferry Peak Orthogneiss (Fig. 3). Xenoliths of the gneiss are seen in the Cooper Mountain batholith near the contact, but were not present at this outcrop. The sample is a medium-grained granodiorite. Zircons are present as inclusions in biotite and plagioclase.

Zircons from the sample are euhedral, colorless, and clear. Inherited cores with overgrowths were present in most grains. Aspect ratios were generally 5:2, but more elongate and rounder grains were also observed. Seven zircon fractions were analyzed and ages ranged from 63 Ma to 47.8 Ma (Fig. 19). Most fractions gave concordant to slightly discordant ages that are within 2σ uncertainty. Three fractions gave ages of approximately 47.9 Ma, which are interpreted as the final crystallization age of the pluton (Figs. 19 and 20). Other ages likely reflect inheritance of older zircon grains.

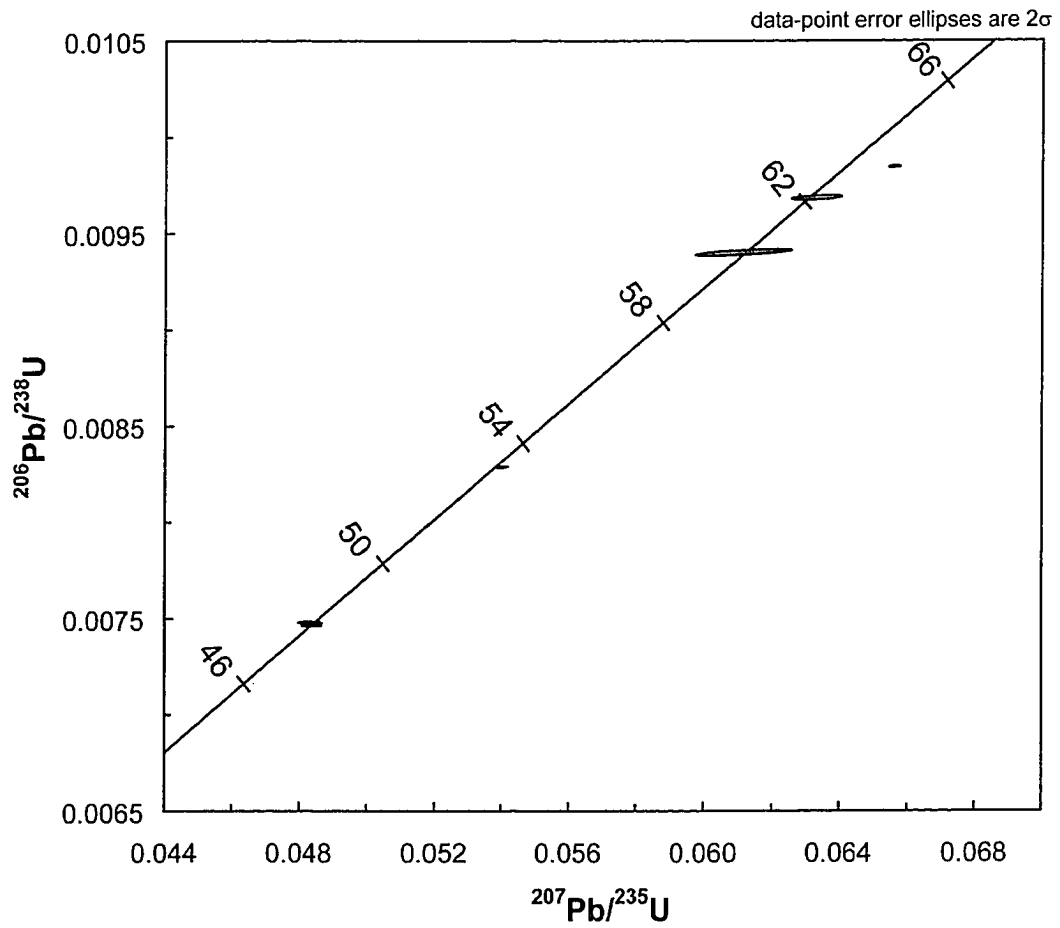


Fig. 19. Concordia plot for all analyzed zircons from the Cooper Mountain batholith (BNC-326-1).

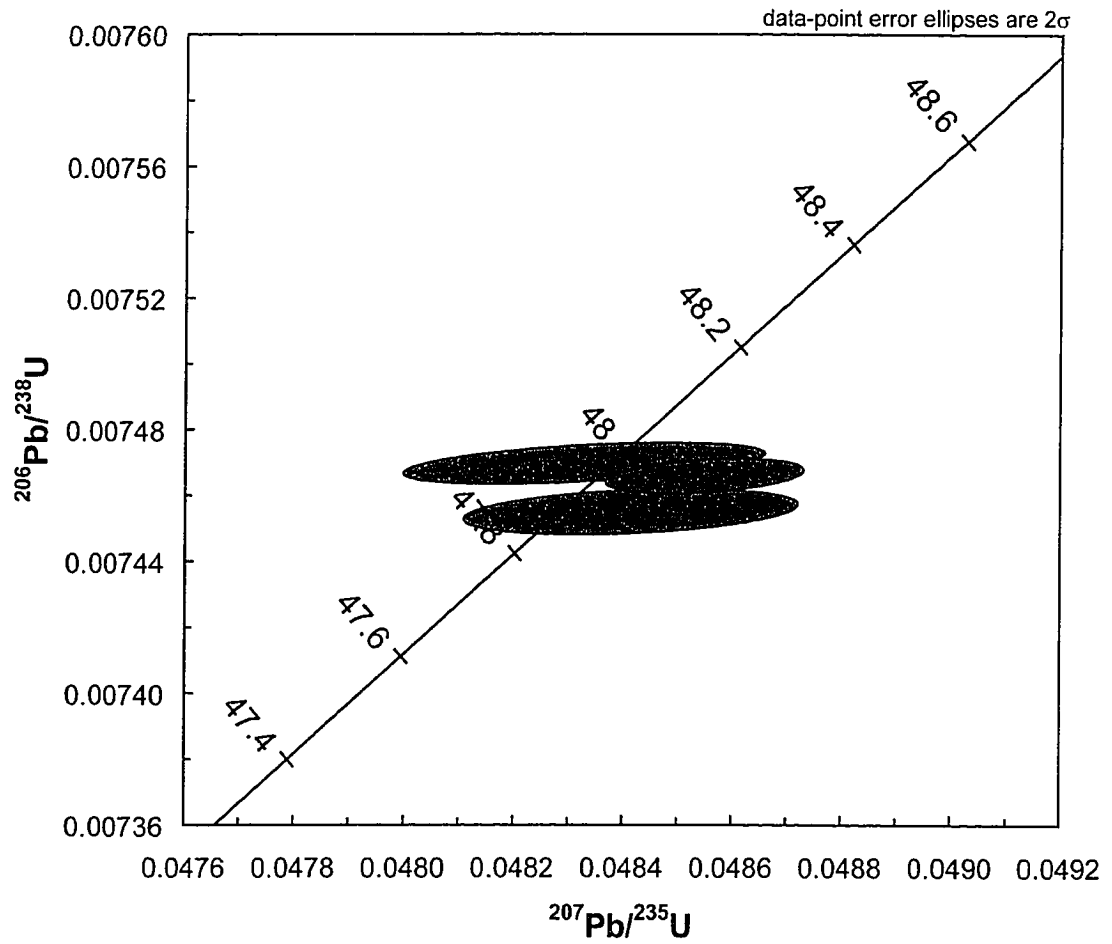


Fig. 20. Magnified concordia plot for zircons from the Cooper Mountain batholith (BNC-326-1). Plot is focused on zircons near the inferred crystallization age.

METAMORPHISM

The temperature and pressure of metamorphism in the study area can be broadly constrained by mineral assemblages and deformation mechanisms present in rocks of the SGC, Bearcat Ridge Orthogneiss, and Cascade-River Holden assemblage. Overall, assemblages indicate amphibolite-facies metamorphism. Specifically, recrystallized hornblende and plagioclase in amphibolites, recrystallized calc-silicate minerals in the Cascade River-Holden assemblage, and sillimanite mats in samples of the Ferry Peak Orthogneiss may indicate high-temperature conditions. Within the Ferry Peak Orthogneiss, the sillimanite-bearing rocks are in close proximity to garnet-hornblende-bearing rocks. Some samples of the Bearcat Ridge Orthogneiss contain biotite-muscovite-garnet assemblages. Cascade River-Holden assemblage rocks vary from garnet-bearing biotite schist to amphibolite. Using the garnet-hornblende-plagioclase assemblage in the Ferry Peak Orthogneiss, minimum temperature is estimated at ~ 500 °C.

STRUCTURE

This chapter describes the foliations, lineations, kinematic indicators, folds, and dike orientations observed and measured during seven weeks of field work. Orientations are expressed using the “right-hand rule.” Structural analysis was performed at a total of 267 stations. Oriented hand samples were collected throughout the field area; preference was given to the rocks of the SGC. Microstructural analysis was conducted on thin sections cut from 60 of these samples.

The southern SGC shows evidence for a complex history of deformation, including multiple phases of folding and non-coaxial shear. Map-scale folding is seen throughout the SGC and is particularly well-developed in the Cascade River-Holden assemblage and Ferry Peak Orthogneiss. However, outcrop-scale folds are absent in much of the complex. Non-coaxial deformation is subdivided into high-temperature and low-temperature deformation based on the relative temperatures inferred from microstructures.

Foliation

Foliation in the SGC and adjacent units is dominantly northwest-striking and moderately to gently dipping (Figs. 21 and 22; Plate 1). In general, rocks west of Lake Chelan dip southwest and rocks east of Lake Chelan dip northeast (Fig. 21; Plate 1). However, dip reversals in both areas are common. In both regions, foliation is generally stronger than lineation ($S \geq L$).

Solid-state foliation, seen in rocks older than 49 Ma, is defined by alignment of biotite, plagioclase, and quartz. Foliation is also defined by compositional layering in the Cascade River-Holden assemblage, rare layered gneiss, and banded

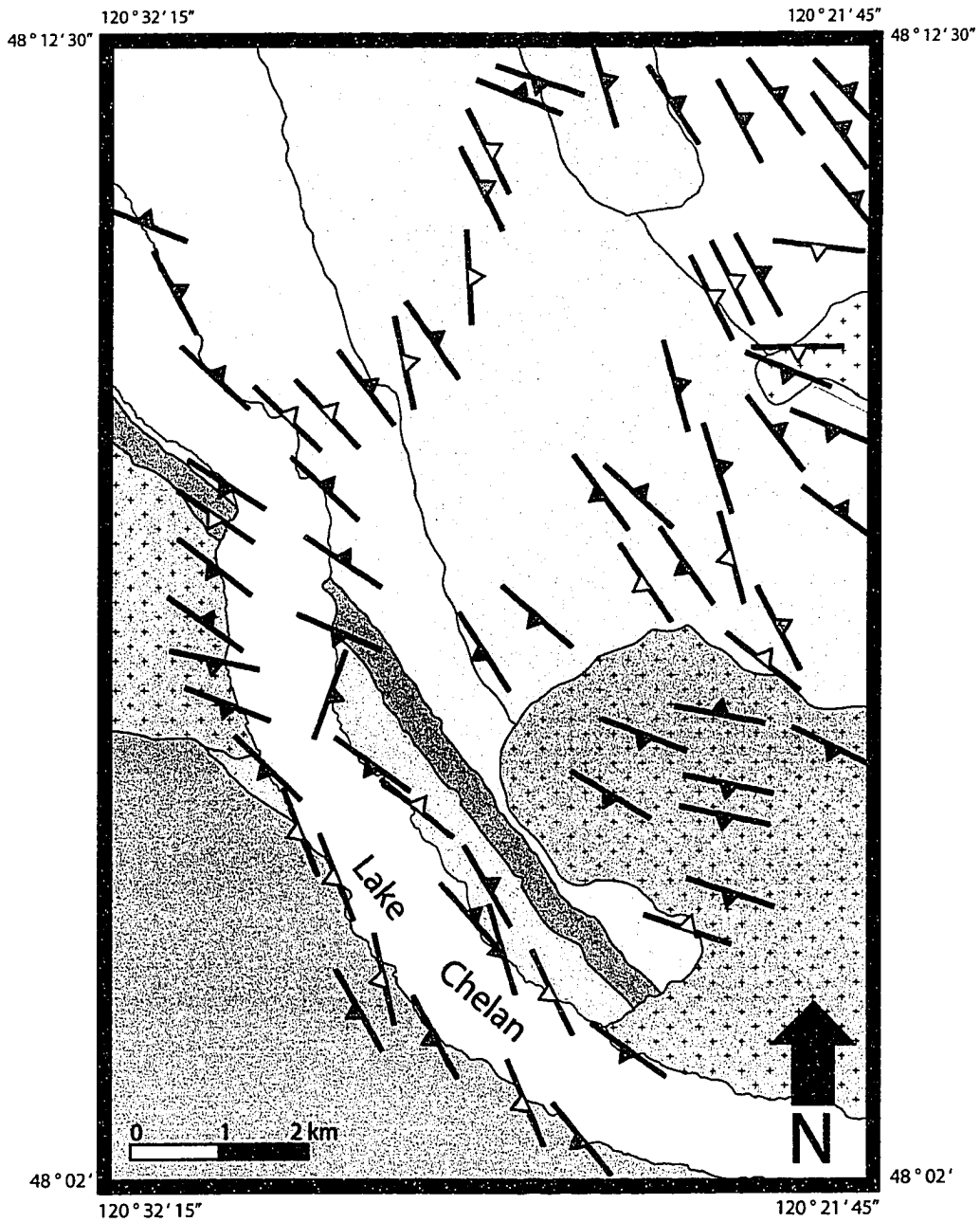


Fig. 21. Simplified map of foliations in the southern Skagit Gneiss Complex and adjacent units. Units with a “+” pattern have magmatic fabric. Color-coding of foliation dip: green, 0-30°, yellow, 31-60°, red from 61-90°.

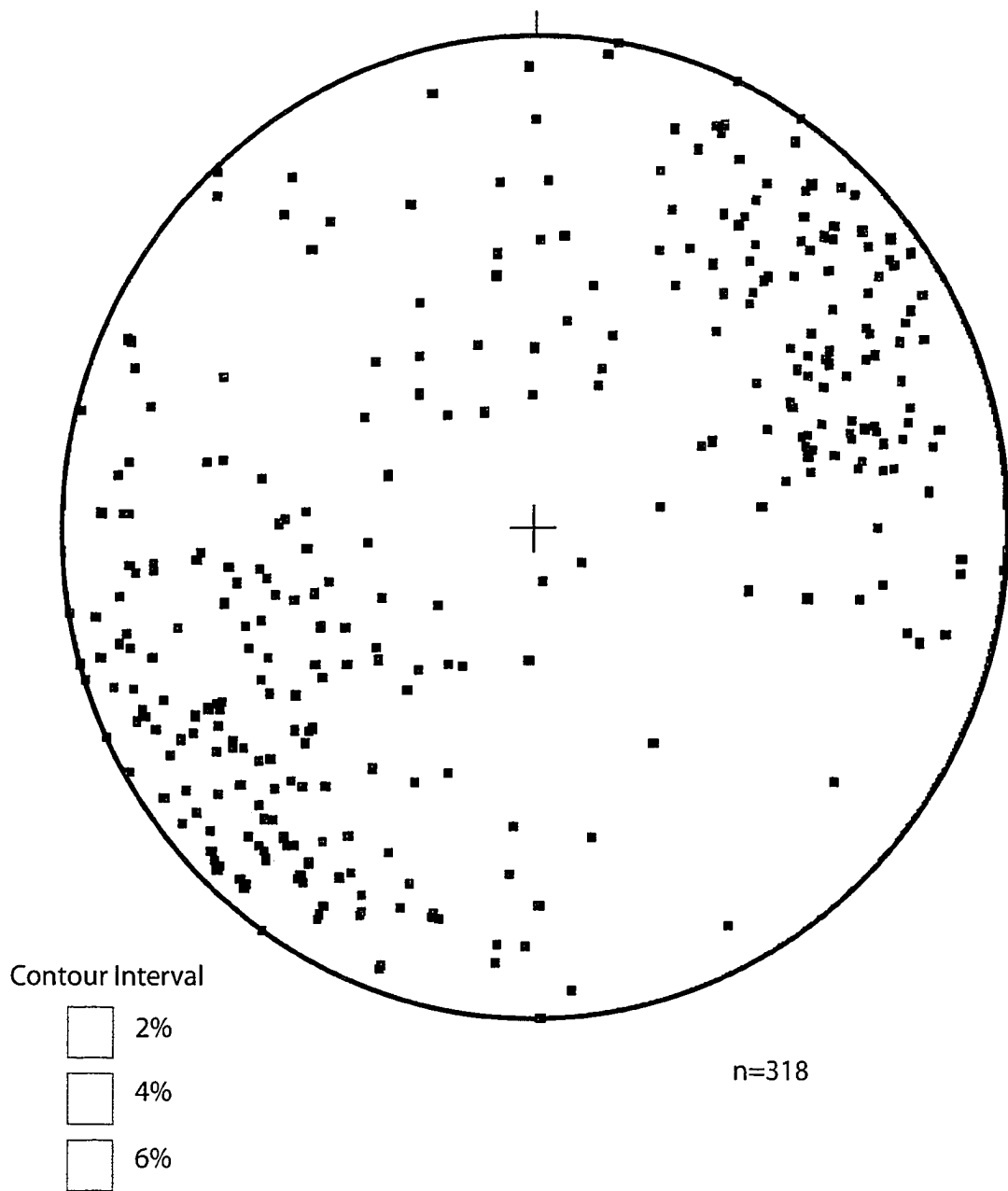


Fig. 22. Lower hemisphere stereographic projection of poles to solid-state foliations in the study area.

migmatite. Foliation intensity across the SGC is moderate, with local areas of intense deformation marked by mylonites.

At a microscopic scale, solid-state foliation in orthogneisses is defined by elongate quartz grains, aggregates of quartz grains, and elongate biotite and plagioclase. Quartz deformation mechanisms include dislocation glide and dislocation creep. Evidence for recovery in quartz includes subgrain rotation recrystallization and recrystallization into mosaics. Plagioclase deformation includes mechanical twinning, brittle fracturing, and dislocation glide. Recrystallization of plagioclase into mosaics is common. Quartz-plagioclase intergrowths can be seen in many plagioclase grains. Biotite grains are tabular, are commonly bent or kinked, and rarely deformed into “fish,” indicating dislocation glide. Brittle fracturing in potassium feldspar is evidenced by microfractures.

A weak, northwest-striking, northeast- or southwest-dipping magmatic foliation is evident in the Railroad Creek pluton, Cooper Mountain batholith, and Sunrise Lake pluton (Fig. 23; Plate 1). These foliations are defined by aligned subhedral to euhedral igneous biotite, plagioclase, and potassium feldspar grains. A minor solid-state overprint is present in the Sunrise Lake pluton and in some samples of the Cooper Mountain batholith, but is absent in the Railroad Creek pluton. This overprint is marked by weakly elongate quartz and evidence for dislocation glide (undulose extinction, elongate grains).

Lineation

Lineations in the SGC, Bearcat Ridge Orthogneiss, and Cascade River-Holden assemblage are broadly southeast-trending and have plunges that range from moderate to gentle (Figs. 24 and 25; Plate 1). Mineral lineations are most commonly defined by elongate biotite, quartz, and quartz aggregates. Alignment of

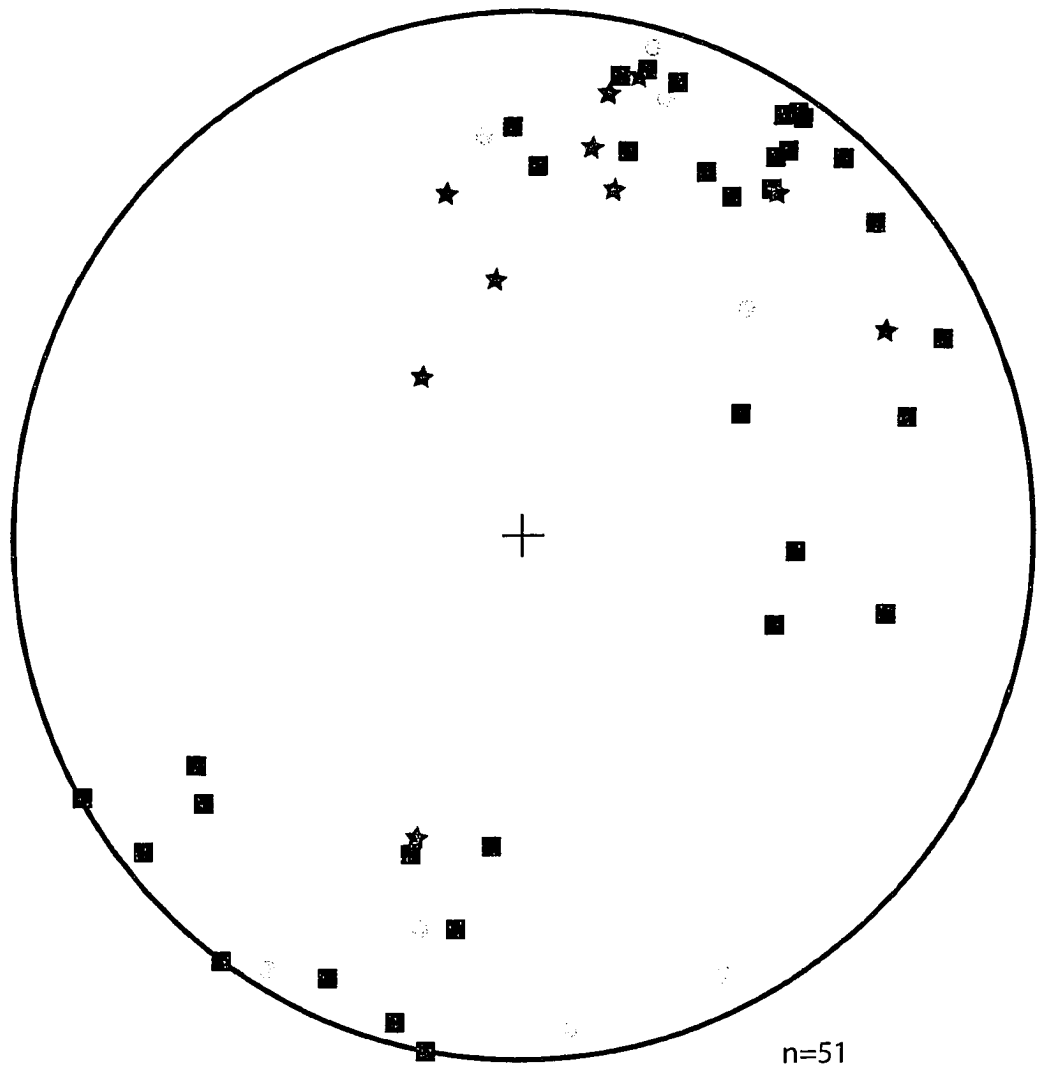


Fig. 23. Lower hemisphere stereographic projection of poles to magmatic foliations in the study area. Red stars = Sunrise Lake pluton, blue squares = Cooper Mountain batholith, green circles = Railroad Creek pluton.

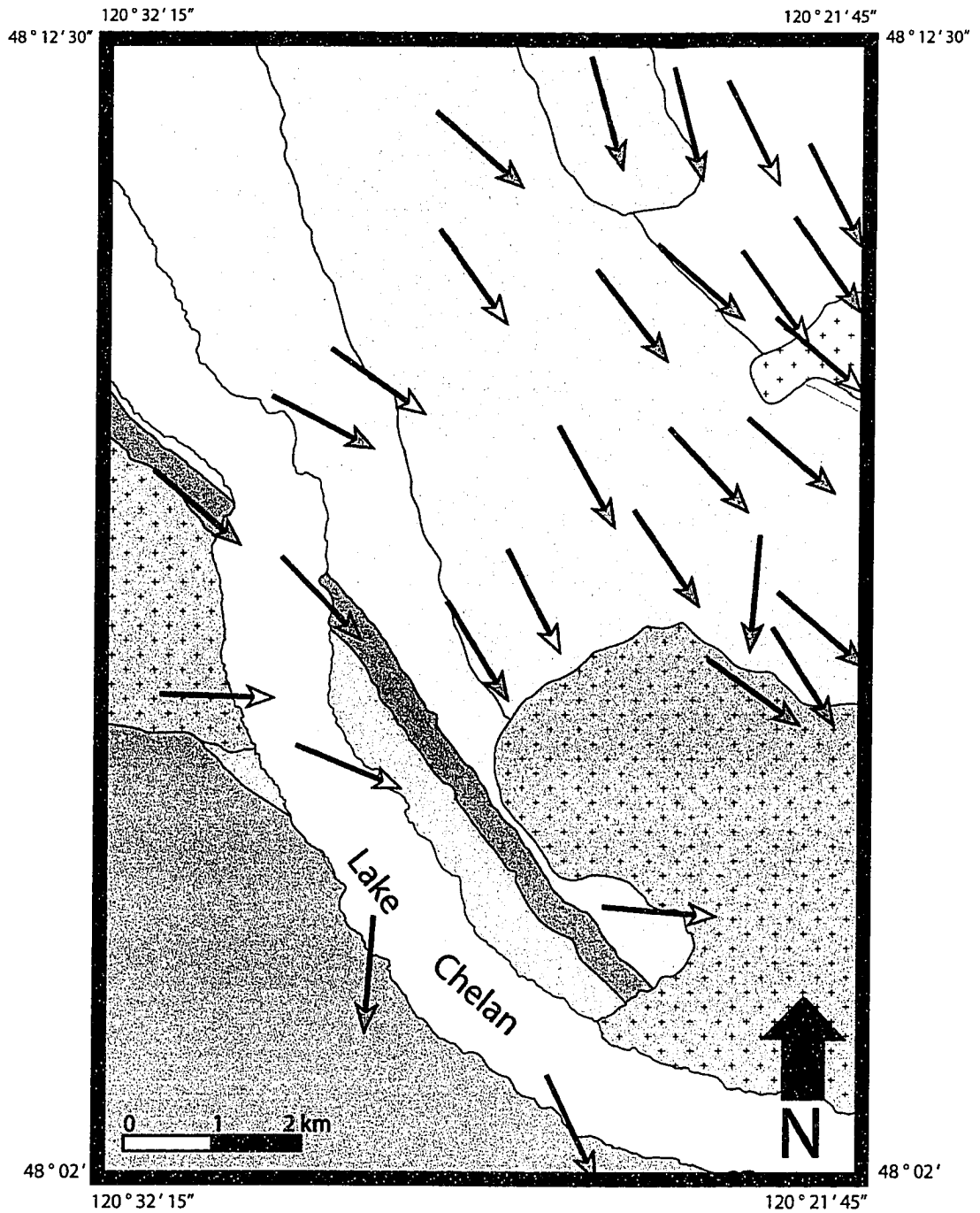


Fig. 24. Simplified map of lineations in the southern Skagit Gneiss Complex and adjacent units. Units with a "+" pattern have magmatic fabric. Color-coding of lineation plunge: green, 0-30°, yellow, 31-60°.

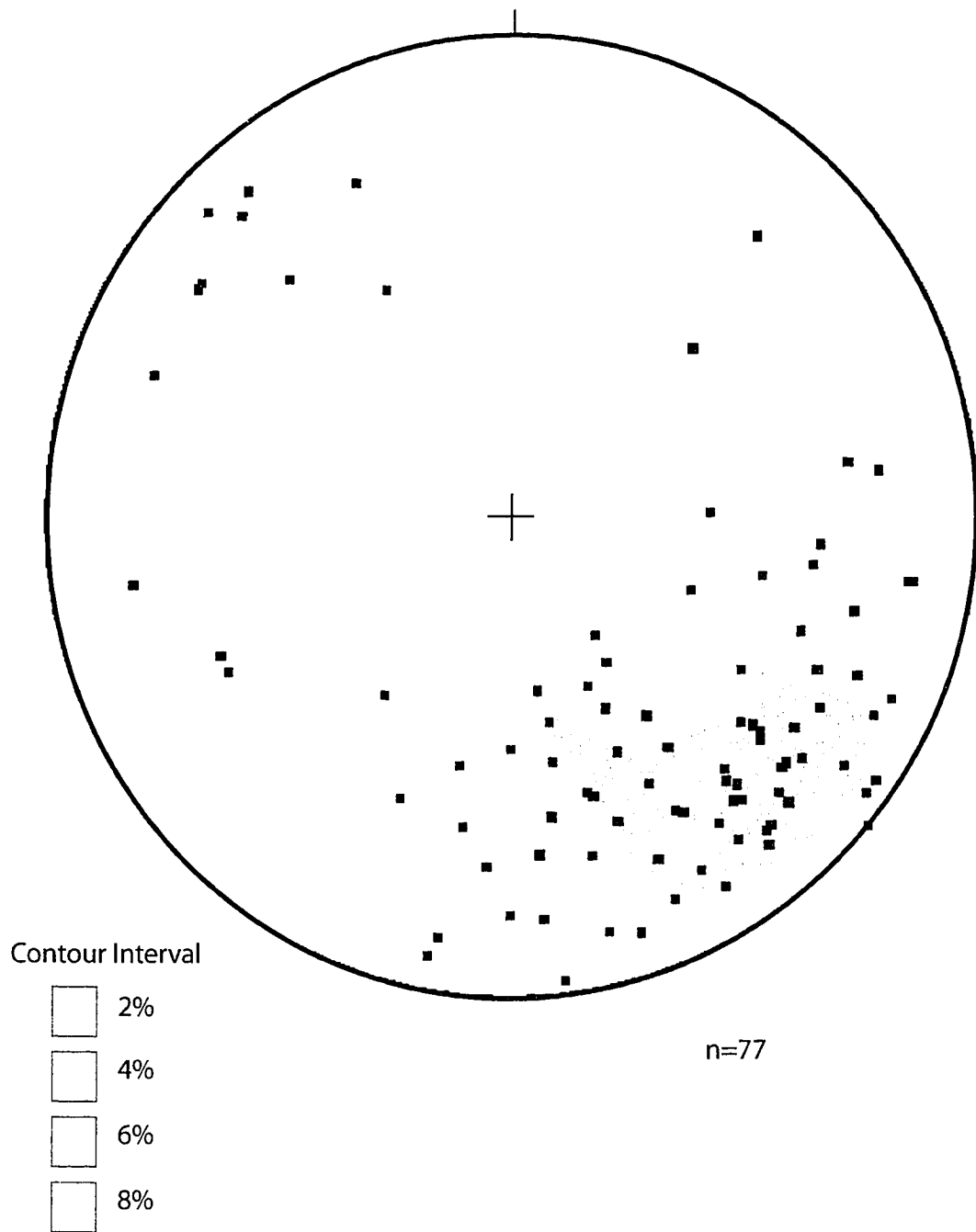


Fig. 25. Stereographic projection of lineations in the Cascade River-Holden assemblage, SGC, and Bearcat Ridge Orthogneiss.

plagioclase and/or potassium feldspar phenocrysts and porphyroclasts defines the lineation in some outcrops. Lineation intensity ranges from weak to strong. In some instances, the Ferry Peak Orthogneiss and the Gray Gneiss display moderate to strong fabrics marked by $L \geq S$.

Magmatic lineation is SE-trending and moderately plunging and is best exhibited within the 49 Ma Sunrise Lake pluton. A weak lineation is distinguished in some outcrops of the Railroad Creek pluton and Cooper Mountain batholith. Lineation is commonly defined by acicular hornblende and, in some places, by weakly aligned plagioclase and potassium feldspar phenocrysts.

Non-Coaxial Shear

Non-coaxial shear is represented throughout the study area by mylonites in ductile shear zones and asymmetric porphyroclasts. This deformation predates large-scale folding (F4 and F5, discussed below) within the region. Non-coaxial deformation can be sub-divided into two groups depending on the relative temperature during deformation, which is inferred from microstructures. Moderate to high-temperature deformation, marked by recrystallization of plagioclase and hornblende, is largely restricted to the Cascade River-Holden assemblage, Ferry Peak Orthogneiss, and Bearcat Ridge Orthogneiss. Lower-temperature non-coaxial deformation, which does not involve the recrystallization of plagioclase, is present in all units older than 49 Ma.

High-Temperature Non-Coaxial Shear

Evidence for moderate- to high-temperature (≥ 450 °C) ductile deformation is present throughout the 76 Ma Ferry Peak Orthogneiss and 69 Ma Bearcat Ridge Orthogneiss in the form of dextral and sinistral ductile shear zones and mylonites.

Mylonites range in intensity from protomylonitic to ultramylonitic. Additionally, xenoliths and septa of Cascade River-Holden assemblage rocks record similar relatively high-temperature deformation.

The Ferry Peak Orthogneiss is cut by distinctive swarms of W- to NW-striking and steeply NE-dipping “melt-filled” ductile shear zones (Fig. 26). These shear zones cut well-foliated and lineated medium-grained Ferry Peak Orthogneiss, are 2 to 3 cm thick, and have diffuse boundaries. Kinematic indicators from the shear zones record dextral strike-slip with a small normal-slip component. Shear zones are filled with a tonalitic “melt” composed of fine-grained plagioclase, biotite, and quartz (Fig. 26). Foliation in the tonalite “melt” is weak and largely magmatic. Based on the curvature of foliation into the shear zones, displacement on individual zones is estimated to be ≤ 10 cm. Melt-filled ductile shear zones occur in swarms of fifty or more in isolated regions (≤ 100 m²) of the orthogneiss.

High-temperature deformation is similarly well-recorded in the Bearcat Ridge Orthogneiss in mylonite zones that range up to 6 m thick; in some locations, these zones are surrounded by protomylonites that are over 50 m thick. These shear zones strike southeast, dip moderately southwest, and record sinistral strike-slip motion. Shear zones contain gently plunging, southeast-trending lineations. Kinematic indicators in the mylonites include sigma- and delta-porphyroclasts and biotite and muscovite fish.

In thin sections of the Bearcat Ridge Orthogneiss, Ferry Peak Orthogneiss, and Cascade River-Holden assemblage, non-coaxial deformation is exhibited by S-C fabric, asymmetric quartz fabric, and porphyroclast tails. Quartz is elongate, and contains subgrains and bulging grain boundaries, suggesting dislocation creep. Quartz recovery is exhibited by subgrains, grain boundary bulging, and subgrain rotation recrystallization. Plagioclase grains are elongate and have deformation

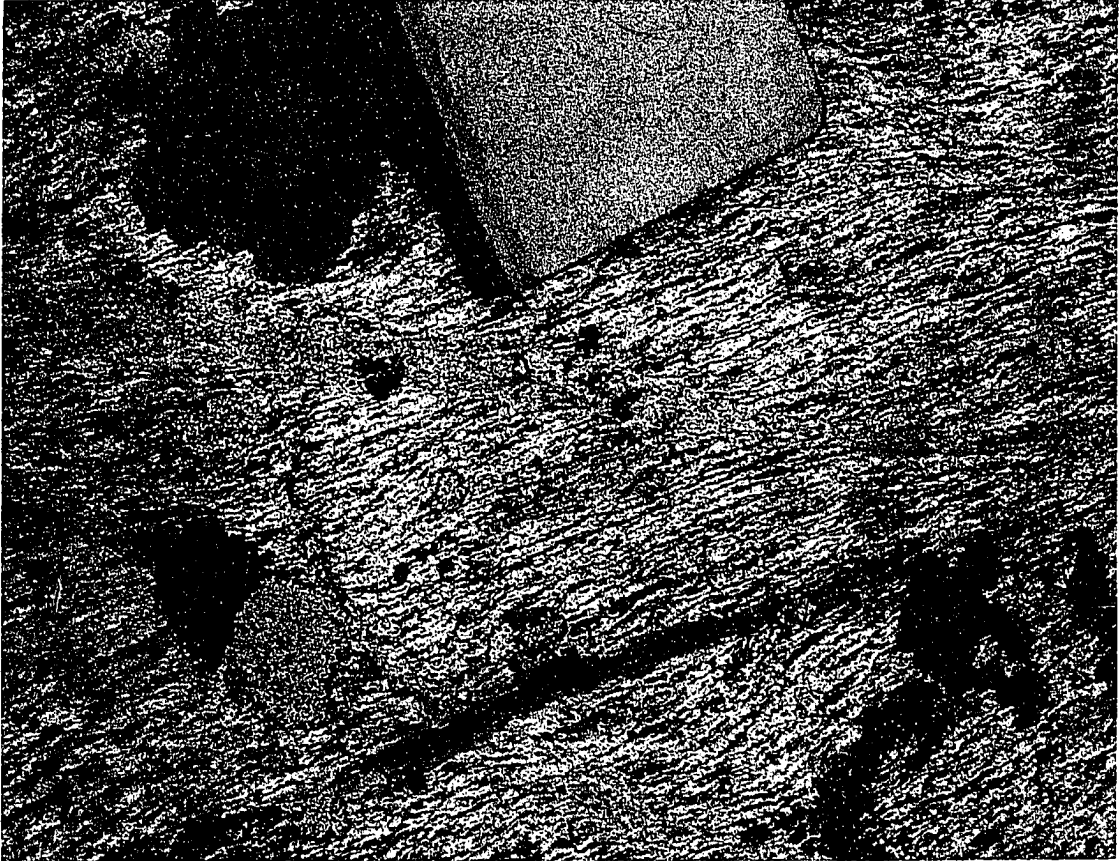


Fig. 26. View of horizontal surface containing dextral (top-to-southeast) “melt-filled” ductile shear zones in the Ferry Peak Orthogneiss. Note the curvature of foliation into the shear zone.

twins and microfractures. Deformation mechanisms in plagioclase include dislocation glide and brittle fracturing. Bent biotite grains provide evidence for dislocation glide. Recrystallization of quartz and plagioclase into medium-grained mosaics is common. S-C fabric is defined by deflected foliation and finely recrystallized biotite, quartz, and muscovite along C-surfaces. Biotite in C-surfaces is lighter in color than that in S-surfaces. S-surfaces are defined by quartz ribbons with aspect ratios of up to 4:1, elongate muscovite and biotite, and plagioclase porphyroclasts. Mica fish are commonly boudinaged and wrap around pre- or syn-tectonic garnets that are $\leq 300 \mu\text{m}$ in diameter. Anastomosing foliation occurs in most mylonites.

Low-Temperature Non-Coaxial Shear

Low-temperature ductile deformation is evident in all rock units in the study area except the Sunrise Lake pluton, Cooper Mountain batholith, and Railroad Creek pluton. Like the higher-temperature deformation, low-temperature ductile deformation is recorded by sinistral and dextral shear zones and mylonites.

Low-temperature ductile deformation is characterized by the lack of recrystallized plagioclase, extensive micro-fracturing of plagioclase (Fig. 27), and sharply defined, narrow (3-5 cm wide) ductile shear zones. These low-temperature shear zones are generally northwest-striking and steeply northeast dipping. Displacement is between five and ten centimeters, based on the offset of gneissic layers and leucocratic veins (Fig. 28). Ductile shear zones occur in sets of several (up to 5) shear zones (Fig. 28), but are not as numerous as the swarms of high-temperature, melt-filled ductile shear zones in the Ferry Peak Orthogneiss. Additionally, fine-grained mylonite zones up to two meters thick have both asymmetric porphyroclasts and S-C fabrics.



Fig. 27. Antithetically faulted plagioclase in a thin section of the Gray Gneiss. "T" indicates up (top) and "S" indicates south.



Fig. 28. Lower-temperature ductile shear zones in a medium-grained biotite tonalite leucogneiss of the Old Maid Orthogneiss. Note the relative lack of curvature of the foliation compared to the ductile shear zone of Fig. 26.

In thin section, low-temperature deformation is typified by ductilely deformed quartz and biotite, but most notably by brittlely deformed plagioclase (Fig. 27) and potassium feldspar. Plagioclase grains commonly have relict zoning, deformation twins, and microfractures. Deformation mechanisms include dislocation glide and brittle fracturing. Aggregates of quartz grains form ribbons that commonly wrap around plagioclase porphyroclasts. Quartz is deformed by dislocation creep. Recovery is evident in the form of subgrains, and subgrain rotation recrystallization is widespread in many quartz grains. Deformation in biotite occurred by translation glide, as evidenced by stretched grains.

S-C fabrics are defined by deflected foliation, with finely recrystallized biotite and quartz in C-surfaces. Biotite along the C-surfaces is lighter in color in plane light than biotite defining S-surfaces. Small, fractured, plagioclase grains are also present in C-surfaces. S-surfaces are characterized by aligned and fractured plagioclase, elongate biotite, and quartz ribbons. Late quartz fills large (up to 1 mm wide) fractures in plagioclase and potassium feldspar grains.

Folds

Four generations of folding have been distinguished in the study area: F2 folds are centimeter- to meter-scale structures within the Cascade River-Holden assemblage; F3 folds are centimeter- to meter-scale structures in the SGC and Cascade River-Holden assemblage; and F4 and F5 folds are large-scale folds that involve the SGC and adjacent units.

F2 Folds

The earliest phase of folding recognized in the field area (F2) consists of open to isoclinal, broadly symmetric folds in outcrops, xenoliths, and the main outcrop belt

of the Cascade River-Holden assemblage. These folds deform both compositional layering and foliation in the assemblage, but do not deform surrounding orthogneiss (Fig. 29). F2 folds have wavelengths that vary from several centimeters to one meter. Axial planes and hinge lines are highly variable in orientation. In places, two generations of folds with broadly parallel hinge lines are distinguished (Fig. 29).

F3 Folds

The second phase of folding (F3) is marked by deformation of the SGC and Cascade River-Holden assemblage. These folds are open to isoclinal, symmetric, and involve compositional layering and foliation (Fig. 30). F3 folds are interpreted as the earliest phase of folding in the SGC based on their relationship with F2 and F4 folds; F2 folds are deformed by F3 and F3 hinge lines are deformed by F4. F3 hinge lines are generally parallel to lineation, have gentle plunges, and vary from east- to southeast-trending. Axial planes vary from east- to southeast-striking and have gentle to moderate dips to the south or southwest. Wavelength is generally a few meters and ranges up to 10 m, but rare outcrops contain crenulated foliation with cm-scale wavelengths (Fig. 31).

F4 Folds

The third phase of folding (F4) involves kilometer-scale, symmetric, gently northwest-plunging folds. Axial planes strike northwest and dip steeply to the northeast. F4 folds range from open to gentle, and have wavelengths mostly between 3 km and 8 km (Plates 2-4). The westernmost and largest of these folds is a northwest-trending antiform that has a hinge line parallel to the dominant lineation (Plates 1-4). This large antiform continues at least 20 km along trend to the northwest and terminates in the south at the Cooper Mountain batholith (Fig. 21;



Fig. 29. F2 folds (arrows) in a xenolith of the Cascade River-Holden assemblage cut by a dike of fine-grained leucogneiss of the heterogeneous gneisses.



Fig. 30. Openly folded xenolith of the Cascade River-Holden assemblage and intrusive veinlets in the Ferry Peak Orthogneiss (F3). Intrusive veinlets are also boudinaged. Note the Ferry Peak Orthogneiss pegmatite above the xenolith that is also folded.



Fig. 31. Crenulated foliation in the Ferry Peak Orthogneiss.

Plate 1). The fold is defined by foliation in rocks on both sides of Lake Chelan, including the Bearcat Ridge Orthogneiss, Ferry Peak Orthogneiss, heterogeneous gneisses, and migmatite. The smaller (3-5 km wavelength) F4 folds to the east of the antiform involve rocks of the SGC older than 49 Ma and the Sunrise Lake pluton (Plates 2-4). Assuming flexural slip, shortening based on line length is at least 25%.

F5 Folds

The final phase of folding, F5, involves foliation and lineation in rocks older than 48 Ma and the hinge lines of older folds. Evidence for this fold is present in data from this study, but is more clearly evident when data east of the field area are incorporated (Miller, 1987; Miller and Bowring, 1990; R.B. Miller, unpublished data). These data reveal a major swing in the foliation strike and lineation trend throughout the length of the central and southern SGC (Figs. 32 and 33). Foliation changes from northwest-striking to east-striking over ~10 km from north to south (Fig. 32). Similarly, lineation changes from southeast- to east-trending (Fig. 33). This large-scale shift in foliation and lineation defines a steeply plunging, map-scale fold in the southern half of the SGC.

Dikes of Intermediate Composition

The orientations of 33 late dikes of intermediate composition were measured throughout the field area. These dikes strike SW (mean orientation of 211/85 SE) and dip steeply SE or NW (Fig. 34). The extension direction inferred from these dikes is NW-SE (301-121), which is subparallel to the orogen. The age of these dikes has not been determined using geochronology, but similar dikes described by Michels (in press) and N. McLean (pers. comm.) are dated at around 49 Ma.

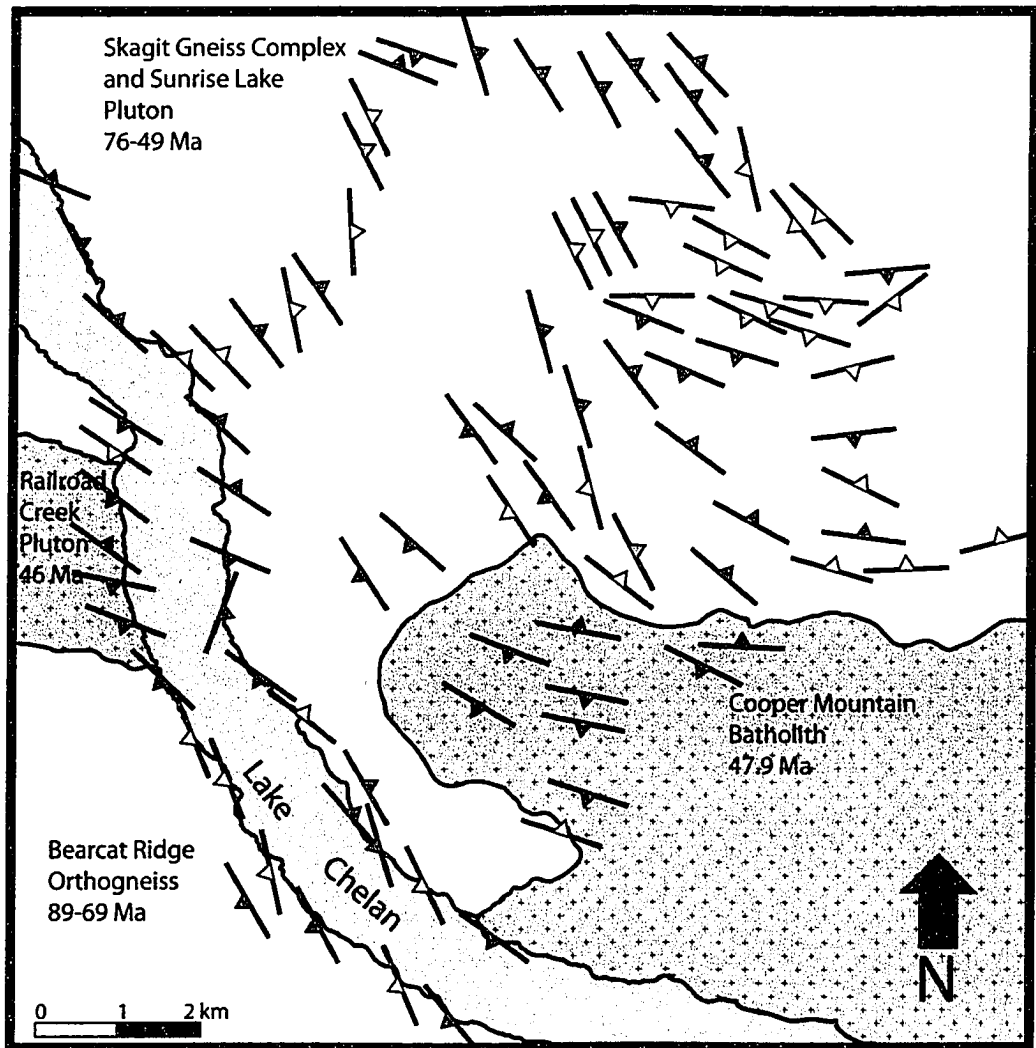


Fig. 32. Simplified map of foliations in the study area combined with foliation data from Miller (1987) and unpublished data of R.B. Miller (pers. comm.). Note the distinct swing in foliation in the SGC that is not present in the Cooper Mountain batholith. Color-coding of foliation dip: green, 0-30°, yellow, 31-60°, red from 61-90°.

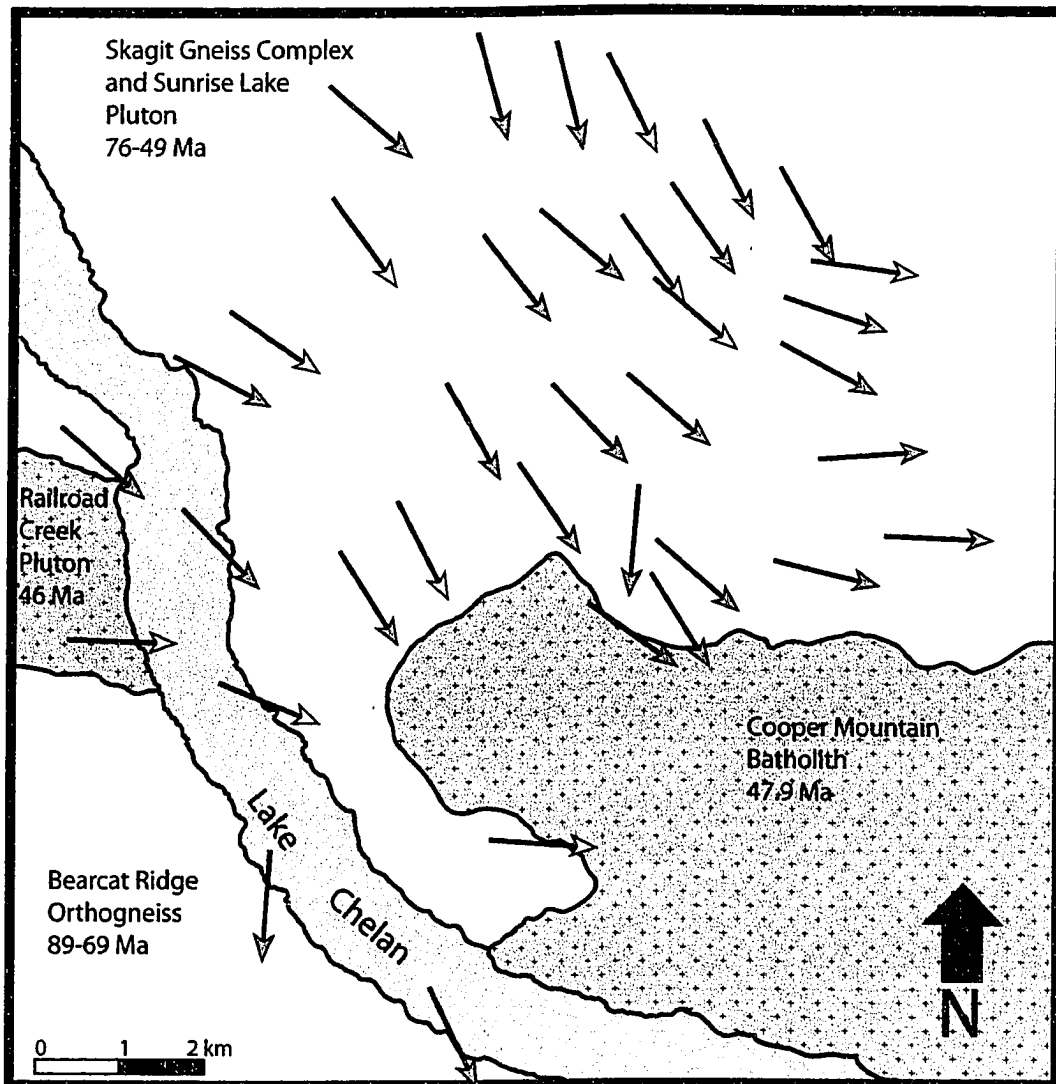


Fig. 33. Simplified map of lineations in the study area combined with data from Miller (1987) and unpublished data (R.B. Miller). Color-coding of lineation plunge: green, 0-30°, yellow, 31-60°.

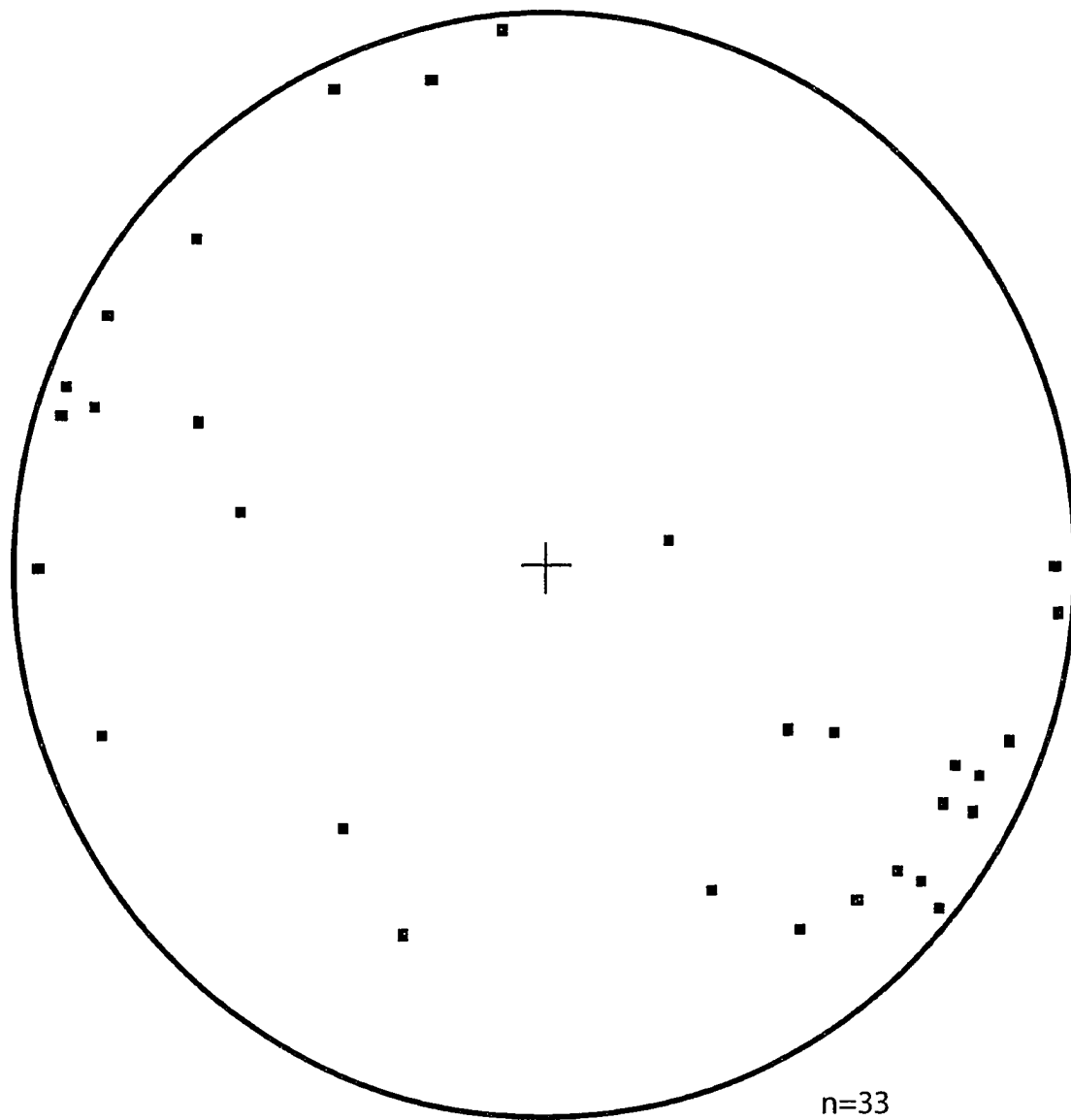


Fig. 34. Lower hemisphere stereographic projection of poles to dikes in the study area.

DISCUSSION

The crystalline core of the North Cascades records a complex history of intrusion, metamorphism, and deformation that spans the Triassic to the Eocene. The range of rock types and ages in the southern SGC has enabled the timing of many events in the field area, and throughout the SGC, to be constrained from cross-cutting relationships. These relationships provide a better understanding of the larger tectonic picture in the region, specifically from 76 Ma to 46 Ma.

Intrusive History

The intrusive history of the southern SGC can be determined using both cross-cutting relationships and geochronology. The oldest unit in the study area, the Triassic Cascade River-Holden assemblage, is generally interpreted as metasedimentary rocks of volcanic and sedimentary origin (Cater and Wright, 1967; Cater, 1982; Miller et al., 1994). In the study area, the assemblage serves as the host rock to the Bearcat Ridge Orthogneiss and intrusions belonging to the southern SGC.

The migmatite of the SGC lies structurally beneath the heterogeneous gneiss unit, and is intruded in places by well-foliated, discordant sheets of the heterogeneous gneiss. The main body of the migmatite is separated from the main belt of heterogeneous gneisses by a thin mantle of the Cascade River-Holden assemblage (Fig. 3; Plates 2-4). Based on the structural level of SGC migmatite and cross-cutting relationships, the migmatite is interpreted as the next oldest unit in the study area after the Cascade River-Holden assemblage. The origin of the migmatite is difficult to determine. However, the intermixing of the SGC migmatite with partially migmatitic Cascade River-Holden assemblage suggests the SGC

migmatite may be a combination of a small amount of partially melted Cascade River-Holden assemblage combined with a larger volume of later igneous intrusions. However, the overall modal mineralogy of the migmatite and the relatively small volume of Cascade River-Holden assemblage available for migmatization make it unlikely that the SGC migmatite originated entirely from the partial melting of metasupracrustal rocks.

The heterogeneous gneisses, which lie structurally above the SGC migmatite, are composed of tonalitic to quartz dioritic sheets and are dominated by solid-state fabric. In some outcrops, the heterogeneous gneisses cut SGC migmatite and overlying Cascade River-Holden assemblage. Xenoliths of SGC migmatite up to ~1 m across (Fig. 5) are also present in the heterogeneous gneisses, and are rotated with respect to foliation of the host gneiss. This relationship suggests intrusion of the heterogeneous gneisses into the migmatite. However, contacts between the heterogeneous gneiss and the migmatite vary from sharp to gradational. At gradational contacts, the heterogeneous gneisses become more felsic as the rock grades into intrusive veinlets (Fig. 6). The gradational contacts between these two units suggests that some of the migmatitic melt was contemporaneous with the heterogeneous gneisses. The variation in contacts between the heterogeneous gneisses and migmatite implies that intrusion of heterogeneous gneisses continued after the end of migmatization.

Sheets of Bearcat Ridge Orthogneiss were dated by Miller et al. (1993) at ~89 Ma and in this study at 69 Ma. These ages, and field relations, suggest that the orthogneiss protoliths were intruded over ~20 Ma. Alternatively, the part of the Bearcat Ridge Orthogneiss studied along Lake Chelan may be a separate gneiss unit from that studied by Miller et al. (1993). In the study area, the Bearcat Ridge Orthogneiss is mostly homogeneous and varies in composition from

garnet-muscovite tonalite to granodiorite. To the west of the study area, the orthogneiss contains abundant tonalite and diorite (Cater, 1982). The range of rock types is compatible with a non-uniform source region for the igneous protolith and/or fractionation. Unfolding F4 folds suggests that the Bearcat Ridge Orthogneiss was intruded as a set of subhorizontal sills. These sills may have incorporated pelitic material from the Cascade River-Holden assemblage to produce garnet and muscovite-bearing layers. More study of the Bearcat Ridge Orthogneiss would provide further insight into the variable nature of this unit.

The Ferry Peak Orthogneiss is the oldest part of the SGC in the study area. The orthogneiss has a relatively homogenous composition, making internal intrusive contacts difficult to discern. However, subtle differences in composition and grain size may indicate separate intrusive bodies with diffuse contacts. Unfolding the upright F4 folds suggests that the Ferry Peak Orthogneiss was intruded as a set of subhorizontal tonalitic sills, similar to the intrusion of the Bearcat Ridge Orthogneiss. The pegmatite of the Ferry Peak Orthogneiss (described earlier) was likely intruded as the final stage of intrusion of the tonalite. The Ferry Peak Orthogneiss grades into structurally underlying heterogeneous gneiss and migmatite over a distance of approximately 100 m. At the contact, the heterogeneous gneiss grades into garnet- and fibrolite-bearing leucogneiss (rare) that grades into the Ferry Peak Orthogneiss. This gradation suggests that formation of at least part of the Ferry Peak Orthogneiss was contemporaneous with formation of the heterogeneous gneiss. Highly localized areas of garnet- and sillimanite-rich rock in the Ferry Peak Orthogneiss are interpreted as melted xenoliths due to their size (less than 3 m across), isolation, and unique mineralogy.

The age of the Old Maid Orthogneiss has not been determined by U-Pb geochronology, but a relative age can be determined for the unit based on xenoliths

of the the Ferry Peak Orthogneiss within the unit. Mingling (Fig. 9) of the Gray Gneiss with the Old Maid Orthogneiss suggests that intrusion of some of the Gray Gneiss was contemporaneous with intrusion of the Old Maid Orthogneiss. Similar to most orthogneisses in the SGC, the Old Maid Orthogneiss shows some minor variability in grain size and composition. Foliation is concordant to that of surrounding units, suggesting that the gneiss was intruded as a set of sills. However, the unit's compositional variability may indicate that intrusion occurred in several temporally discrete pulses.

The Cub Lake Orthogneiss was emplaced after the Old Maid Orthogneiss was intruded, judging from xenoliths of the latter within the former. This relative age is further supported by the greater magnitude of deformation in the Old Maid Orthogneiss, implying a longer history of deformation. Alternatively, strain may have been partitioned into the Old Maid Orthogneiss. The magnitude of deformation and the composition of the Cub Lake Orthogneiss differ distinctly from those of older units in the SGC. Older units are more tonalitic than the Cub Lake Orthogneiss, which is granodioritic and has a more aluminous character. However, concordant contacts of the Cub Lake Orthogneiss with adjacent units suggests that the orthogneiss was intruded as a sill.

The Gray Gneiss forms tonalitic sills that do not intrude the Bearcat Ridge Orthogneiss, but intrude all units in the southern SGC. The Gray Gneiss cuts the Cub Lake Orthogneiss, but mingles with the older Old Maid Orthogneiss. These relationships suggest that intrusion of the Gray Gneiss spanned the ages of these two units. The Gray Gneiss was not seen in the Cooper Mountain batholith or the Railroad Creek pluton, indicating that intrusion likely ended by 48 Ma.

The broad range of zircon ages obtained within individual samples (Table 1) suggests that inherited zircons are important constituents of many of the studied

orthogneisses. These orthogneiss bodies likely assimilated older plutonic and/or metasedimentary rocks as they were emplaced, releasing xenocrystic zircons. These xenocrysts are surrounded by younger zircon, producing a range of ages depending on the amount of overgrowth. This is most evident in the Gray Gneiss (ES-02), where zircon ages range from 83 Ma to 47 Ma, and the Bearcat Ridge Orthogneiss (ES-19), where ages range from 88 Ma to 68 Ma. Small amounts of sillimanite (fibrolite) in the Cub Lake Orthogneiss, rare garnet in the heterogeneous gneiss, and isolated garnet- and sillimanite-bearing rocks in the Ferry Peak Orthogneiss support the idea that metasedimentary material was incorporated into many orthogneiss protoliths.

The highly felsic composition of the SGC and Bearcat Ridge Orthogneiss suggests that during the main period of magmatism, which lasted until ~49 Ma, the southern SGC and Bearcat Ridge Orthogneiss had very little interaction with mafic intrusive material. Neither unit shows evidence for physical mixing (e.g. enclaves) with more mafic (e.g. dioritic) material. However, dioritic material is present in the heterogeneous gneisses and migmatite, which are presumed to be broadly contemporaneous with the SGC and Bearcat Ridge Orthogneiss, based on cross-cutting relationships with the Gray Gneiss. A proposed explanation for the felsic nature of these bodies is modified from the ideas of Hogan and Gilbert (1995) and Hogan et al. (1998). These authors propose that strength anisotropies in the crust may serve as “barriers” to mafic intrusions. The location of such a barrier in the study area may have been located between the base of heterogeneous gneisses and the base of the Ferry Peak Orthogneiss (Fig. 35), resulting in felsic rocks above and relatively more mafic rocks below. Further study of the heterogeneous gneisses would allow this hypothesis to be tested further.

The youngest plutonic bodies in the study area, the Sunrise Lake pluton (49

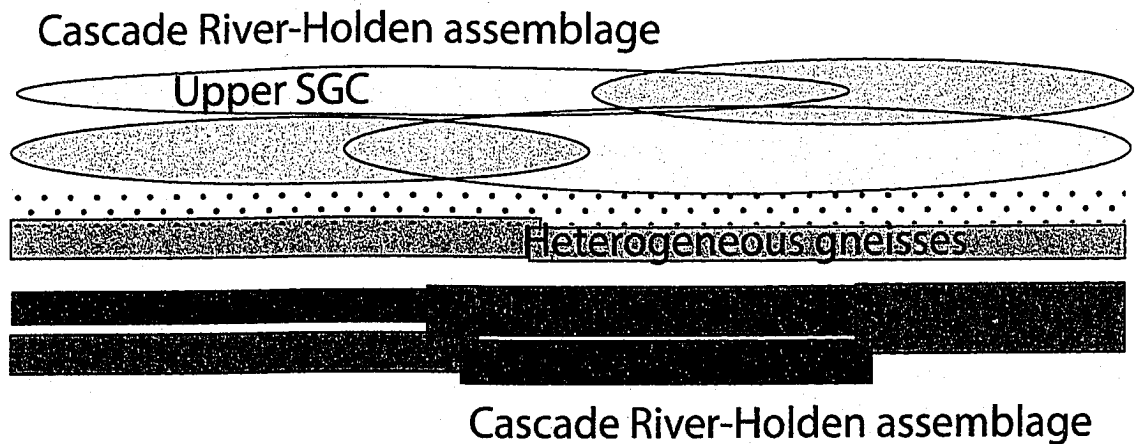


Fig. 35. Schematic sketch of the southern SGC, based on a diagram for the eastern Transverse Ranges by A. Barth and S. Paterson (pers. comm.). Diagram is based on the unfolding of F4 folds and shows the stratification of the SGC: upper SGC rocks (Ferry Peak Orthogneiss, Old Maid Orthogneiss, Cub Lake Orthogneiss), heterogeneous gneisses, and SGC migmatite. All SGC-rocks are intruded into the Cascade River-Holden assemblage. The felsic nature of the upper SGC rocks may be due to a subhorizontal strength anisotropy located between the heterogeneous gneisses and Ferry Peak Orthogneiss (represented by dotted area above). This anisotropy may have served as a barrier to mafic intrusions, resulting in relatively felsic rocks above the barrier and relatively mafic rocks below.

Ma; McLean et al., 2006), Cooper Mountain batholith (48 Ma), and Railroad Creek pluton (~46 Ma; N. McLean, pers. comm.) have all been dated using U-Pb geochronology. These plutons are compositionally and structurally different from the dominantly tonalitic gneisses of the SGC. The Sunrise Lake pluton is dominantly quartz dioritic in the study area, whereas the Cooper Mountain batholith and Railroad Creek pluton are granitic and granodioritic, respectively.

The range in compositions of these relatively late-forming plutons may be related to contemporaneous ridge subduction that probably occurred at the latitude of northern Washington at ~50 Ma (Cowan, 2003; Madsen et al., 2006). In some interpretations, this ridge subduction formed a slab window beneath the North Cascades (Madsen et al., 2006). This postulated slab window, caused by the separation of the Resurrection and Farallon plates beneath the North American crust, would have produced significant magmatic and structural changes in the region. Each slab window environment is unique, but most are characterized by alkalic to tholeiitic and calc-alkalic magmatism, and extensional or transtensional structures in the overriding plate (Thorkelson et al., 1996). In the southern SGC, a change from tonalite-dominated magmatism (e.g., Ferry Peak Orthogneiss) to more potassium-feldspar-rich (Cub Lake Orthogneiss) and finally to more mafic (Sunrise Lake pluton) and granitic/granodioritic-dominated magmatism (Cooper Mountain batholith and Railroad Creek pluton) occurred at this time. Additionally, transtension in the region was roughly coeval with ridge subduction, providing additional support for this hypothesis. Other interpretations (e.g. Dostal et al., 2003) place the slab window north of the Cascades core, requiring a different source for the late plutons in the study area (Matzel et al., 2006).

Deformation History

The study area preserves a complex structural history. Multiple phases of non-coaxial shear and folding are seen in the SGC and adjacent units and span from the Cretaceous to Eocene. Determining the absolute timing of events is difficult without more geochronologic work; however, relative timing for some events can be determined.

Foliation in the study area is dominantly northwest-striking and steeply dipping. A large antiform (~8 km wavelength) and several smaller folds (~3 km) defined by foliation are considered part of the F4 phase of folding (Plates 2-4). In the southern SGC, foliation can be restored to a subhorizontal configuration by the removal of the upright F4 folds. Based on their presence in the 49 Ma Sunrise Lake pluton, these folds in part formed coevally with or shortly after emplacement of the pluton. This timing suggests that foliation and contacts in the study area may have had an initially gentler dip that can be crudely restored through the unfolding of F4 folds. This inferred subhorizontal arrangement suggests that most of the gneisses in the study area were intruded as sills and were underlain by migmatite and partially migmatitic paragneiss (Fig. 35). The majority of rocks in the study area show evidence for stronger foliation than lineation; thus implying an oblate-flattening strain ellipsoid.

The subhorizontal orientation and shape of the flattening-type ellipsoid may be explained by several tectonic scenarios. In one speculative hypothesis, the structures result from the buildup and collapse of a thick orogenic plateau in the North Cascades between the Early and Late Cretaceous (Whitney et al., 2004). This hypothetical plateau presumably formed as the result of crustal thickening associated with Cretaceous contraction and the accretion of Wrangellia to the North

American continent. In the thickened region of the plateau, the mid- to lower-crust would have experienced high temperatures and pressures, promoting anatexis, as evidenced in the southern SGC by migmatite and partially melted Cascade River-Holden assemblage. The gravitational force acting on the deep crust would have promoted vertical shortening and horizontal extension, resulting in a subhorizontal foliation (Rey et al., 2001). Over-thickening or changes in regional strain, such as a transition from transpression to transtension, caused divergent gravitational collapse of the thickened crust, which served to reduce the energy stored in the thickened region through thinning and crustal flow. Alternatively, the strain ellipsoid may have been caused by distributed thrusting throughout the region. Ductile shear zones in the SGC may be evidence for this thrusting.

The overall southeast trend and gentle plunge of lineation suggests that orogen-parallel flow occurred in the southern SGC. Lineation is interpreted as an indicator of the direction of flow of material, but at least two explanations for flow exist. The first explanation is that lineation development was contemporaneous with foliation development, but preceded F4 folding. In this scenario, lineation may have formed as a result of crustal thickening and orogenic collapse. The lineation then would indicate the direction of the flow of lower crustal material away from the plateau. The second explanation is that the lineation development was contemporaneous with F4 folding and represents extension (NW-SE) parallel to the fold axes and perpendicular to the regional shortening direction. The parallel trends of lineation and F4 fold hinges make determining the timing of lineation formation relative to F4 folding and foliation development difficult; with parallel trends, F4 folds do not affect the lineation orientation to any great extent.

Non-coaxial deformation in the region is difficult to decipher, owing to the variety of shear senses that are recorded by both high- and low-temperature

deformation. As currently oriented, non-coaxial shear zones in the study area indicate dominantly strike-slip motion with either sinistral or dextral shear senses. High-temperature deformation in the study area is evident in the Ferry Peak Orthogneiss (76 Ma), Bearcat Ridge Orthogneiss (69 Ma), and Triassic Cascade River-Holden assemblage. As noted above, microstructures in these units indicate temperatures were ≥ 450 °C during deformation. Restoration of F4 folds orients shear zones and mylonites to a subhorizontal configuration. In this orientation, high-temperature non-coaxial deformation gives subhorizontal southeast-vergent thrust- or normal-sense shear (Fig. 36). Uncertainties in the original dips of these structures make it difficult to determine if they record thrust- or normal-kinematics. The timing of this deformation is difficult to constrain and may have continued until the initiation of low-temperature non-coaxial deformation prior to 49 Ma.

Low-temperature, non-coaxial deformation is present in all rock units older than 49 Ma. This deformation is not associated with recrystallized plagioclase, indicating temperatures ≤ 450 °C. However, quartz deformation occurs by dislocation glide and dislocation creep, suggesting temperatures ≥ 300 °C (Passchier and Trouw, 2005). After unfolding F4 folds, low-temperature shear zones indicate northwest-vergent, thrust- or normal-sense deformation (Fig. 36).

The change from dominantly southeast-vergent, relatively high-temperature deformation to northwest-vergent, relatively low-temperature deformation is constrained by the age of the 69 Ma Bearcat Ridge Orthogneiss, which has southeast-vergent mylonites, and the 49 Ma Sunrise Lake pluton, which shows no evidence for strong non-coaxial deformation. The Bearcat Ridge and Sunrise Lake ages provide a 20 m.y. window during which deformation changed from southeast-vergent and relatively warm (≥ 450 °C) to northwest-vergent and relatively cool (300 °C – 450 °C). This change in kinematics is interpreted as

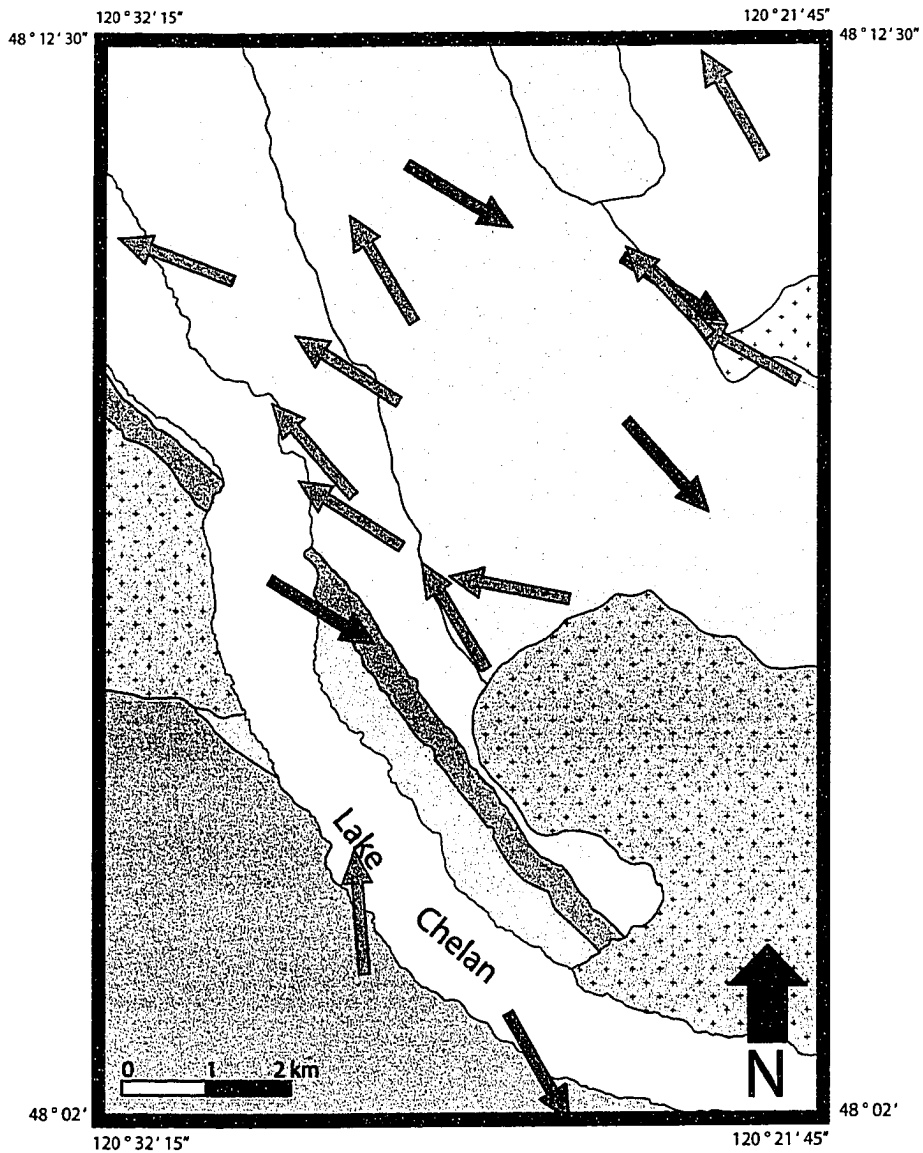


Fig. 36. Simplified map of non-coaxial deformation in the study area. Arrows indicate direction of upper plate. Red arrows indicate high-temperature deformation, green arrows indicate low-temperature deformation.

evidence for a significant shift in the direction of non-coaxial deformation and flow of crustal material in the southern SGC and Bearcat Ridge Orthogneiss. The driving mechanism for this kinematic reversal is uncertain and there is no obvious reason why flow should be top-to-the-SE. The reversal may be linked to the change in regional strain from transpression to transtension, which is interpreted to have occurred at ~ 55 Ma (e.g., Miller and Bowring, 1990; Cowan, 2003).

Northwest-vergent deformation in the southern SGC may be linked to exhumation to the south that occurred at least in part by north-vergent shear on subhorizontal surfaces during regional transtension (Paterson et al., 2004). This link is compatible with the relatively lower-temperature deformation of the mylonites and shear zones.

Large-scale folding in the study area occurred after non-coaxial deformation. As stated above, non-coaxial deformation is absent in the Sunrise Lake pluton, but F4 and F5 folds involve the pluton. Smaller wavelength folds (F2, F3) in the Cascade River-Holden assemblage and Ferry Peak Orthogneiss are interpreted to have occurred prior to or contemporaneous with non-coaxial deformation.

F2 folds in xenoliths of the Cascade River-Holden assemblage have variably trending and plunging hinge lines and variably striking and dipping axial planes. The inconsistent orientation and lack of involvement of later gneissic units suggest that F2 folds formed prior to intrusion of the Skagit orthogneisses. As xenoliths of the assemblage were incorporated into intruded bodies, they likely rotated, leading to variation in fold orientations.

F3 folds are typified by variably oriented hinge lines and axial planes. The scattered orientations and isolated occurrences of F3 folds suggests that these folds are local perturbations in the Ferry Peak Orthogneiss, making them difficult to relate to the larger tectonic picture.

F4 folds provide evidence for orogen-perpendicular shortening that lasted until

approximately 49 Ma. Intrusion of the late intermediate dikes is interpreted to have occurred contemporaneously with or shortly following this folding, based on the similar strain fields (NW-SE extension) and lack of folded dikes. The onset of folding is difficult to determine but may have followed intrusion of the Cub Lake Orthogneiss or Gray Gneiss, as these units are relatively young but are folded. These folds are unlikely to be the result of wrench strain caused by the Ross Lake fault zone, as they trend nearly parallel to the strike of the fault ($\leq 10^\circ$ deviation). This subparallel alignment is compatible with a transpressional relationship between the folds and the fault zone. In this case, the fault zone and the folds partition regional transpressional strain (e.g., Robin and Cruden, 1994; Tikoff and Teyssier, 1994).

The folding of lineation, foliation, and earlier fold hinge lines by the F5 fold signifies the end of significant orogen-parallel flow in the SGC. The steeply plunging F5 fold is tightly constrained by the ages of the Sunrise Lake pluton (49 Ma), which is folded, and the Cooper Mountain batholith (47.9 Ma), which is not. The F5 fold is most obvious in the southern SGC, and more data are needed to determine whether the fold involves the Bearcat Ridge Orthogneiss to the west. It is not obvious how far north the F5 fold affects the SGC, but evidence for the fold is found at least 30 km north of the study area in the central SGC. In this region, a wide swing in foliation from NW-striking to NNE-striking and in lineation from SE-trending to NE-trending is present (Adams, 1961; Michels et al., 2007) and is interpreted as part of the F5 fold.

The late-forming dikes of intermediate composition may also have been influenced by the F5 fold; the extension direction derived from these dikes shows a similar swing from the southern to the central SGC. In the central SGC, the dike extension direction is parallel to the lineation in the area, suggesting that the

NNE-SSW extension lasted through the emplacement of the dikes (Michels et al., 2007). Based on cross-cutting relationships, dikes were emplaced prior to 48 Ma in the southern SGC and after 48 Ma in the central SGC. The regional nature of the F5 fold raises several important questions: How was space accommodated for the fold? Why does the fold not deform the contacts between units in the SGC? What drove the folding? The fold may be broadly related to movement on the Ross Lake fault zone, but this fault zone is relatively far away and folds associated with strike-slip are generally gently plunging.

CONCLUSIONS

The southern Skagit Gneiss Complex (SGC) is an important example of the exhumed core of a continental magmatic arc. This study has shown that:

- (1) The southern SGC can be broken up into six sub-units: Ferry Peak Orthogneiss, Old Maid Orthogneiss, Gray Gneiss, Cub Lake Orthogneiss, and heterogeneous gneisses and migmatite concentrated on the western edge of the complex.
- (2) U-Pb dating of zircon indicates crystallization of the Ferry Peak Orthogneiss at ~76 Ma, Bearcat Ridge Orthogneiss at ~68 Ma, Gray Gneiss at 60 Ma, and the Cooper Mountain batholith at 47.9 Ma.
- (3) Foliation in the southern SGC strikes NW with moderate to steep NE or SW dip.
- (4) Lineation in the southern SGC is SE-trending with gentle to moderate plunge.
- (5) Solid-state lineation and foliation, which can be restored to a subhorizontal orientation after unfolding F4, are interpreted as evidence for orogen-parallel flow in the southern SGC.
- (6) Two periods of non-coaxial deformation are recorded in the southern SGC.
- (7) High-temperature deformation is seen only in the Cascade River-Holden assemblage, Ferry Peak Orthogneiss, and Bearcat Ridge Orthogneiss and records southeast-vergent shear.
- (8) Low-temperature deformation is present in all rock units older than 49 Ma and records northwest-vergent shear.
- (9) Four phases of folding are recorded in the study area. The extent of the first phase (F2) is difficult to determine while folds of the second phase (F3) are likely due to local effects. The last two phases (F4-F5) are due to regional strain.
- (10) F4 folds are NW-striking, large-wavelength (3-8 km) structures with subhorizontal hinge lines, indicating orogen-perpendicular shortening.

(11) The F5 fold is a large, steeply plunging structure that signifies the end of major orogen-parallel flow. Timing of this event is constrained between 49 and 48 Ma.

REFERENCES CITED

- Adams, J.B., 1961, Petrology and structure of the Stehekin-Twisp Pass area, northern Cascades, Washington [Ph.D. thesis]: Seattle, University of Washington, 172 p.
- Brandon, M.T., Cowan, D.S., and Vance, J.A., 1988, The Late-Cretaceous San Juan thrust system, San Juan Islands, Washington: Geological Society of America Special Paper 221, 81 p.
- Cater, F.W., and Wright, T.L., 1967, Geologic map of the Lucerne quadrangle, Chelan County, Washington: U.S. Geological Survey Geologic Quadrangle Map GQ-647, 1 sheet, scale 1:62,500.
- Cater, F.W., 1982, Intrusive rocks of the Holden and Lucerne quadrangles, Washington—The relation of depth zones, composition, textures, and emplacement of plutons: U.S. Geological Survey Professional Paper 1220, 108 p.
- Cowan, D., 2003, Revisiting the Baranof-Leech River hypothesis for early Tertiary coastwise transport of the Chugach-Prince William terrane: *Earth and Planetary Science Letters*, v. 213, p. 463-475, doi: 10.1016/S0012-821X(03)003000-5.
- Doran, B., and Miller, R., 2006, Structure of the Swauk basin and Teanaway dike swarm, central Cascades, Washington: *Geological Society of America Abstracts with Programs*, v. 38, no. 5, p. 17.
- Doran, B., Miller, R., and Michels, Z., 2007, Structure and implications of Eocene dike swarms in the Washington Cascades: *Geological Society of America Abstracts with Programs*, v. 39, no. 4, p. 10.
- Dostal, J., Breitsprecher, K., Church, B.N., Thorkelson, D., and Hamilton, T.S., 2003, Eocene melting of Precambrian lithospheric mantle: analcime-bearing volcanic rocks from the Challis-Kamloops belt of South Central British

- Columbia: Journal of Volcanology and Geothermal Research, v. 126, p. 303-326.
- Gordon, S.M., Whitney, D.L., Miller, R.B., McLean, N., Bowring, S., 2008, The Skagit gneiss (North Cascades, Washington) revisited: New P-T results from recently discovered Al₂SiO₅-bearing gneiss: Geological Society of America Abstracts with Programs, v. 40, no. 6, p. 516.
- Johnson, S.Y., 1985, Eocene strike-slip faulting and nonmarine basin formation in Washington, *in*: Biddle, K.T., and Christie-Blick, N., eds., Strike-slip deformation, basin formation, and sedimentation: Society of Economic Paleontologists and Mineralogists Special Publication 37, p. 283-302.
- Krogh, T.E., 1973, A low contamination method for the hydrothermal decomposition of zircon and extraction of U and Pb for isotopic age determinations: *Geochimica et Cosmochimica Acta*, v. 46, p. 637-649.
- Haugerud, R.A., van der Heyden, P., Tabor, R.W., Stacey, J.S., and Zartman, R.E., 1991, Late Cretaceous and early Tertiary plutonism and deformation in the Skagit Gneiss Complex, North Cascade range, Washington and British Columbia: *Geological Society of America Bulletin*, v. 103, p. 1297-1307.
- Hogan, J.P. and Gilbert, M.C., 1995, The A-type Mount Scott Granite sheet: importance of crustal magma traps: *Journal of Geophysical Research*, v. 100, p. 15,779-15,793.
- Hogan, J.P., Price, J.D., and Gilbert, M.C., 1998, Magma traps and driving pressure: consequences for pluton shape and emplacement in an extensional regime: *Journal of Structural Geology*, v. 20, p. 1155-1168.
- Jaffey, A.H., Flynn, K.F., Glendenin, L.E., Bentley, W.C., and Essling, A.M., 1971, Precision measurement of half-lives and specific activities of ²³⁵U and ²³⁸U: *Physical Review C*, v. 4, p. 1889-1906.
- Madsen, J.K., Thorkelson, D.J., Friedman, R.M., and Marshall, D.D., 2006,

- Cenozoic to Recent plate configurations in the Pacific Basin: Ridge subduction and slab window magmatism in western North America: *Geosphere*, v. 2, p. 11-34, doi:10.1130/GES00020.1.
- Mattinson, J.M., 2005, Zircon U-Pb chemical abrasion (“CA-TIMS”) method: Combined annealing and multi-step partial dissolution analysis for improved precision and accuracy of zircon ages: *Chemical Geology*, v. 220, p. 47-66.
- Matzel, J.E.P., Bowring, S.A., and Miller, R.B., 2006, Time scales of pluton construction at differing crustal levels: Examples from the Mount Stuart and Tenpeak intrusions, North Cascades, Washington: *Geological Society of America Bulletin*, v. 118, p. 1412-1430, doi:10.1130/B25923.1.
- McLean, N.M., Bowring, S.A., Miller, R., Whitney, D., and Gordon, S., 2006, North Cascades, WA: The collapse of a continental magmatic arc: *Eos, Transactions, American Geophysical Union Fall Meeting Supplement*, v. 87, p. 199.
- McGroder, M.F., 1991, Reconciliation of two-sided thrusting, burial metamorphism, and diachronous uplift in the Cascades of Washington and British Columbia: *Geological Society of America Bulletin*, v. 103, p. 189-209.
- Michels, Z.D., Miller, R.B., and McLean, N., 2007, Structures of the central part of the Skagit Gneiss Complex, North Cascades, Washington: *Geological Society of America Abstracts with Programs*, v. 39, no. 4, p. 10.
- Miller, R.B., 1987, *Geology of the Twisp River-Chelan Divide region, North Cascades, Washington*: Washington Division of Geology and Earth Resources Open File Report 87-17, 12 p., 12 pl.
- Miller, R.B., 1994, A mid-crustal contractional stepover zone in a major strike-slip system, North Cascades, Washington: *Journal of Structural Geology*, v. 16, p. 47-60.
- Miller, R.B., and Bowring, S.A., 1990, Structure and chronology of the Oval Peak

- batholith and adjacent rocks: Implications for the Ross Lake fault zone, North Cascades, Washington: *Geological Society of America Bulletin*, v. 102, p. 1361-1377.
- Miller, R.B., and Paterson, S.R., 2001, Influence of lithological heterogeneity, mechanical anisotropy, and magmatism on the rheology of an arc, North Cascades, Washington: *Tectonophysics*, v. 342, p. 351-370.
- Miller, R.B., Brown, E.H., McShane, D.P., and Whitney, D.L., 1993, Intra-arc crustal loading and its tectonic implications, North Cascades crystalline core, Washington and British Columbia: *Geology*, v. 21, p. 255-258.
- Miller, R.B., Haugerud, R.A., Murphy, F., and Nicholson, L.S., 1994, Tectonostratigraphic framework of the northeastern Cascades: Washington Division of Geology and Earth Resources Bulletin 80, p. 73-92.
- Miller, R.B., Paterson, S.R., Lebit, H., Alsleben, H., and Luneburg, C., 2006, Significance of composite lineations in the mid- to deep crust: a case study from the North Cascades, Washington: *Journal of Structural Geology*, v. 28, p. 302-322, doi:10.1016/j.jsg.2005.11.003.
- Miller, R.B., Bowring, S., Doran, B., Gordon, S., McLean, N., Michels, Z., Shea, E., and Whitney, D.L., 2007, Eocene tectonic evolution of the North Cascades: *Geological Society of America Abstracts with Programs*, v. 39, no. 4, p. 10.
- Misch, P., 1966, Tectonic evolution of the northern Cascades of Washington State – a west Cordilleran case history. Canadian Institute of Mining and Metallurgy, Special Volume 8, p. 101-148.
- Misch, P., 1968, Plagioclase compositions and non-anatectic origin of migmatitic gneisses in the Northern Cascade Mountains of Washington State: *Contributions to Mineralogy and Petrology*, v. 17, p. 1-70.
- Monger, J.W.H., Price, R.A., and Tempelman-Kluit, D.J., 1982, Tectonic accretion

- and the origin of the two major metamorphic and plutonic belts in the Canadian Cordillera: *Geology*, v. 10, p. 70-75.
- Passchier, C.W., and Trouw, R.A., 2005, *Micro-tectonics*: Berlin, Springer-Verlag, 366 p.
- Paterson, S.R., Miller, R.B., Alsleben, H., Whitney, D.L., Valley, P.M., and Hurlow, H., 2004, Driving mechanisms for >40 km of exhumation during contraction and extension in a continental arc, Cascades core, Washington: *Tectonics*, v. 23, TC3005, doi:10.1029/2002TC001440.
- Rey, P., Vanderhaeghe, O., and Teyssier, C., 2001, Gravitational collapse of the continental crust; definition, regimes, and modes: *Tectonophysics*, v. 342, p. 435-449.
- Robin, P.F., and Cruden, A.R., 1994, Strain and vorticity patterns in ideally ductile transpression zones: *Journal of Structural Geology*, v. 16, p. 447-466.
- Rubin, C.M., Saleeby, J.B., Cowan, D.S., Brandon, M.T., and McGroder, M.F., 1990, Regionally extensive mid-Cretaceous west-vergent thrust system in the northwestern Cordillera; implications for continent-margin tectonism: *Geology*, v. 18, p. 276-280.
- Schmitz, M.D., and Schoene, B., 2007, Derivation of isotope ratios, errors, and error correlations for U-Pb geochronology using ^{205}Pb - ^{235}U -(^{233}U)-spiked isotope dilution thermal ionization mass spectrometric data: *Geochemistry, Geophysics, Geosystems*, v. 8, Q08006, doi:10.1029/2006GC001492.
- Shea, E.K., Miller, R.B., Michels, Z.D., and McLean, N.M., 2007, *Structural Geology of the Skagit Gneiss Complex (SGC), North Cascades, Washington*: Geological Society of America Abstracts with Programs, v. 39, no. 4, p. 10.
- Tabor, R.W., Frizzell, V.A., Vance, J.A., and Naeser, C.W., 1984, Ages and stratigraphy of lower and middle Tertiary sedimentary and volcanic rocks of the

- central Cascades, Washington; application to the tectonic history of the Straight Creek fault: *Geological Society of America Bulletin*, v. 95, p. 26-44.
- Tabor, R.W., Haugerud, R.A., and Miller, R.B., 1989, Accreted terranes of the North Cascades Range, Washington: *Field Trip Guidebook*, AGU, Washington, D.C., v. T307, 62 p.
- Tabor, R.W., Haugerud, R.A., Hildreth, W., and Brown, E.H., 2003, Geologic map of the Mount Baker 30- by 60-minute quadrangle, Washington: U.S. Geological Survey Geological Investigations Series 1-2660, scale 1:100,000, 1 sheet.
- Thorkelson, D.J., 1996, Subduction of diverging plates and principles of slab window formation: *Tectonophysics*, v. 255, p. 47-63, doi:10.1016/0040-1951(95)00106-9.
- Tikoff, B., and Teyssier, C., 1994, Strain modeling of displacement-field partitioning in transpressional orogens: *Journal of Structural Geology*, v. 16, p. 1575-1588, doi:10.1016/0191-8141(94)90034-5.
- Whitney, D.L., 1992a, Origin of CO₂-rich fluid inclusions in leucosomes from the Skagit migmatites, North Cascades, Washington: *Journal of Metamorphic Geology*, v. 10, p. 715-725.
- Whitney, D.L., 1992b, High-pressure metamorphism in the Western Cordillera of North America: an example from the Skagit Gneiss, North Cascades: *Journal of Metamorphic Geology*, v. 10, p. 71-85.
- Whitney, D.L., Paterson, S.R., Schmidt, K.L., Glazner, A.F., and Kopf, C., 2004, Growth and demise of continental arcs and orogenic plateaux in the North American Cordillera: from Baja to British Columbia, *in*: Grocott, J., Tikoff, B., McCaffrey, K.J.W., and Taylor, G., eds., *Vertical coupling and decoupling in the lithosphere*: Geological Society of London Special Publication, v. 227, p. 167-176.

NOTE TO USERS

Oversize maps and charts are microfilmed in sections in the following manner:

LEFT TO RIGHT, TOP TO BOTTOM, WITH SMALL OVERLAPS

This reproduction is the best copy available.

UMI[®]

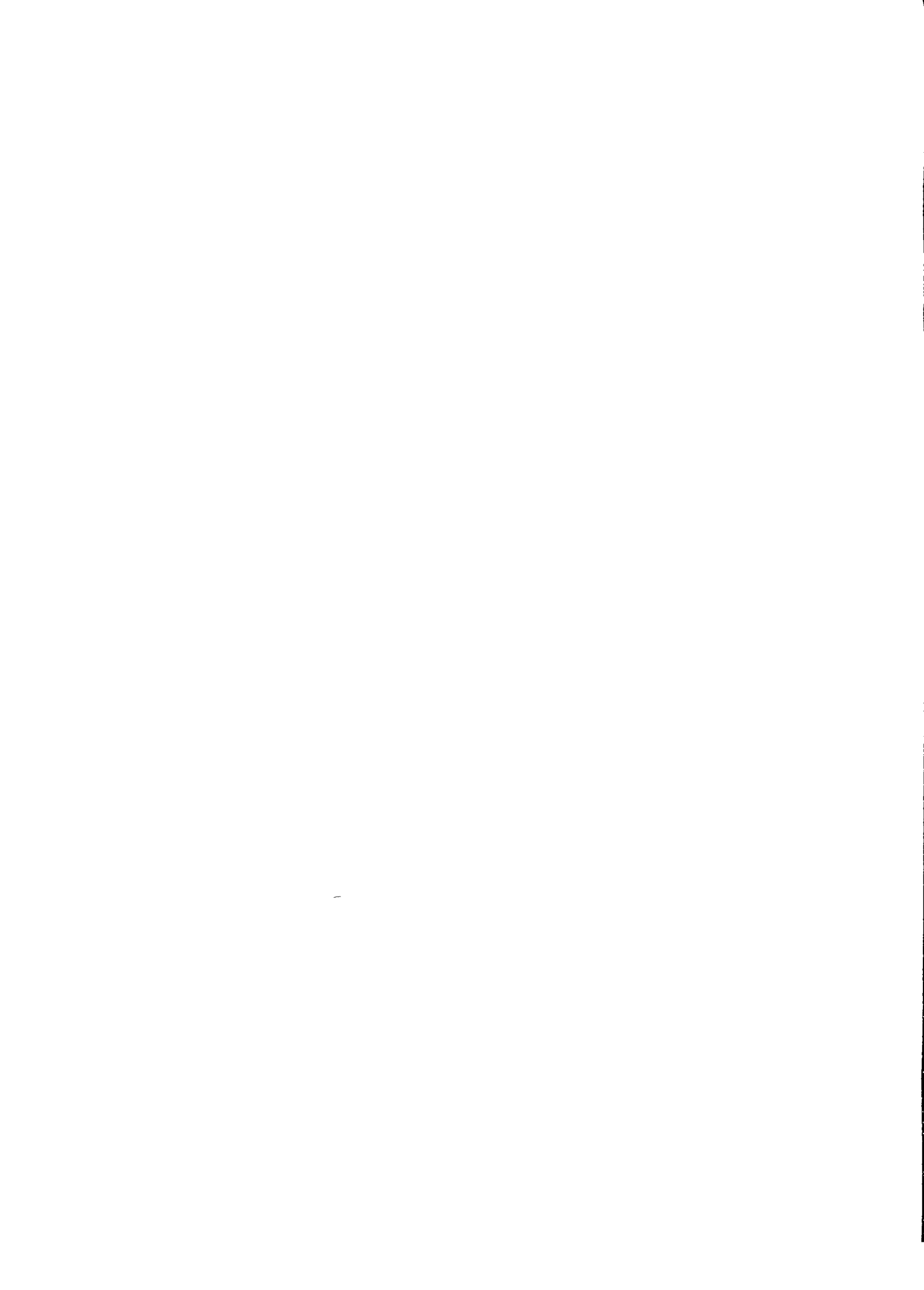
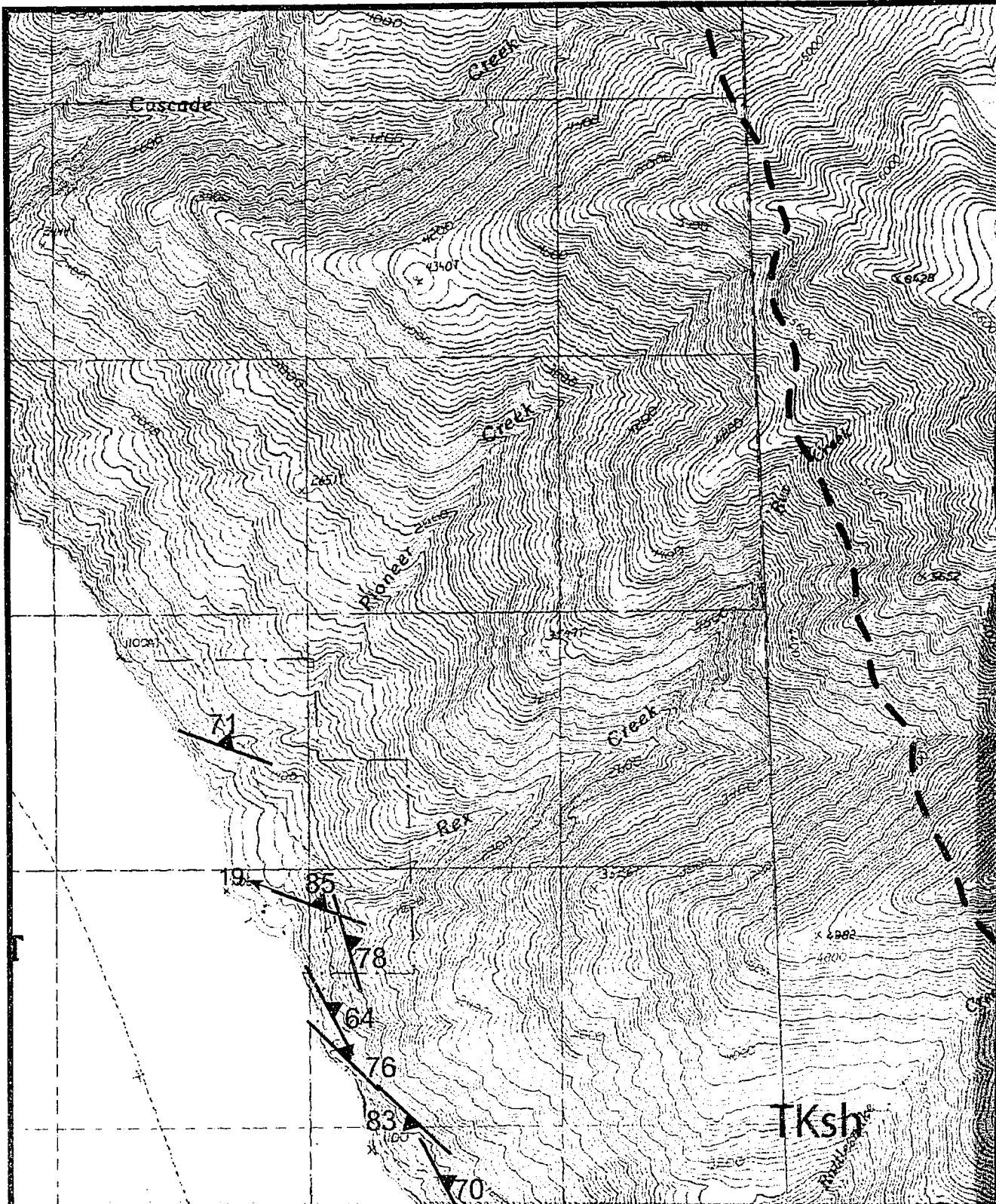
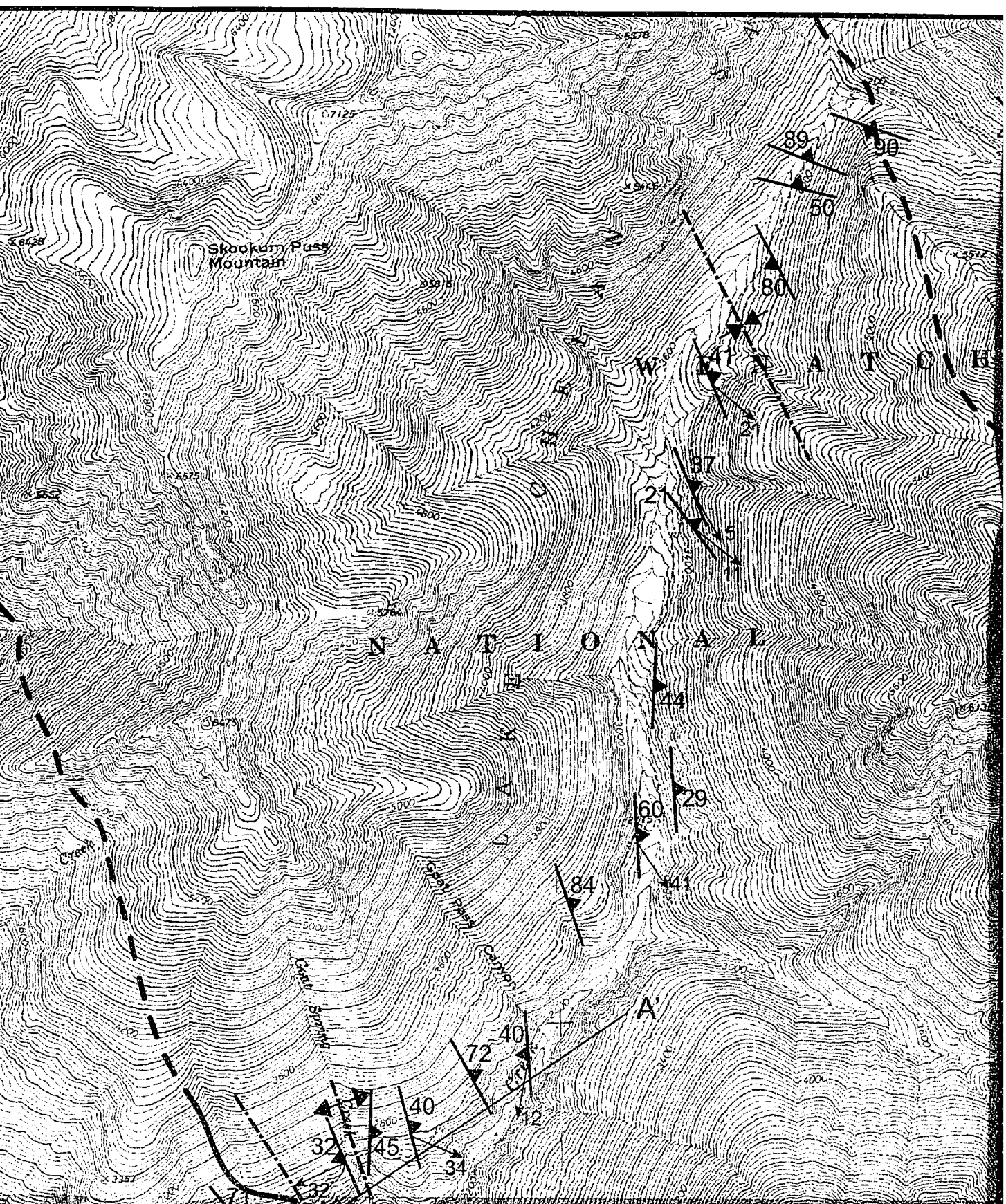


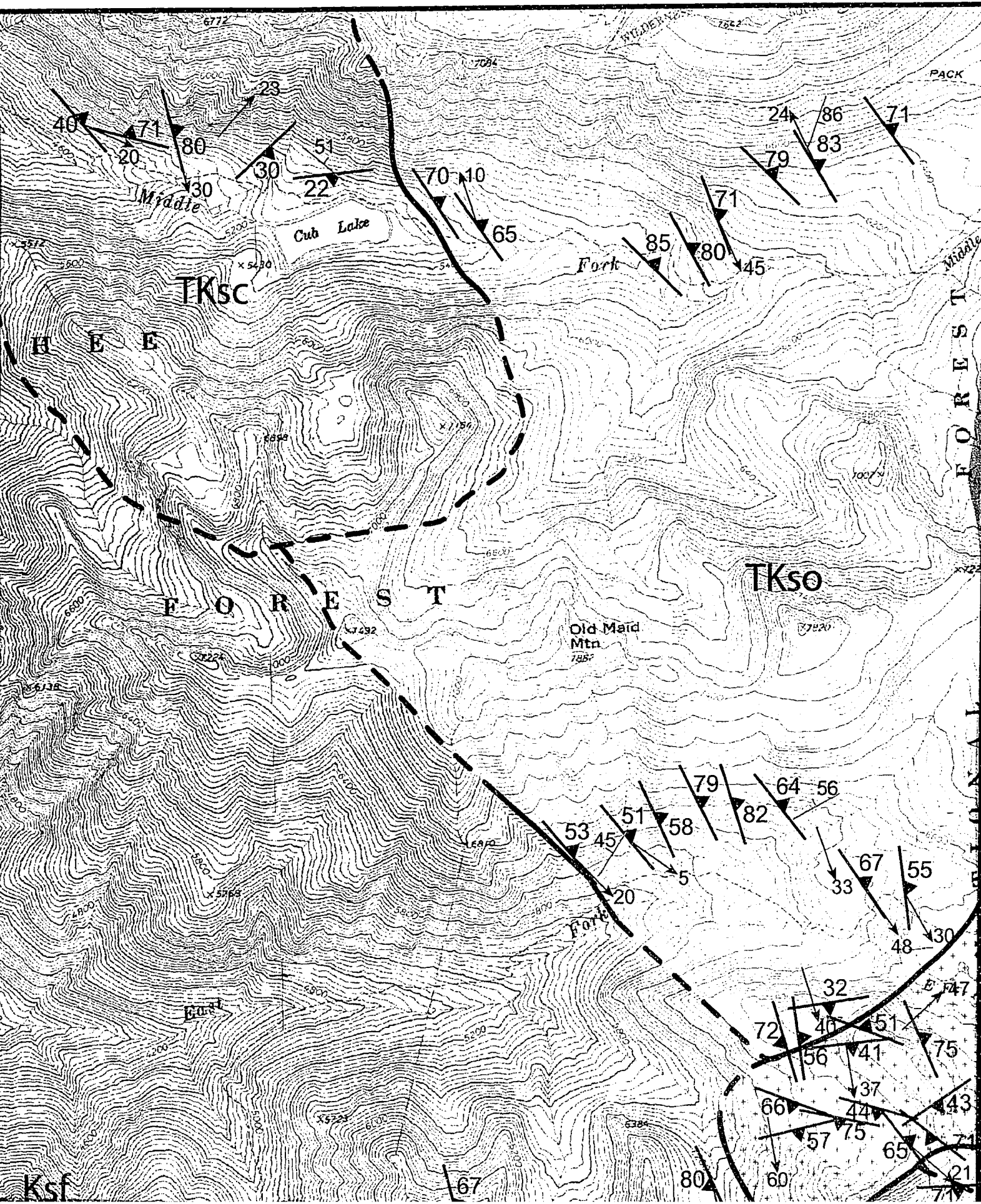
Plate 1

120° 32' 15"

48° 12' 30"

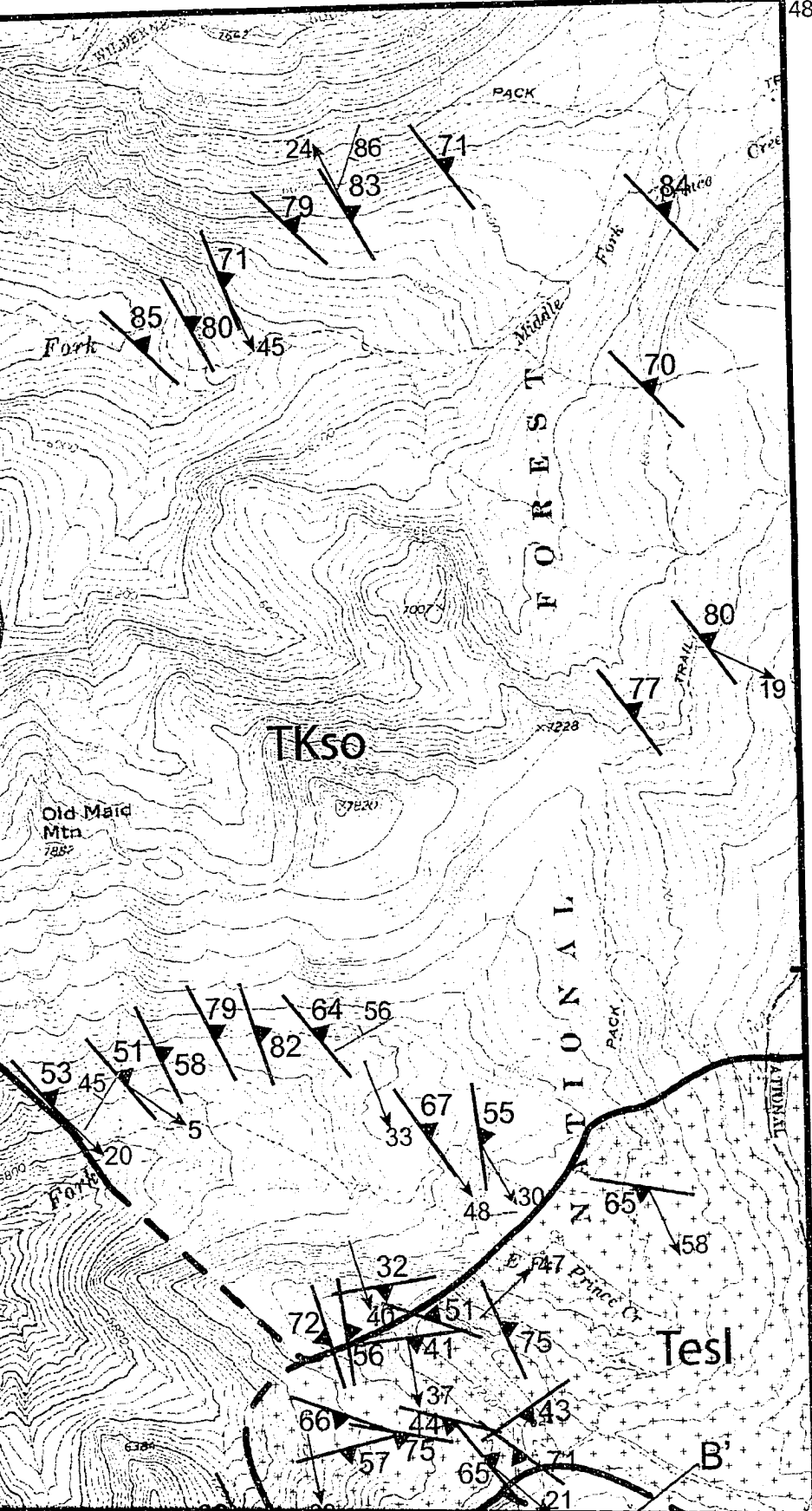


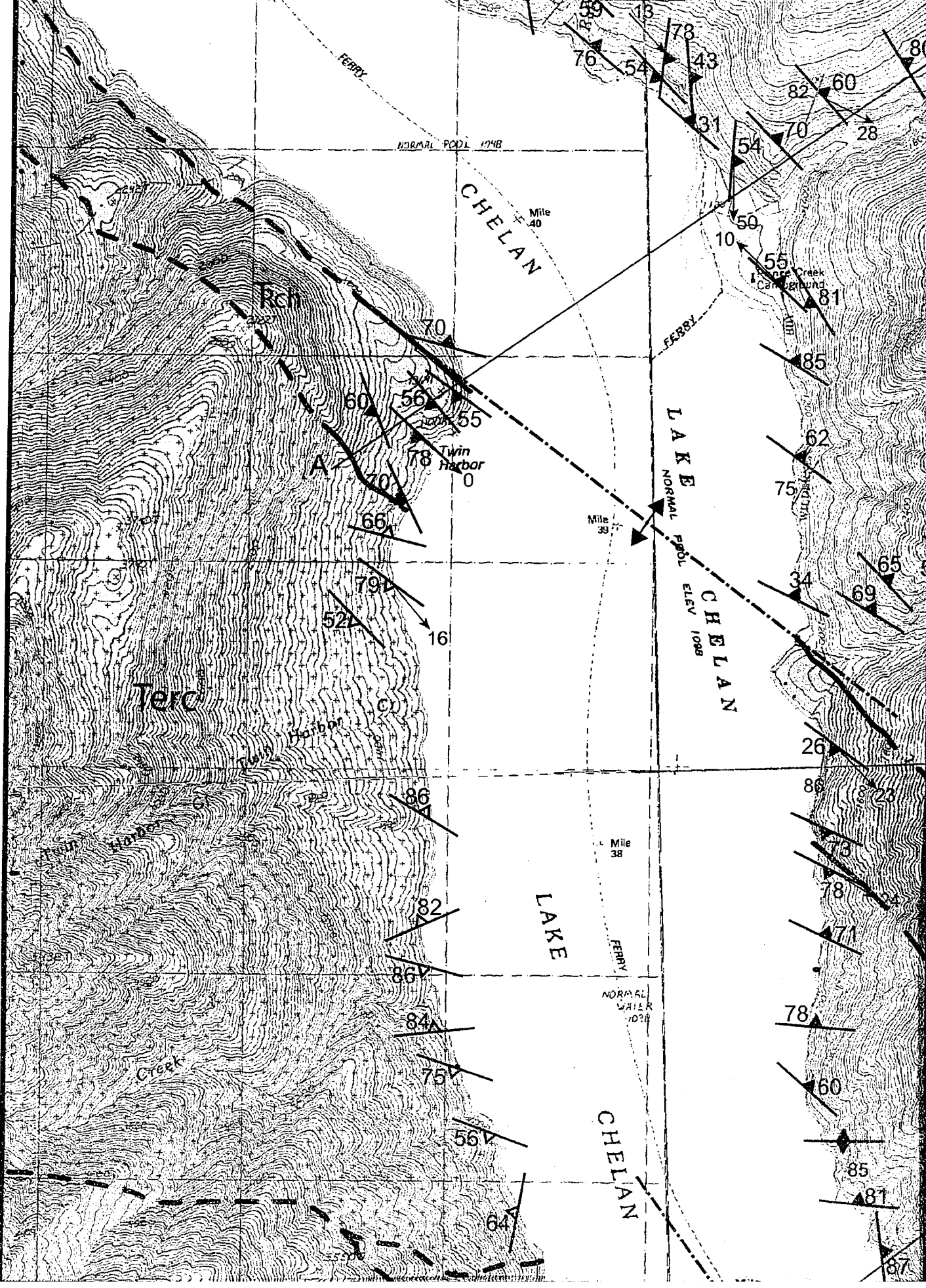


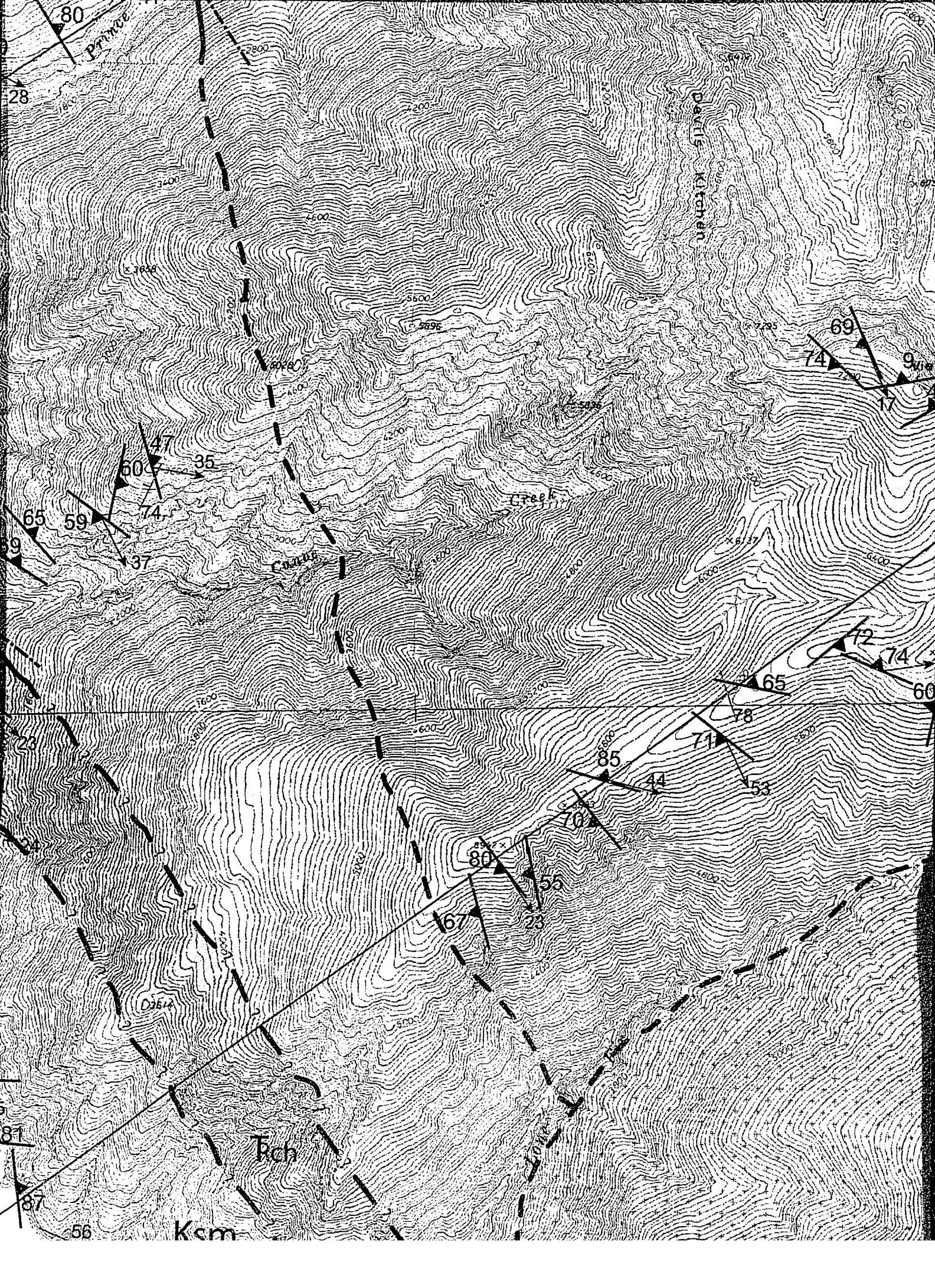


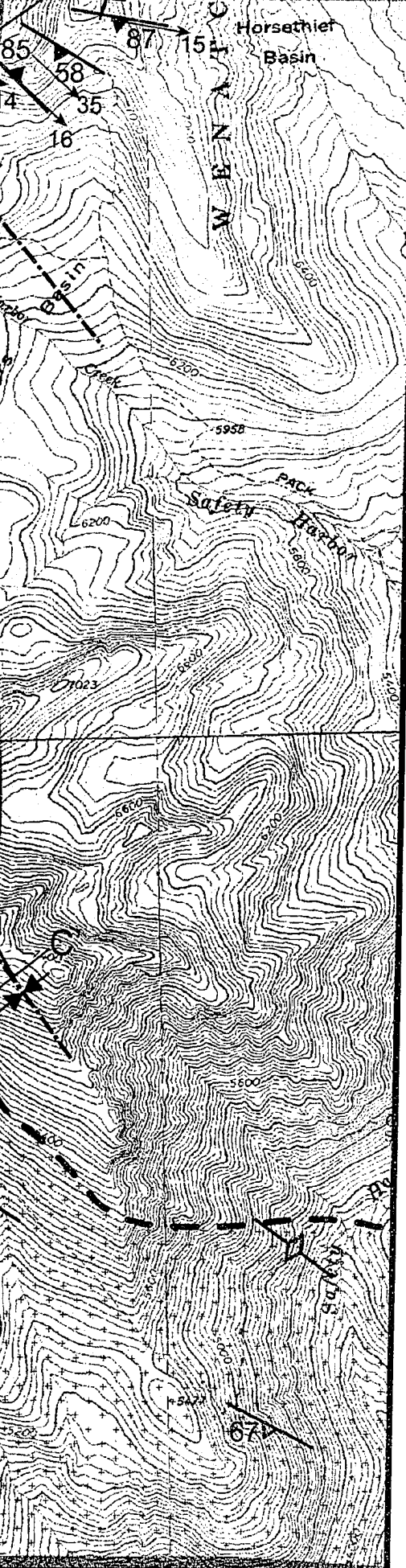
120° 21' 45"

48° 12' 30"









Explana

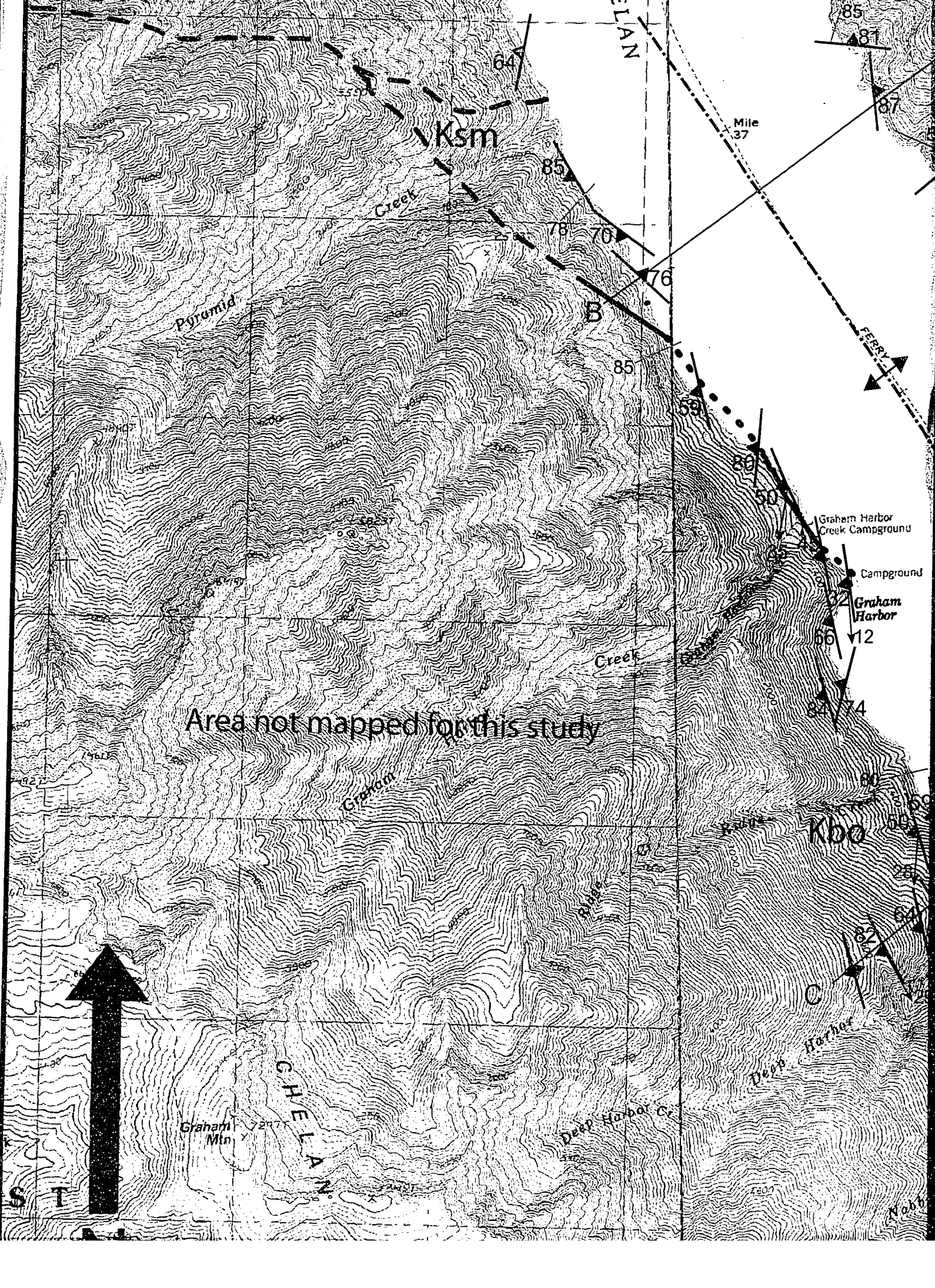
Rock Units

Explanation

Rock Units

85
—△—

Magmatic foliation
strike and dip



Ksm

85

81

87

Mile 37

64

85

78

70

76

B

85

59

80

50

Graham Harbor Creek Campground

Campground

Graham Harbor

60

12

84

74

Pyramid

Creek

Creek

Graham

Kbo

C

Deep Harbor

Deep Harbor Cr

Graham Mtn

GHELLAN

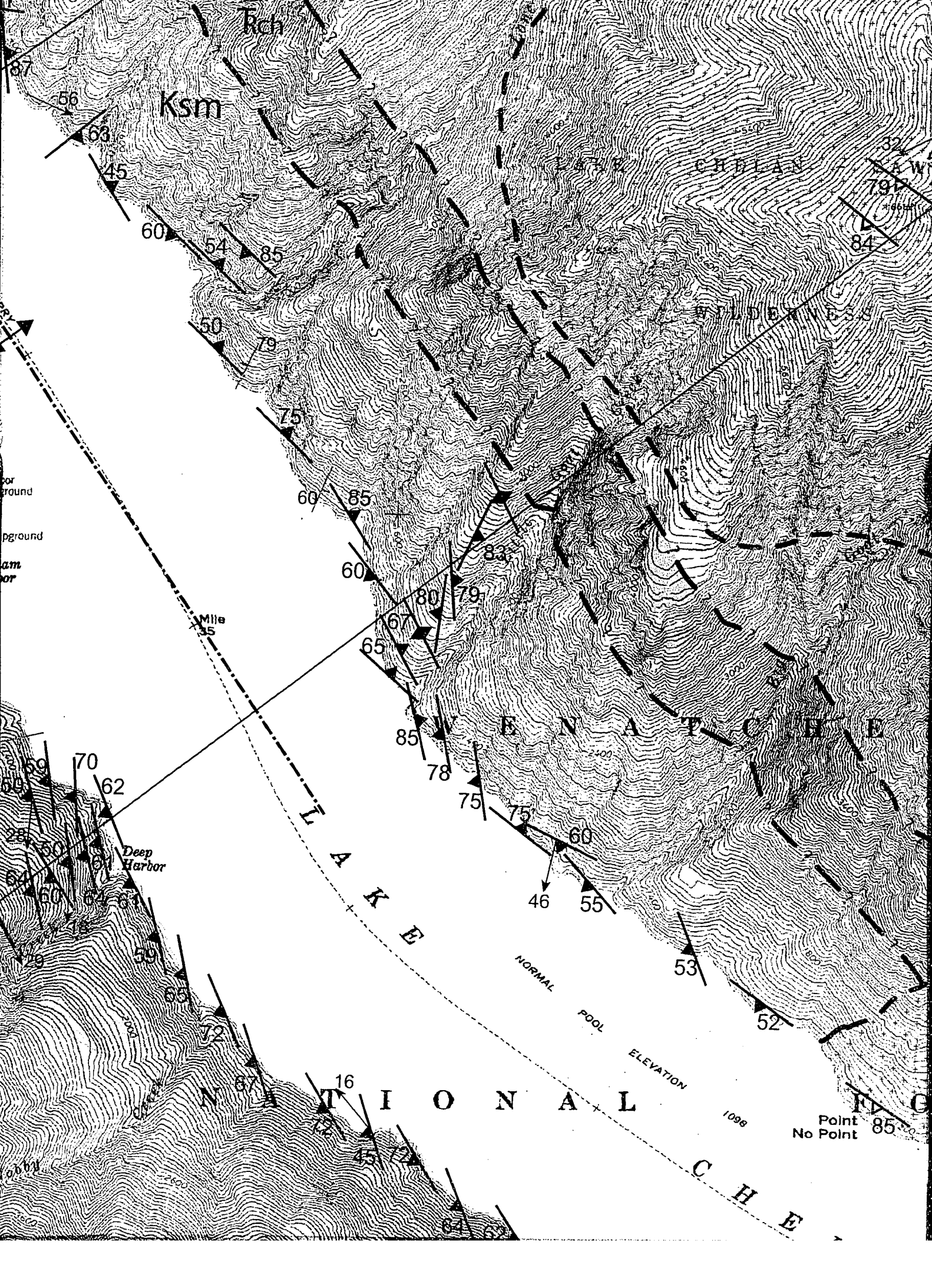
Nobb

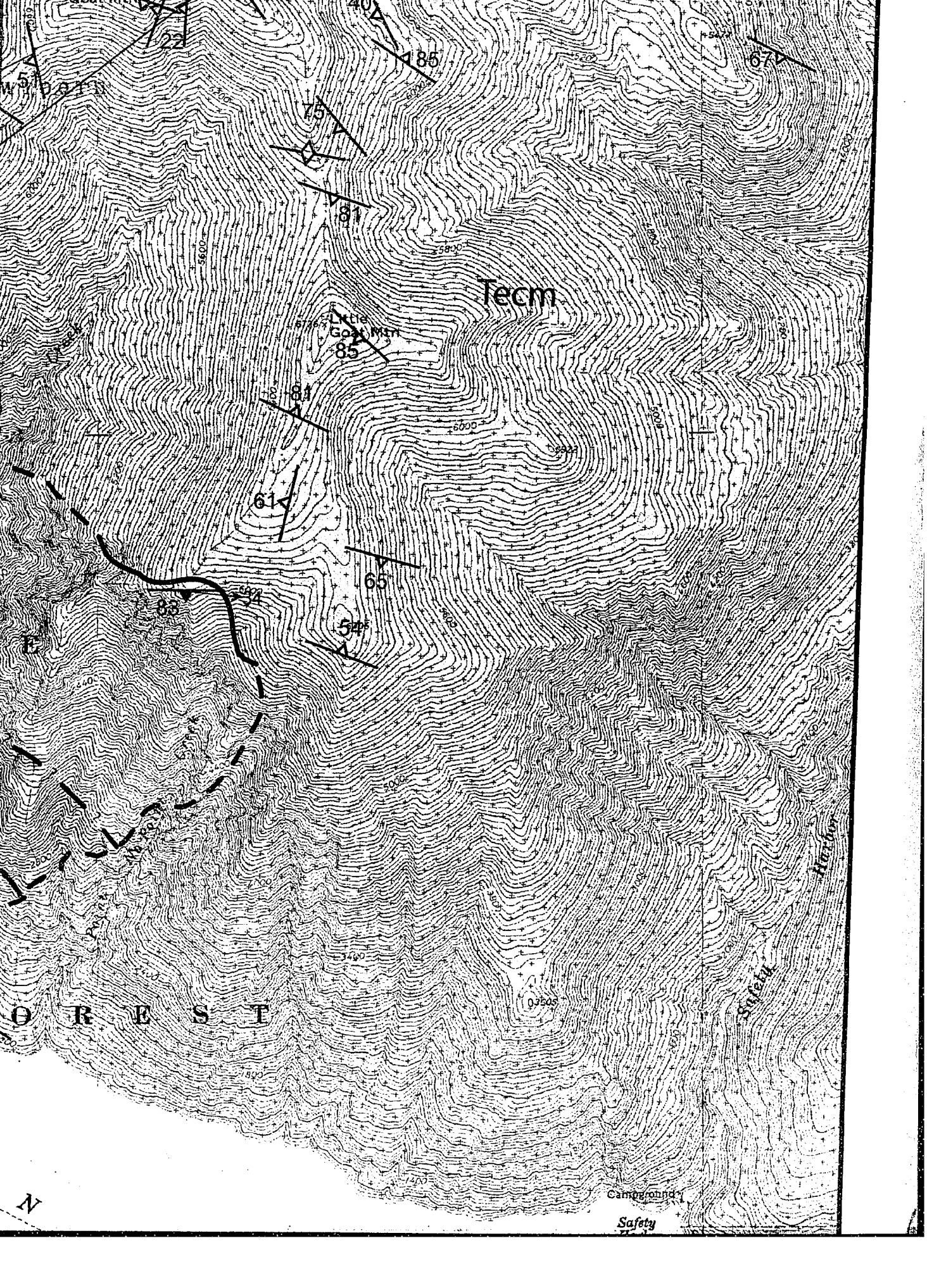
Area not mapped for this study



S T

A B





122

185

75

81

85

61

65

54

63

57

50

40

Tern

Little
Cove
Mtn

FOREST

Safety



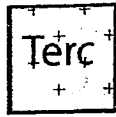
Campanella

Safety

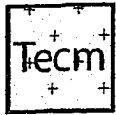


Explanation

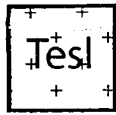
Rock Units



Railroad Creek Pluton
(46 Ma)



Cooper Mountain
Batholith (48 Ma)



Sunrise Lake Pluton
(49 Ma)

SKAGIT GNEISS COMPLEX



Cub Lake Orthogneiss



Old Maid Orthogneiss



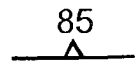
Heterogeneous Gneiss



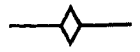
Ferry Peak
Orthogneiss (76 Ma)



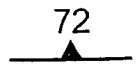
Migmatite



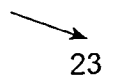
Magma
strike and
dip



Vertical
foliation



Solid-state
strike and
dip



Lineation
plunge



Vertical
foliation



Mafic
dip



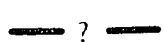
Approximate



Mapped



Concealed



Inferred



Antiform

Explanation

Rock Units

rc

Railroad Creek Pluton
(46 Ma)

m

Cooper Mountain
Batholith (48 Ma)

sl

Sunrise Lake Pluton
(49 Ma)

Ksc

Cub Lake Orthogneiss

Kso

Old Maid Orthogneiss

Ksh

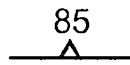
Heterogeneous Gneiss

Ksf

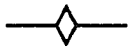
Ferry Peak
Orthogneiss (76 Ma)

Ksm

Migmatite



Magmatic foliation
strike and dip



Vertical magmatic
foliation



Solid-state foliation
strike and dip



Lineation trend and
plunge



Vertical solid-state
foliation



Mafic dike strike and
dip



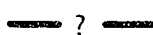
Approximate contact



Mapped contact



Concealed contact

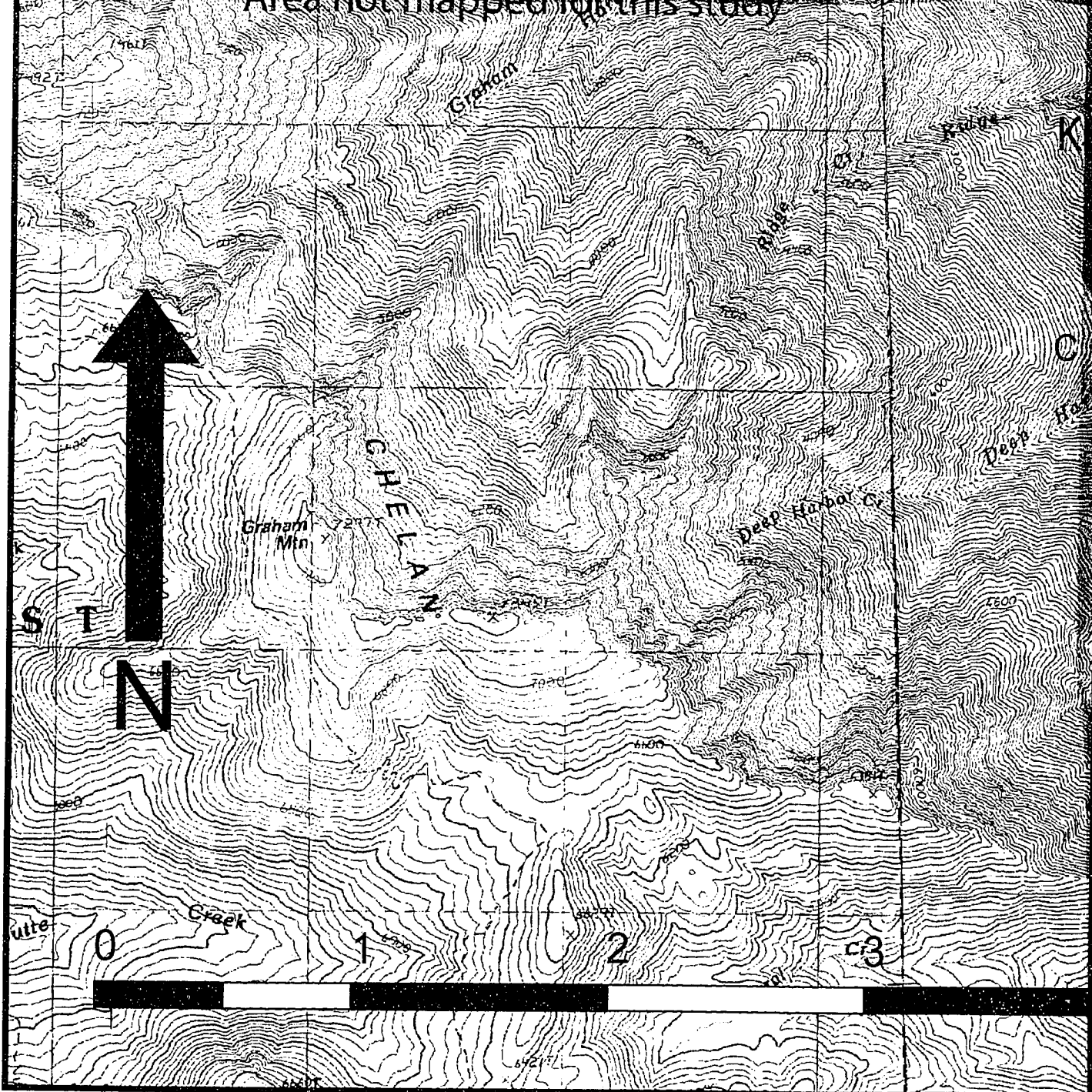


Inferred contact



Antiform

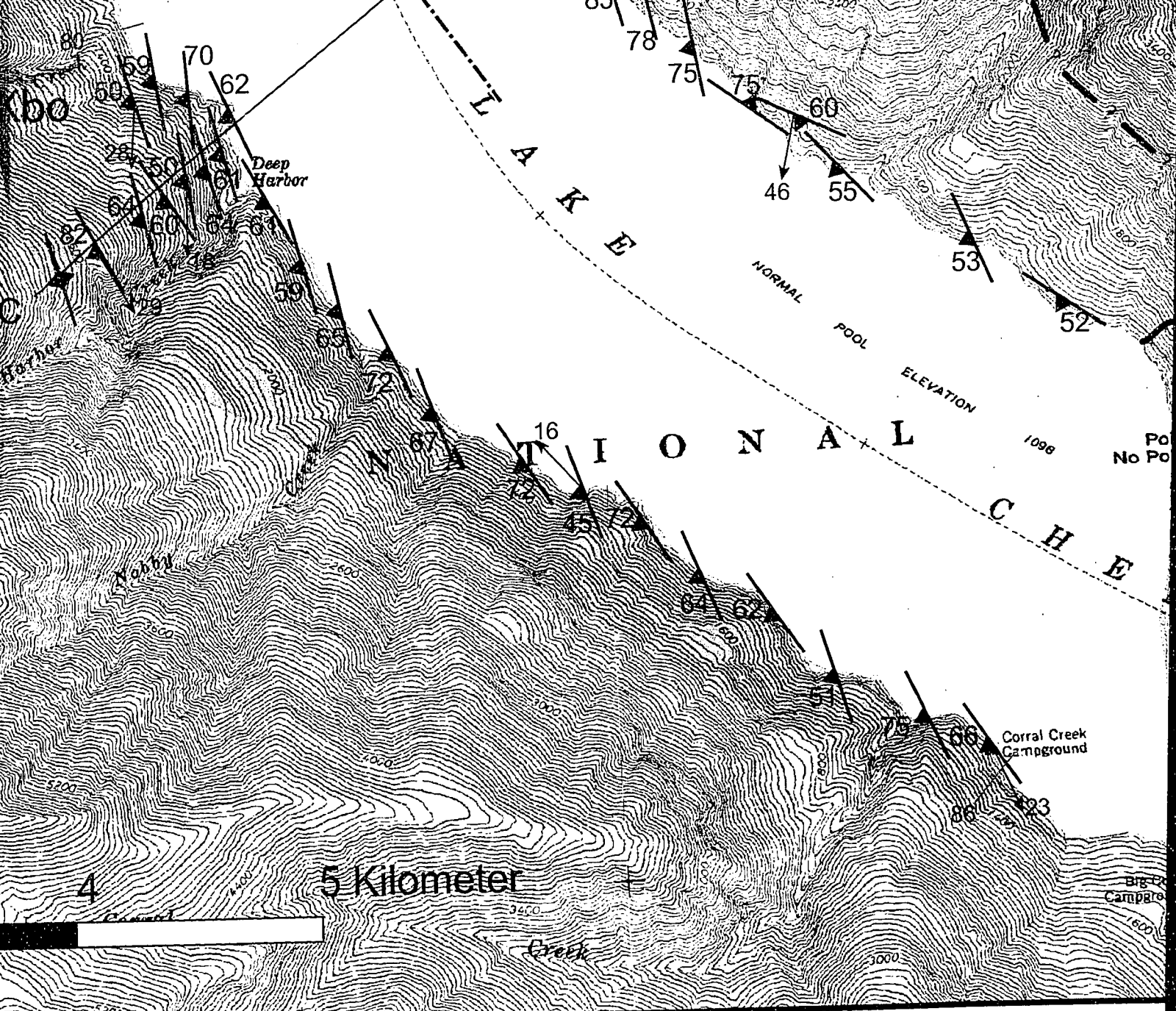
Area not mapped for this study



48° 02'

120° 32' 15"

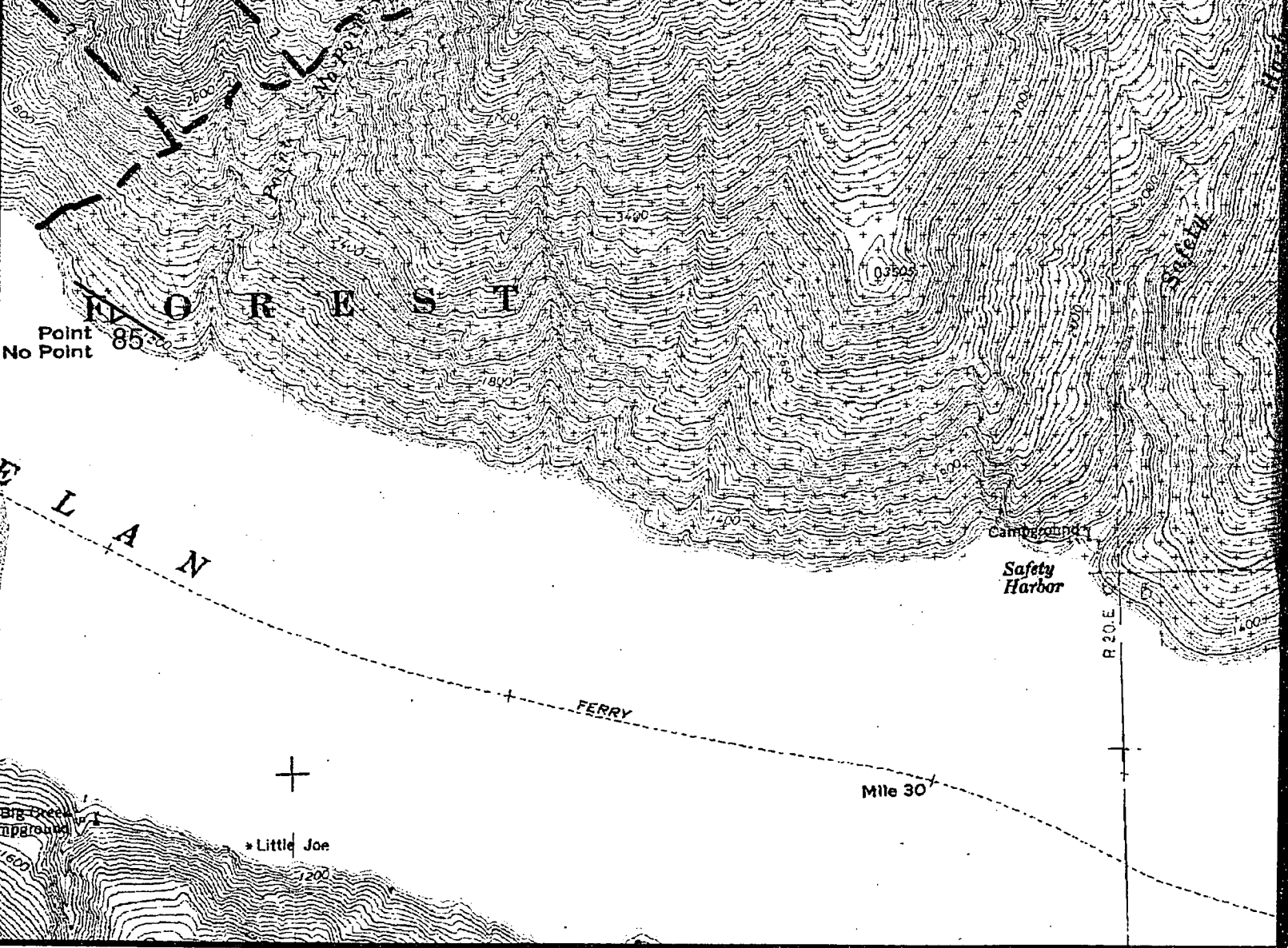
Bedrock Geology



SCALE 1:24,000

Topographic Map of the Southern Skagitzi National Forest, Washington

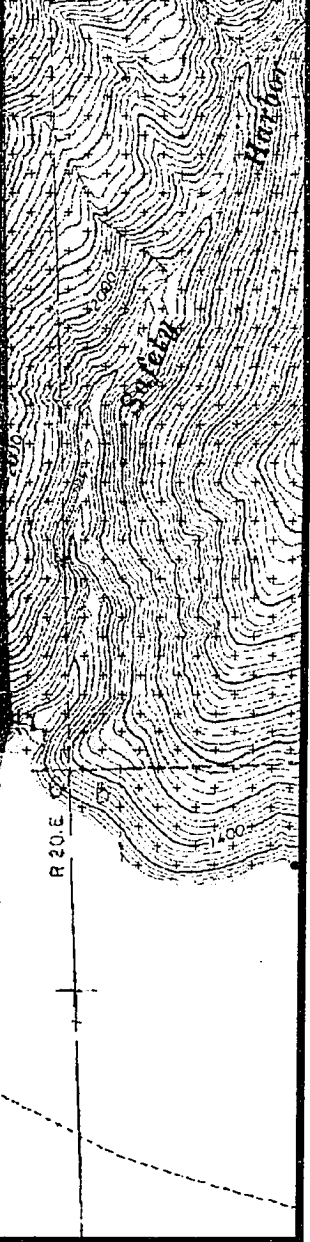
By
Erin Shea
2008



120° 21'

Bit Gneiss Complex

n



SKAGIT GNEISS C

TKsh

Heterogeneous Gneiss

————— M

Ksf

Ferry Peak Orthogneiss (76 Ma)

..... Co

Ksm

Migmatite

— ? — In

Kbo

Bearcat Ridge Orthogneiss (89-69 Ma)

↕ A

Rch

Cascade River-Holden Assemblage (Triassic)

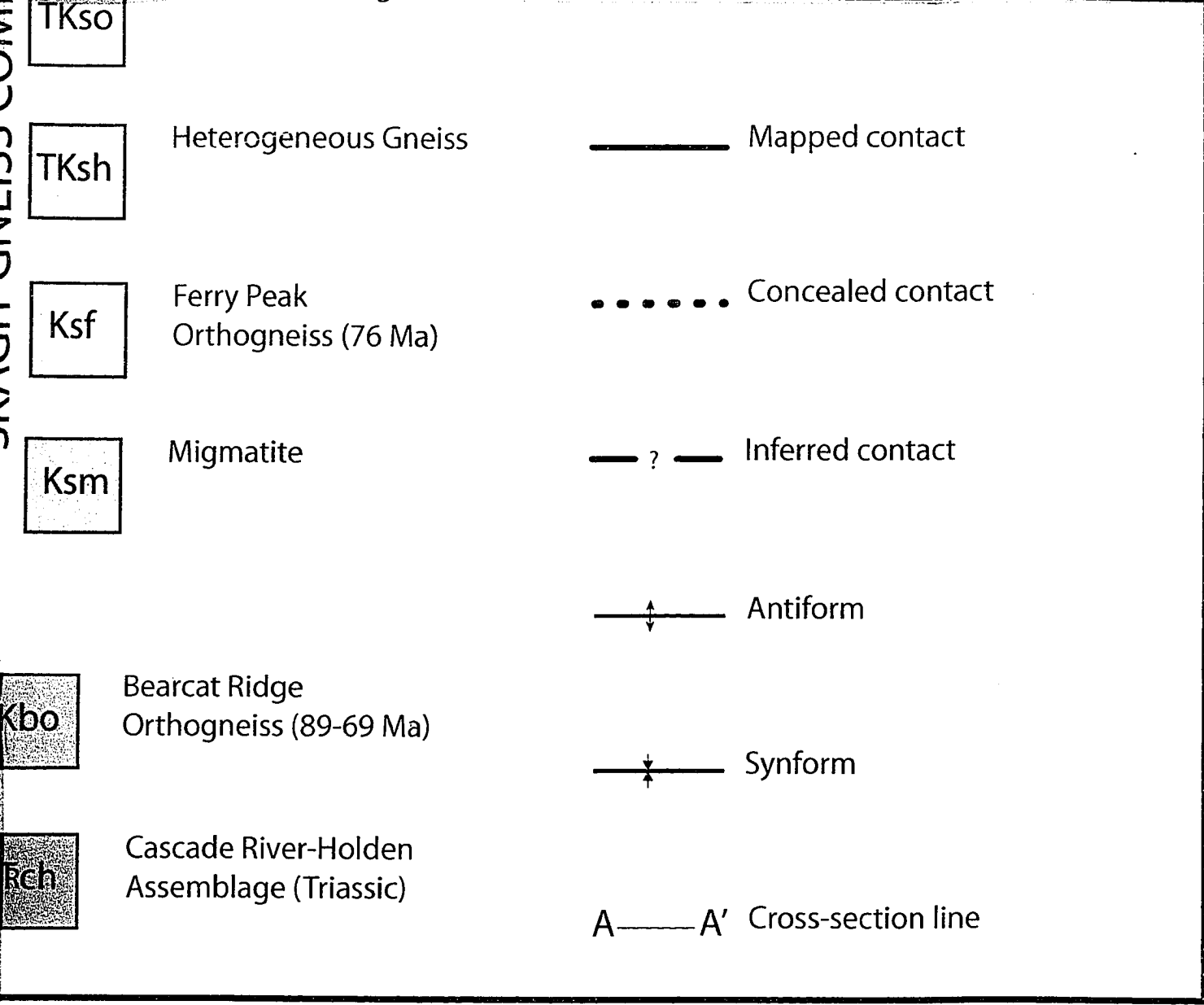
⊕ Sy

A—A' C

48° 02'

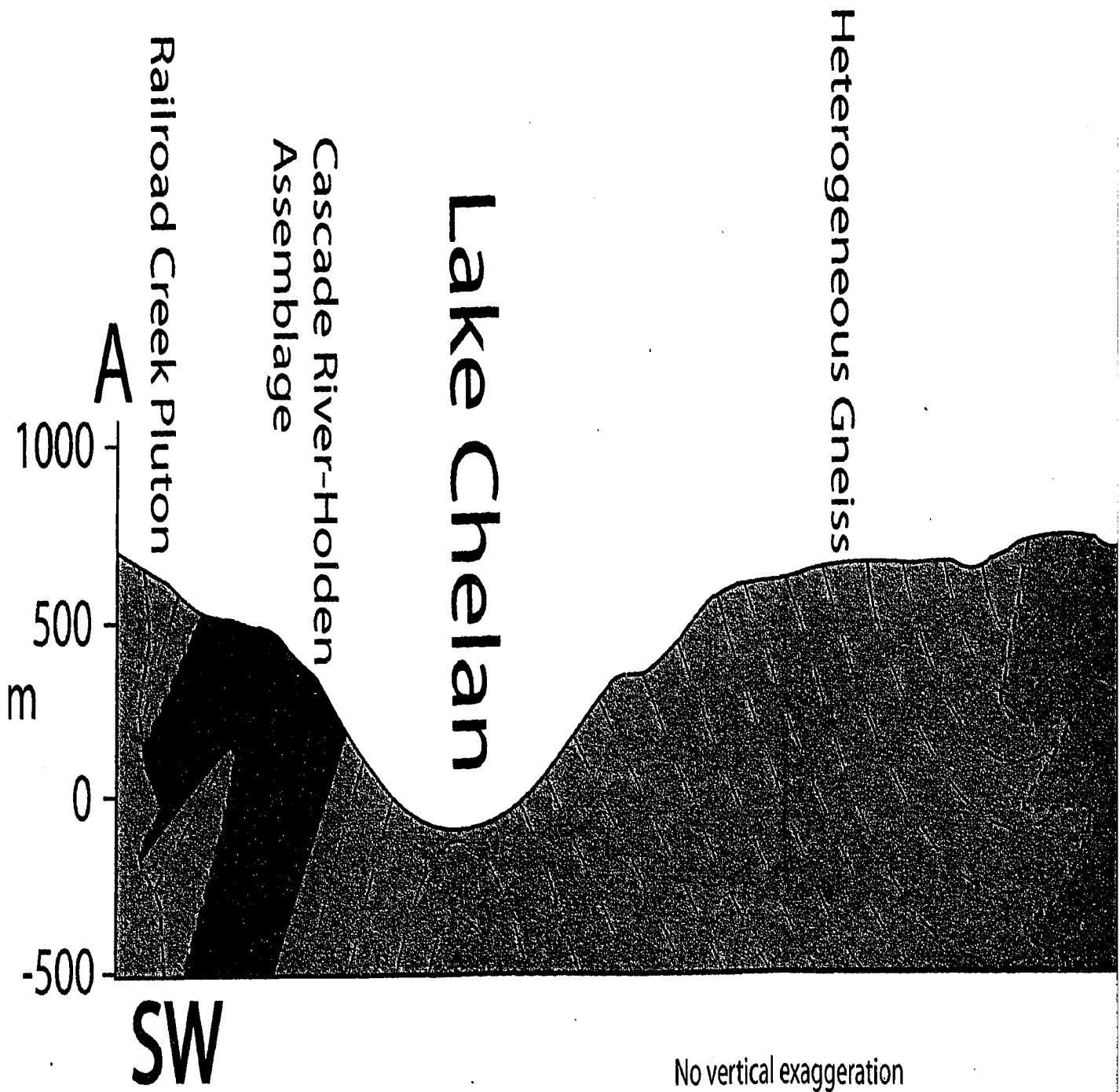
120° 21' 45"

Base map taked from the
 Lucerne
 Prince Creek
 Martin Peak
 Pyramid Mountain
 Big Goat Mountain
 South Navarre



Base map taked from the following USGS 7.5 minute quadrangles;
 Lucerne
 Prince Creek
 Martin Peak
 Pyramid Mountain
 Big Goat Mountain
 South Navarre

Plate 2



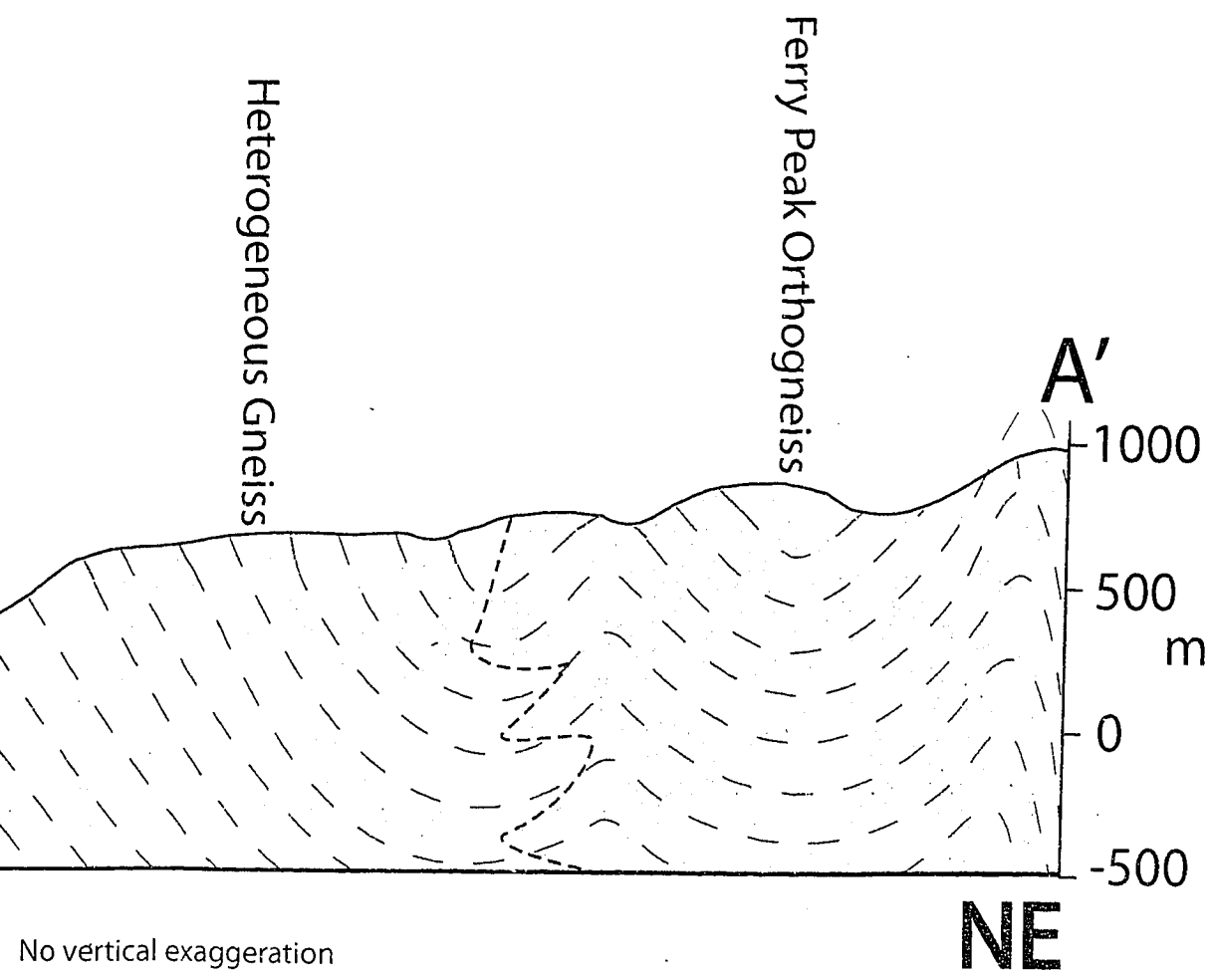
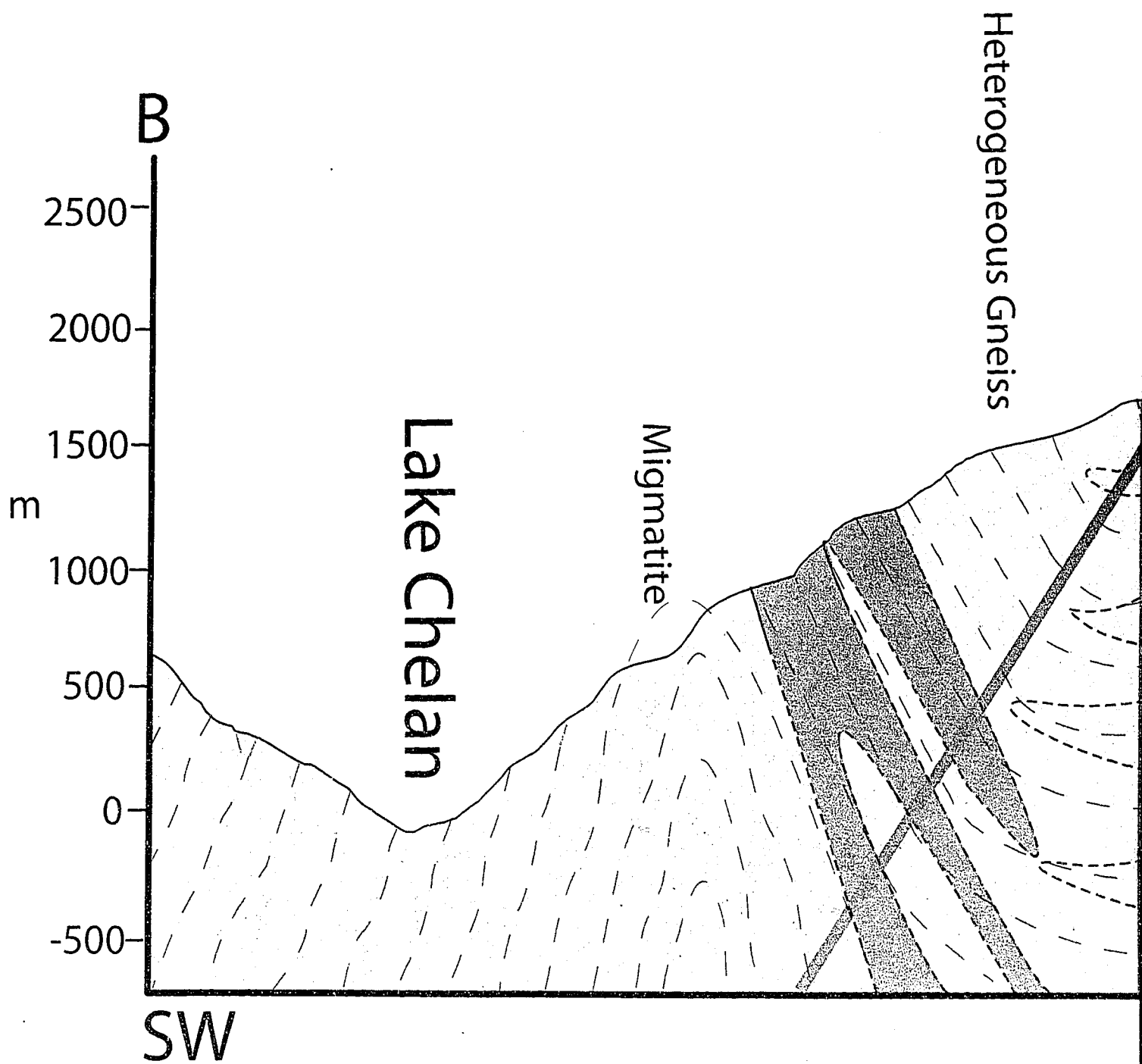
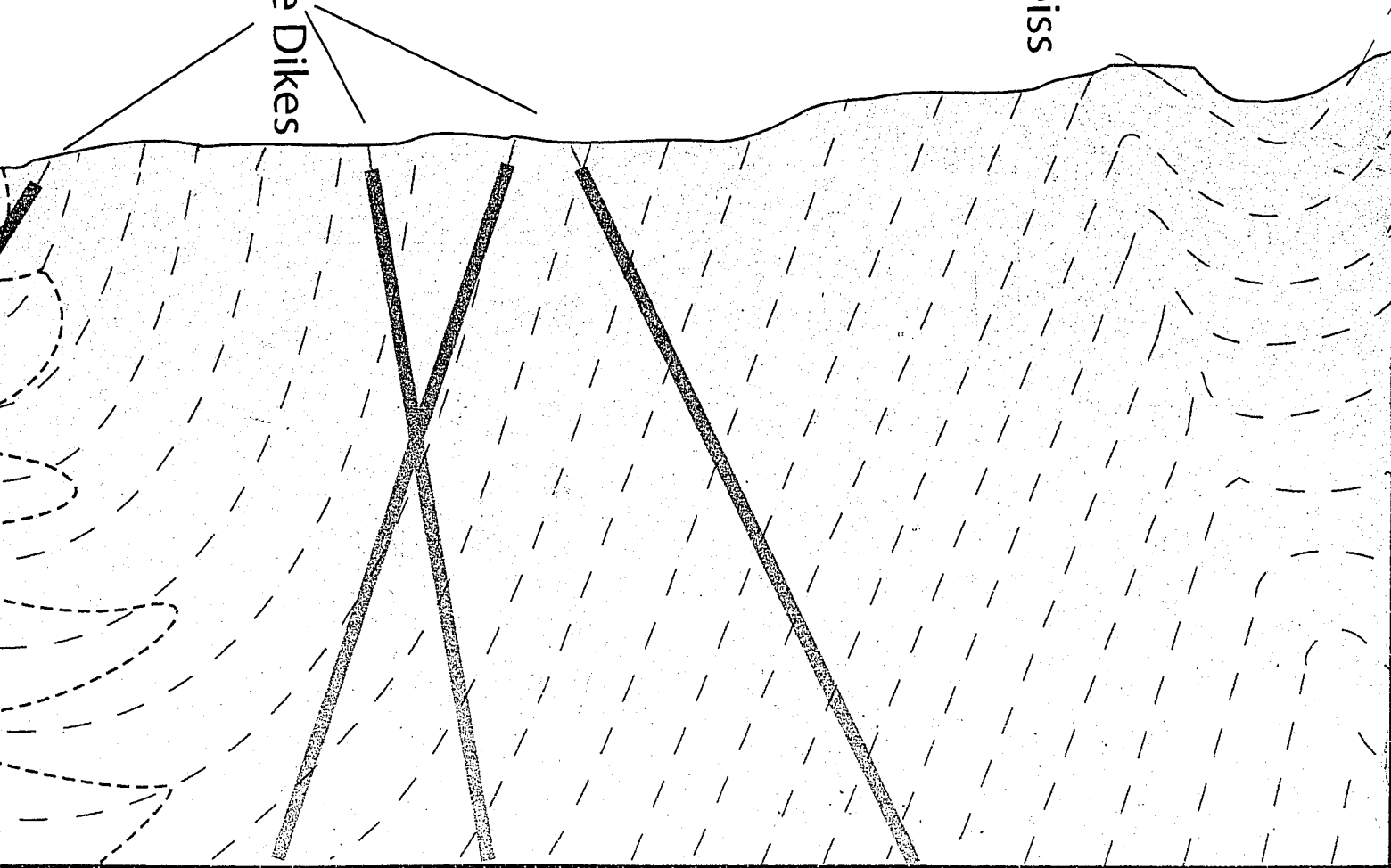


Plate 3



Ferry Peak Orthogneiss

Granodiorite Dikes



No vertical exaggeration

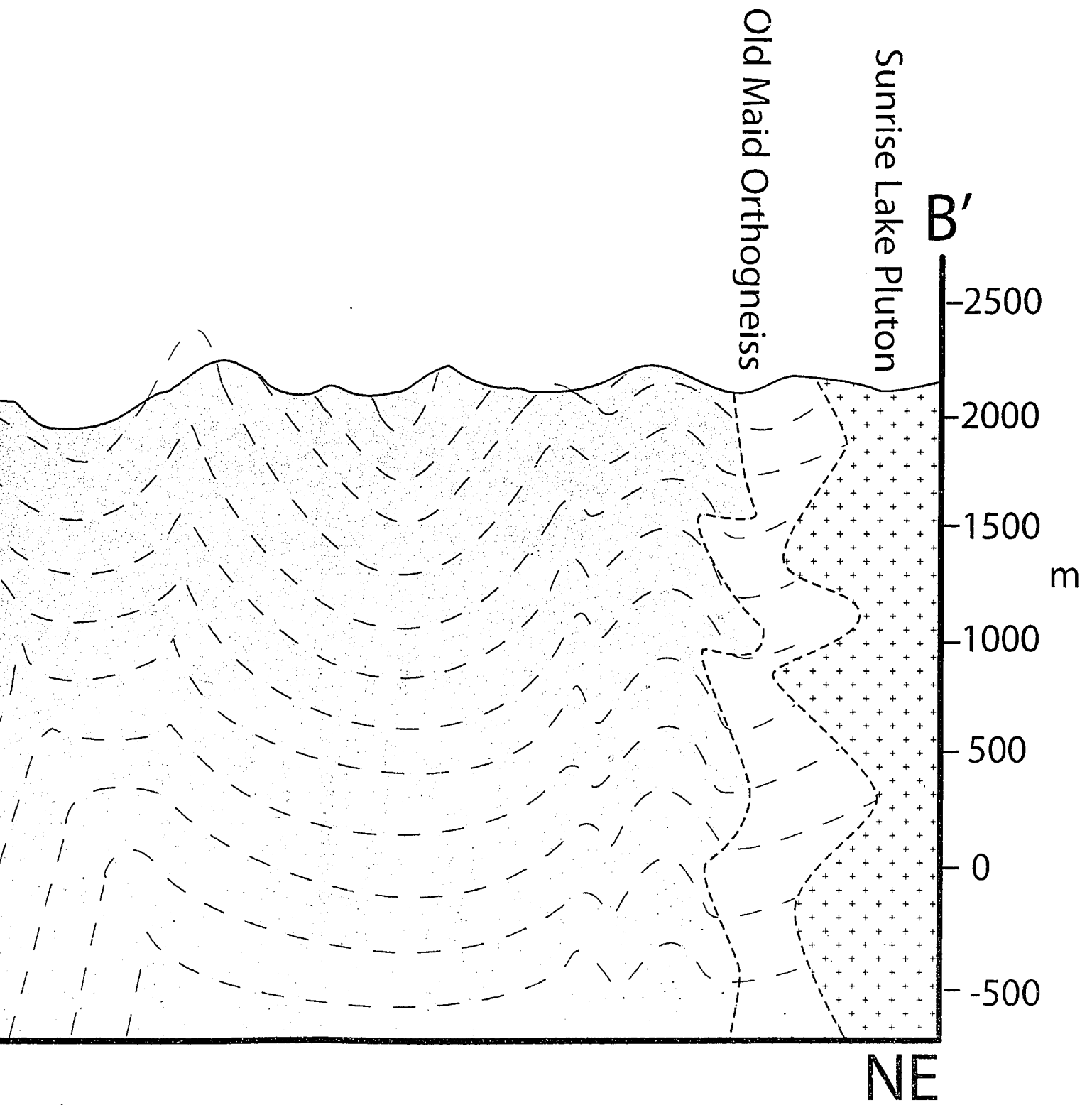
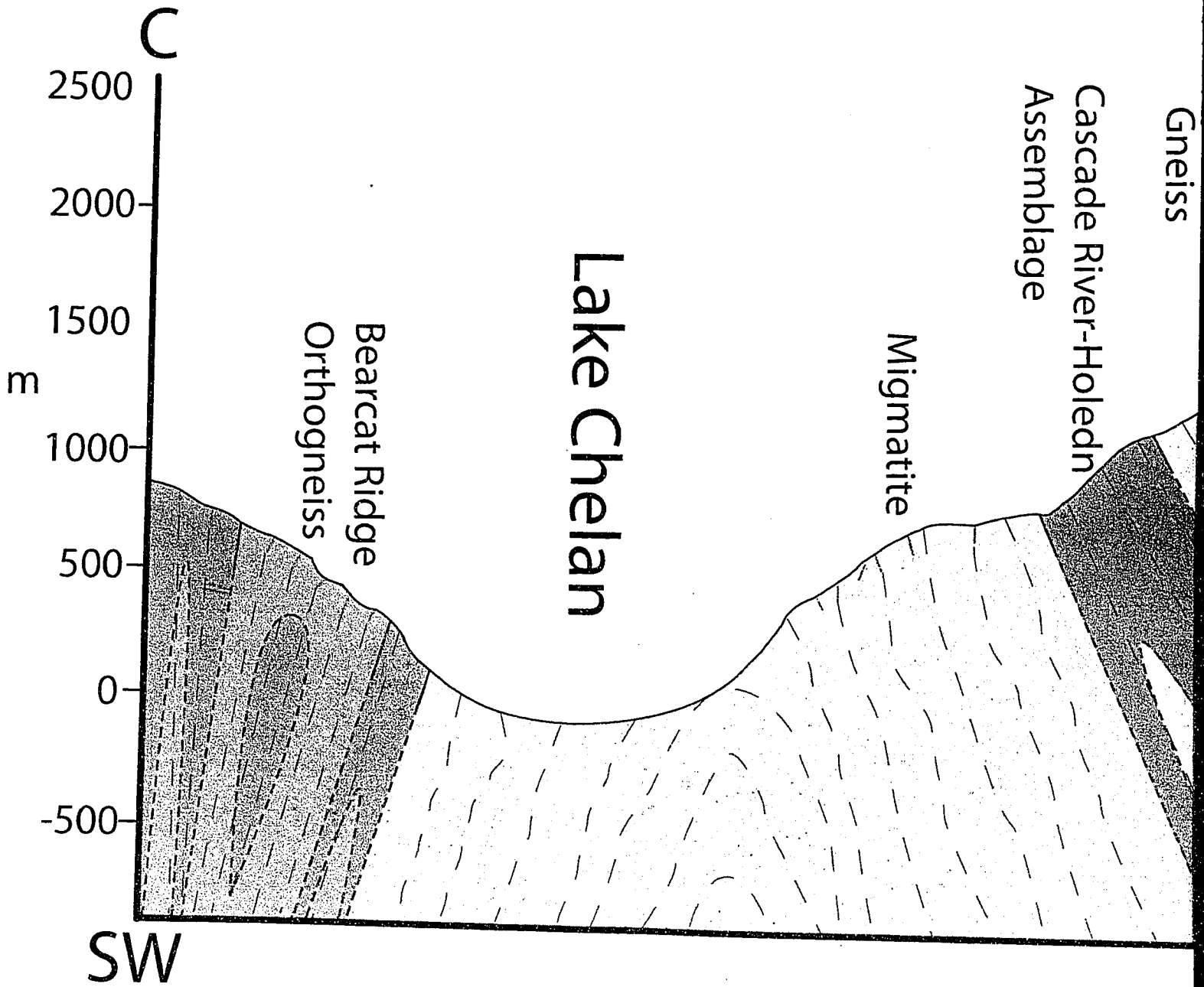


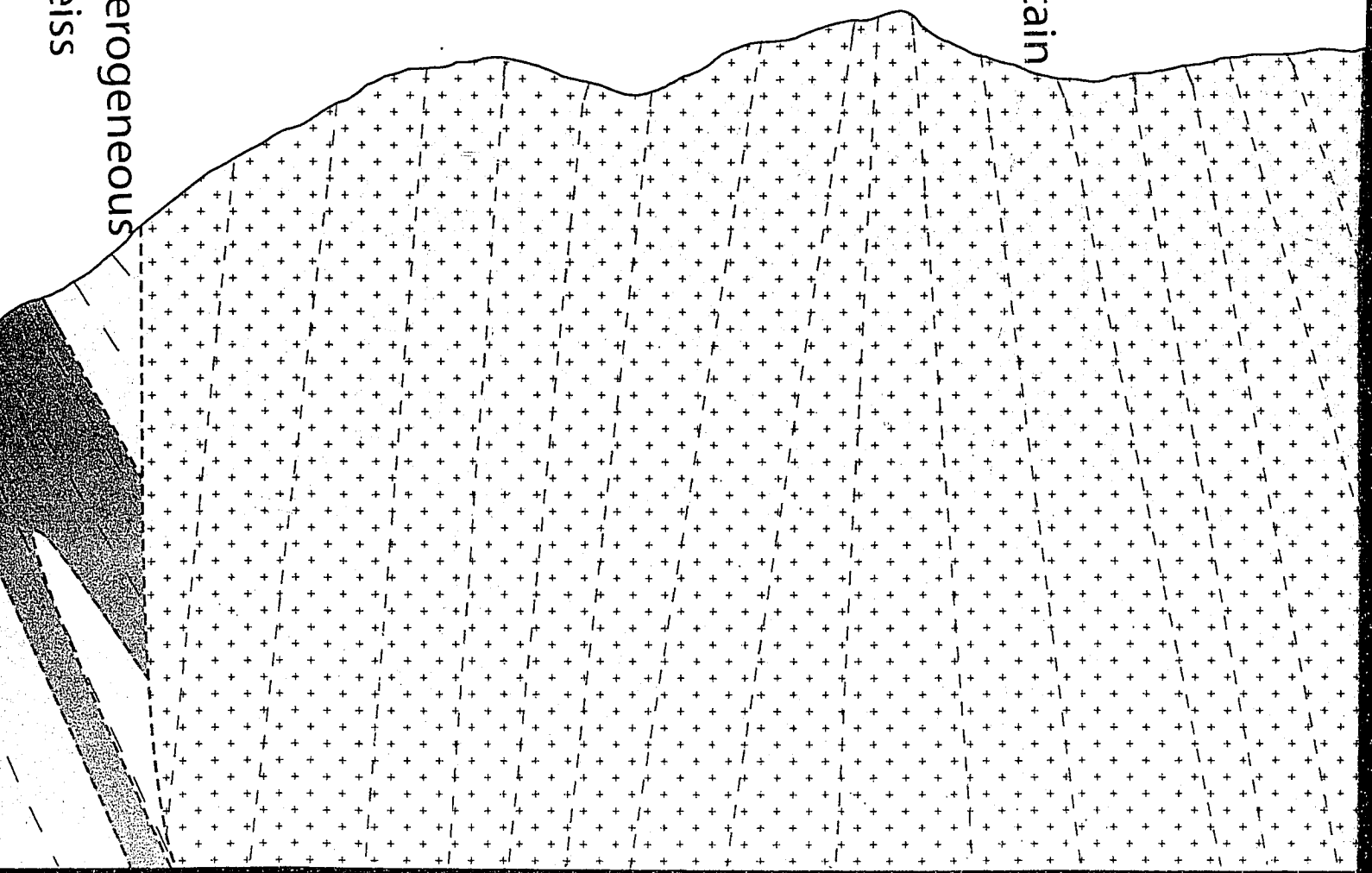
Plate 4





Cooper Mountain
Batholith

Heterogeneous
Gneiss



No vertical exaggeration



